TECHNISCHE UNIVERSITÄT WIEN

Master Thesis

Catalyst-Free Visible Light-Driven Hydroacylation by Direct Photoexcitation of 4-Acyl Hantzsch Esters

Ausgeführt am
Institut für Angewandte Synthesechemie

unter der Leitung von
Univ. Prof. Dipl.-Ing. Dr. techn. Katharina Schröder

Eingereicht an der Technischen Universität Wien
am 7.6.2023

von
Florian Ehrschwendtner, BSc
[redacted]

=:

Note of thanks

I would like to thank my family for their continuous financial support, without which I would have faced far more obstacles throughout studying and especially the support of not only both my parents (Karin Roithner, formerly Ehrschwendtner and Michael Sahiner, formerly Weyermayr) and step-parents (Christian Roithner and Songül Sahiner) but also my grandparents Harald and Gertrude Ehrschwendtner who provided food and shelter, should be highlighted. Furthermore, even though this is perceived as a matter of course in most civilised nations, I would like to thank the state of Austria for bearing the majority of the costs universities need to educate people. If support of both, family and state, had been absent, my chances of studying would be nigh zero and my life would have been forced to take a completely different direction.

My decision to study chemistry probably goes back to Dr. Mag. Elisabeth Weigel, at that time a very ambitious chemistry teacher at my school, who understood to spark my and many others' interest in chemistry.

I would like to thank the group I had the pleasure to work with and whose people were not only friendly, kind and patient but also very skilled and therefore provided a work atmosphere in which it was fun to work and interesting to learn new things. Of course, none of this would have happened, if Univ.Prof. Dr. Katharina Schröder (formerly Bica) hadn't squeezed me into her already crowded lab, finding me a place to work, for which I am very grateful. I am also thankful for all her ideas and support during my work. Finally, any master student will feel pressed about thanking their supervisor; however, I can proudly say that Univ.Ass. Dr.techn. MSc Ádám Márk Pálvölgyi did not only earn my thanks but also my respect for the insane amount of work he puts into his research while still flexibly taking the time whenever needed and teaching me a lot of practical work (especially related to photochemistry) as well as giving me a more nuanced view on scientific work while doing so.

Abstract

This work focused on an alternative photochemical hydroacylation strategy for electron-poor alkenes. Using 4-acyl Hantzsch esters as radical reservoirs, an efficient hydroacylation protocol has been developed, which requires neither a photocatalyst nor any kind of additives for efficient acyl transfer. After optimisation of reaction conditions, a substrate scope based on benzylidenemalononitrile derivatives and enones was established. The 4-acyl group on acyl-Hantzsch esters was also varied to further investigate electronic and steric influence from the reagent side. This hydroacylation approach also enabled one-pot derivatisations, providing straightforward access to a set of formal alkenylation products.

Detailed mechanistic studies were conducted to elucidate the reaction mechanism. This revealed, that the reaction proceeds *via* a non-chain radical mechanism, initiated by the direct photoexcitation of the Hantzsch ester species at 460 nm, and the generated acyl radical reacts with the activated alkene substrate in a Giese-like manner.

Kurzfassung

Die vorliegende Arbeit konzentrierte sich auf die Entwicklung einer alternativen photochemischen Hydroacylierungsstrategie für elektronenarme Alkene. Unter Verwendung von 4-Acyl-Hantzsch-Estern als Radikalreservoir wurde ein effizientes Hydroacylierungsprotokoll entwickelt, das weder einen Photokatalysator noch irgendwelche Additive für den effizienten Acyltransfer benötigt. Nach Optimierung der Reaktionsbedingungen wurde ein Substratspektrum basierend auf Benzylidenmalonitril-Derivaten und Enonen etabliert. Die 4-Acylgruppe an Acyl-Hantzsch-Estern wurde ebenfalls variiert, um den elektronischen und sterischen Einfluss von Seiten der Reagenzien weiter zu untersuchen. Dieser Hydroacylierungsansatz ermöglichte auch Eintopfderivatisierungen, die einen direkten Zugang zu einer Reihe von formalen Alkenylierungsprodukten boten.

Detaillierte mechanistische Studien wurden durchgeführt, um den Reaktionsmechanismus aufzuklären. Dabei zeigte sich, dass die Reaktion nicht über einen radikalischen Kettenmechanismus abläuft, dass sie durch die direkte Photoanregung der Hantzsch-Ester-Spezies bei 460 nm initiiert wird, und dass das so erzeugte Acylradikal mit dem aktivierten Alken-Substrat auf Giese-ähnliche Weise reagiert.

List of abbreviations

Alkyl-HE – Alkylated Hantzsch ester

Acyl-HE – Acylated Hantzsch ester

BET – Back electron transfer

bipy – 2,2'-Bipyridyl

DCM – Dichloromethane (methylenechloride)

dHAT – Direct hydrogen atom transfer

EDA – Electron donor-acceptor complex

EnT – Energy transfer

EtOH – Ethanol

HAT – Hydrogen atom transfer

HE – Hantzsch ester; 2,6-dimethyl-3,5-dicarboxylethylester-1,4-dihydropyridine

HIC – Hypervalent iodine species

HOMO – Highest occupied molecular orbital

HPyr – Hantzsch pyridine; 2,6-dimethyl-3,5-dicarboxylethylesterpyridine

iHAT – Indirect hydrogen atom transfer

LED – Light emitting diode

LUMO – Lowest unoccupied molecular orbital

*n*Hex – n-Hexyl

PC - Photocatalyst

PRC-H – Polarity reversal catalyst

PRC* - Polarity reversal catalyst radical

PS – Photosensitiser

RHAT – Reverse hydrogen atom transfer

SOMO – Single occupied molecular orbital

SUMO – Single unoccupied molecular orbital

SET – Single electron transfer

TEMPO - (2,2,6,6-Tetramethylpiperidin-1-yl)oxyl

TLC – Thin layer chromatography

TMS - Tetramethylsilane

UV – Ultraviolet

Table of contents

1 Introduction 1

1.1 Early examples[1] 1

1.2 Basics of photochemistry 3

1.2.1 Comparing thermal and photochemical reactions[16,17] 3

1.2.2 Quantum mechanics[16,17,20] 4

1.2.3 HOMO, LUMO, SOMO, SUMO 6

1.2.4 Multiplicity (singlet, duplet, triplet, …)[16,17,20] 6

1.2.5 Absorption and Excitation [16,17,20] 7

1.2.6 Jablonski diagram[16,17,20] 9

1.2.7 Types of photochemical reactions[24] 10

1.3 Direct photoexcitation[16,17] 12

1.3.1 Photosensitation, Photoredox Catalysis & Atom Transfer[30–32] 14

1.3.2 Electron donor-acceptor complexes and exciplexes[24,38] 17

1.4 Instrumentation and set-up[17,39,40] 20

1.4.1 Wavelength and light sources 20

1.4.2 Light intensity 22

1.4.3 Quantum yield[17] 23

1.4.4 Temperature 24

1.4.5 Impurities 24

1.5 Introduction to Acylation and Hydroacylation 25

1.6 Free Radical Hydroacylations 28

2 Aim of the thesis 32

3 Results and discussion 35

3.1 Preparation of benzylidenemalononitrile substrates 35

3.2 Preparation of Hantzsch esters 36

3.3 Optimisation 38

3.4 Hydroacylation reactions 40

3.4.1 Saturated photoproducts 40

3.4.2 Towards furane-formation 42

3.4.3 Synthesis of formal alkenylation products 46

3.4.4 Trial for silylation 47

3.5 Mechanistic considerations 47

4 Summary 53

5 Experimental part 54

5.1 Materials & methods 54
5.2 The photochemical setup 55
5.3 Synthesis of malononitrile substrates 56
5.3.1 Benzylidenemalononitrile (36-A, CAS: 2700-22-3) 56
5.3.2 2-(2-Methylbenzylidene)malononitrile (36-B, CAS: 2698-44-4) 56
5.3.3 2-(3-Methylbenzylidene)malononitrile (36-C, CAS: 15728-26-4) 57
5.3.4 2-(4-Methylbenzylidene)malononitrile (36-D, CAS: 2826-25-7) 57
5.3.5 2-(4-Methoxybenzylidene)malononitrile (36-E, CAS: 2826-26-8) 57
5.3.6 2-(2-Nitrobenzylidene)malononitrile (36-F, CAS: 2826-30-4) 57
5.3.7 2-(3-Nitrobenzylidene)malononitrile (36-G, CAS: 2826-32-6) 58
5.3.8 1-Naphthylmethylidenemalononitrile (36-I, CAS: 2972-83-0) 58
5.3.9 2-(4-Cyanobenzylidene)malononitrile (36-J, CAS: 36937-92-5) 58
5.4 Synthesis of Hantzsch esters 59
5.4.1 Glyoxal synthesis 59
5.4.2 Hantzsch ester synthesis 59
5.5 Synthesis of saturated photoproducts 62
5.5.1 2-(2-Oxo-1,2-diphenylethyl)malononitrile (133-A, CAS: 312307-43-0) 62
5.5.2 2-(1-(4-Methoxyphenyl)-2-oxo-2-phenylethyl)malononitrile (133-B, CAS: n.a.) 63
5.5.3 2-(1-(4-Chlorophenyl)-2-oxo-2-phenyl)malononitrile (133-C, CAS: n.a.) 63
5.5.4 2-(1-(4-Bromophenyl)-2-oxo-2-phenyl)malononitrile (133-D, CAS: n.a.) 63
5.5.5 2-(1-(Naphthen-1-yl)-2-oxo-2-phenylethyl)malononitrile (133-E, CAS: n.a.) 63
5.5.6 3-Benzoylcyclopentan-1-one (135, CAS: 92516-43-3) 64
5.5.7 3-Benzoylcyclohexanone (137, CAS: 58753-28-9) 64
5.6 Synthesis of formal alkenylation-type photoproducts 65
5.6.1 2-(2-Oxo-1,2-diphenylethylidene)malononitrile (146-A, CAS: 23195-86-0) 65
5.6.2 2-(1-(4-Methoxyphenyl)-2-oxo-2-phenylidene)malononitrile (146-B, CAS: n.a.) 65
5.6.3 2-(1-(4-Chlorophenyl)-2-oxo-2-phenylidene)malononitrile (146-C, CAS: n.a.) 66
5.6.4 2-(1-(4-Bromophenyl)-2-oxo-2-phenylidene)malononitrile (146-D, CAS: n.a.) 66
5.6.5 (2-(1-(Naphthalen-1-yl)-2-oxo-2-phenylethylidene)malononitrile (146-E, CAS: n.a.) ... 66
5.6.6 2-(1-(4-Cyanophenyl)-2-oxo-2-phenylethylidene)malononitrile (146-F, CAS: n.a.) 67
5.7 Furane formation 67
5.7.1 2-Amino-5-(naphthalene-1-yl)-4-phenylfuran-3-carbonitrile (146-Ab, CAS: n.a.) 67
5.7.2 2-Amino-4-(4-cyanophenyl)-5-phenylfuran-3-carbonitrile (146-J, CAS: n.a.) 67
5.8 Silylation trials 69
6 Appendix 70
6.1 List of figures and schemes 70

7 Literature 73

1 Introduction

1.1 Early examples[1]

One of the first documented photochemical experiments was performed in 1719 by Johann Heinrich Schulze[2,3], where he used a nitric acid HNO_3(aq.) / silver nitrate $AgNO_3$(aq.) solution left-over from purifying gold, and put powdered chalk in it. What he saw was the precipitation of elemental silver particles Ag^0 on chalk upon light irradiation, which resulted in a grey colour according to the following equation:

$$2\ AgNO_3 \xrightarrow{h\nu} 2\ Ag + 2\ NO_2 + O_2$$

This discovery was a predecessor to the first photochemical application: photography. According to findings on SciFinder, most, if not all, effort was put to advance the newly found photograph technology, often resulting in patents.[4–6] The first organic photochemical reaction was reported in 1834 by Hermann Trommsdorff[7], where he observed that santonin crystals cracked and changed their colour from colourless to yellow upon irradiation with blue or purple light. Later, other photochemical reactions were discovered, such as the first photo dimerisation by Carl Julius Fritzsche in 1867[8], the first [2+2]-cycloaddition by Carl Theodor Liebermann in 1877[9], the first photo isomerisation by William Henry Perkin in 1881[9], the first photo-induced halogenation by Paul Jannasch in 1875[10] and the first photoreduction by Heinrich Klinger in 1886[9]. So far, the organic photochemical repertoire was limited to isomerisations, reactions of substances with themselves and functional group conversions. One major milestone for organic photochemistry was the first set of photochemical syntheses performed by Heinrich Klinger published in 1886[11] and extended in 1888[12] as he successfully reacted phenanthrene-9,10-quinone (**1**) with various aldehydes (acetaldehyde (**3**), benzaldehyde, isovaleraldehyde) to form a product **4** of increased complexity (Scheme 1). The initial photochemical reduction of phenanthrene-9,10-quinone (**1**) to **2** was followed by esterification with an aldehyde. The aromatisation of the phenanthrene part seems to play an important role during this reaction, as it locks the enol form to undergo esterification.

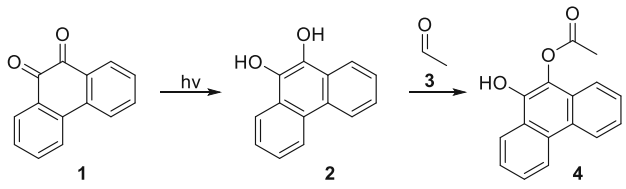

Scheme 1: Photochemically triggered aromatisation and enol formation followed by acetylation[11,12].

One has to keep in mind that the analytical methods available at that time were rather limited[13], photometry was quite imprecise and the Michelson interferometer or X-ray diffraction for instance

were developed as late as 1892[14] or 1955[15] respectively. Experiments were carried out by putting a solution out into direct sunlight on a non-cloudy day, concentration was given as „putting a lot of water on it“ and temperature (in a control experiment of Schulze) was determined by „so much heat, that my hands can barely hold the hot glass“. As the solutions were not stirred and just sunlight was used, reactions could take weeks to months to complete while standing next to a window and becoming prey to the next stormy day. Despite all these difficulties, clever scientists developed theories and rules for what is now known as photochemistry.

1.2 Basics of photochemistry

1.2.1 Comparing thermal and photochemical reactions[16,17]

In conventional, thermal reactions the activation energy is applied in the form of heat. In contrast, photochemical reactions utilise an electronically excited state, which is formed when the ground state molecule absorbs a photon. The photon's energy will be completely consumed and added to the ground state's energy, promoting an electron to higher energy levels and therefore creating the excited state. It is important to note that this electronically excited state acts as an isomer of the ground state and therefore has different properties.[18] The different nature of the ground and excited state also enables different reaction pathways as opposed to thermal reactions, which is mostly attributed to the radical character of the electronically excited state. Once the molecule is selectively brought to the excited state the difference in free Gibbs energy between the starting material and product (ΔH_R) is no longer crucial for whether the reaction takes place or not. Instead, the energy gap between the excited state and the product(s) is important and it is noteworthy, that the thermodynamically most stable product does not necessarily need to be the major product either. This enables photochemistry to aim for different products than those of conventional chemistry, such as in the case of isomerisation, where, for example, one (more stable) isomer is periodically and selectively excited and its excited state is given the chance to be converted to either isomer. After some time, most of the (more stable) isomer will completely drained giving the (less stable) isomer as the major product as long as the (less stable) isomer is not also excited by the light source[19].

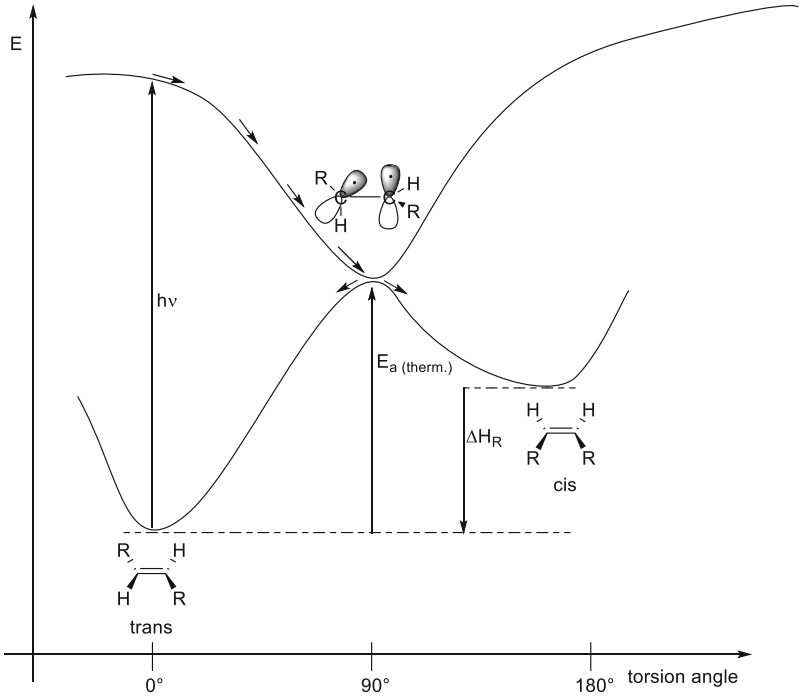

Figure 1: Schematic representation of photoisomerisations (redrawn from literature[19]).

1.2.2 Quantum mechanics[16,17,20]

The core part of photochemistry is the generation of electronically excited states *via* photon absorption, so we first need to answer the questions of what an electronically excited state is, how we get it and what happens after its generation.

Something that was anticipated until now is the Grotthuss-Draper law, which states that photochemical reactions can only occur *via* light absorption. How this absorption takes place is defined by Stark-Einstein law, which states that every molecule can only absorb one photon (as always, exceptions exist[21]). To describe the absorption more mechanistically, we need quantum mechanics.

Without going into mathematical details, by asking the question "Where are the electrons" (= solving Schrödinger's equation) a set of solutions (wave functions) is obtained, which, if quadrated, give functions that represent the probability of finding the electron at a certain point in space. A fraction of that infinite space can be defined as orbital - a volume of a certain shape (Figure 1), that has a 90% probability to include the electron of interest. We conveniently say/assume that an electron is in an orbital even if this might not be the case with the simple explanation that this is easier to imagine/visualise.

Each orbital is - because of quantisation - associated with a discrete energy level based on the principal quantum number n (n = 0, 1, 2, …) and the angular-momentum quantum number l (l = 0, 1, 2, … n-1). The shape and therefore the type of orbital (s, p, d, f, g, …) depends on l. As there are 2l+1 orbitals of the same shape with the same n - and therefore the same energy - these orbitals can be only discriminated by their orientation within an external magnetic field, where the orientation is described by the magnetic quantum number m (m = -l, -l+1, -l+2, …, +l). Based on the "Aufbau" principle, if an atom were formally filled with electrons those electrons would be found within the lowest energy orbitals first, which are not already filled. The Pauli principle states, that two electrons with the same quantum numbers must not be in the same orbital, which is where the fourth quantum number - the spin quantum number s (s = -½, +½) - comes into play. As each orbital can contain up to two electrons, they, therefore, need to have different spin quantum numbers, which are generally visualised by drawing upward and downward arrows. Hund's rule states that orbitals of the same energy are formally filled with single electrons before paired with a second one or more generally that the multiplicity M = 2S + 1 is to be maximized, where S is the sum of the electron's spin quantum numbers s across the atom. The last set of orbitals with the same n and l (with the exception of e.g. inorganic complexes and their high and low spin configuration) is the only one that may contain unpaired electrons because based on the "Aufbau" principle all lower orbitals would have been filled with two electrons first. As these electrons must have opposing spin quantum numbers based on the Pauli principle, that means that all those "lower" orbitals equal themselves out (-½ + ½ = 0) and it can be sufficient to look at the "highest" orbitals (as mentioned: with exceptions).

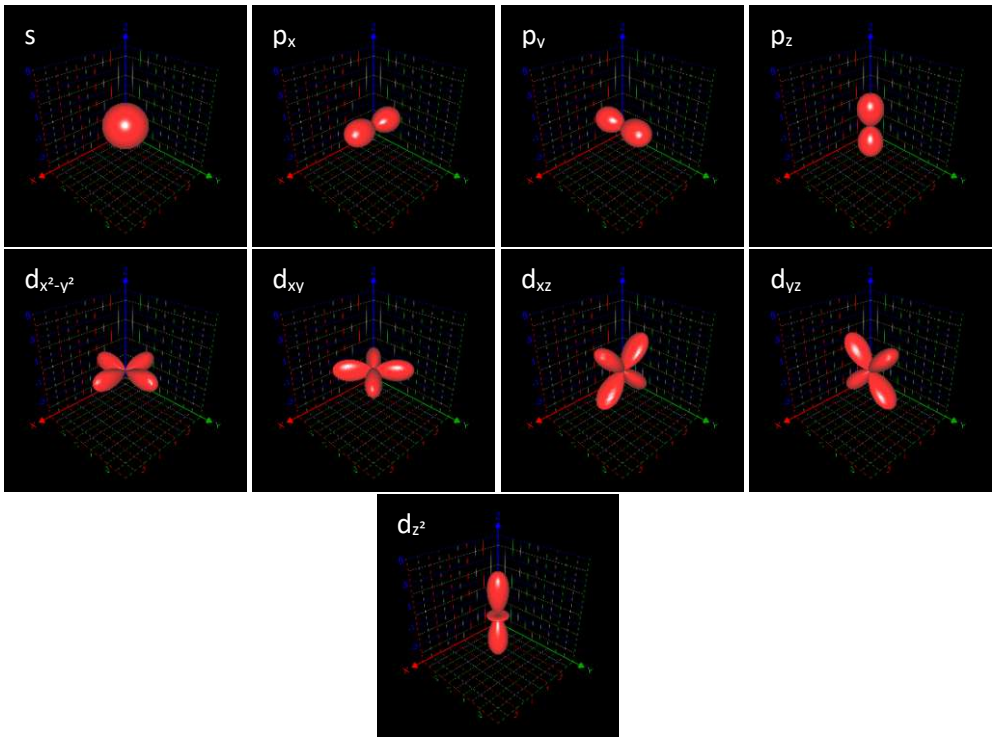

Figure 2: Representation (program: Graphing calculator 3D) of the squared angular part (not the actual orbitals) of the wave functions for s, p, and d orbitals, which are arbitrarily scaled for better representation.

So far, this is all true for the hydrogen atom alone, as it is the only one the Schrödinger's equation can be calculated exactly. For other elements or molecules methods to give approximate results exist[22]. In order to describe molecules, the molecular orbital theory uses the linear combination of atomic orbitals, in which the wave functions of e.g. two atomic orbitals are both added and subtracted from one another to give two molecular orbitals. It is noteworthy that also more than two atomic orbitals can be combined, such as in the case of conjugated systems (e.g. benzene), but for each atomic orbital combined, there needs to be exactly one molecular orbital formed. These molecular orbitals can have either bonding or antibonding properties, based on whether the overlap of the wave functions (which the orbitals are based on) lead to (partial) constructive interference and thereby increase electron density between them or (partial) destructive interference, reducing the electron density between them. The more nodes a molecular orbital has, the more antibonding it is. The same rules apply for formally filling molecular orbitals with electrons as mentioned above for atomic orbitals. It can happen that electrons from an atom cannot participate in bonding interaction due to a lack of symmetry (two wave functions having different algebraic signs) or geometric reasons (no bonding partner in range).

Bonding molecular orbitals can be subdivided into different groups: sigma (σ), pi (π), delta (δ), … bonds. Their antibonding counterparts are denoted with a star symbol (e.g. σ*). "*In the case of two-centre bonds, a π-bond has a nodal plane that includes the internuclear bond axis, whereas a σ-bond has no such nodal plane. (A δ-bond in organometallic or inorganic molecular species has two nodes.)*"[18]. In terms of energy, σ-bonds are generally lower in energy than π-bonds, meaning that more energy is

needed to break σ-bonds as opposed to π-bonds, while non-bonding orbitals, generally denoted with n, lie in between bonding and antibonding molecular orbitals.

1.2.3 HOMO, LUMO, SOMO, SUMO

Chemistry is basically the science of electrons and this becomes the most apparent when talking about the HOMO and LUMO concept. Generally speaking, in conventional reactions the highest occupied molecular orbital (HOMO) of molecule A is reacting with the lowest unoccupied molecular orbital (LUMO) of molecule B. For example, if we take an S_N2 reaction, the nucleophile's (Lewis base) HOMO is generally a lone pair, which it donates into an antibonding σ* orbital (LUMO) of the electrophile. Since electrons are filled into an antibonding orbital, this helps dissociate the leaving group from the soon-to-be-formed substituted product. HOMO/LUMO are by definition either filled or empty, while the so-called single occupied molecular orbitals (SOMO) are half-filled, and single unoccupied molecular orbitals (SUMO) are half-empty. A SOMO-SUMO pair can be generated *via* photoexcitation for example, in which the SUMO contains the remaining electron of the former completely filled orbital and the SOMO contains the electron that is promoted to a higher energy level. They are therefore generally needed to describe radicals, which are commonly encountered in photochemistry.

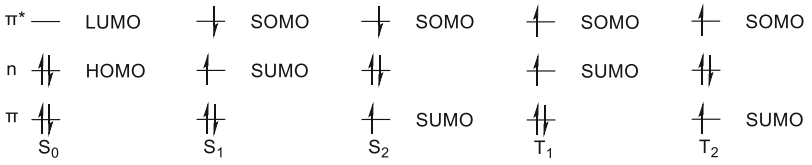

Figure 3: Schematic representation of HOMO, LUMO, SOMO and SUMO is a recreation from literature[17] (giving formaldehyde as an example).

1.2.4 Multiplicity (singlet, duplet, triplet, …)[16,17,20]

The formula for multiplicity M = 2S + 1 gives results of natural numbers. If the result is 1, the according state is called a singlet, 2 for duplets, 3 for triplets, 4 for quartets and so on. Of importance for organic photochemistry are singlet and triplet states, where singlet states are the default ones. This is because a ground-state molecule usually has a closed shell, where all electrons are paired. Its total electron spin is therefore S = 0 and its multiplicity M = 1, a singlet. If an electron within that molecule is promoted to a higher level, this must happen with spin retention, which is why excited states usually are also singlets. As shown below, by intersystem crossing the spin of the excited molecule may be inverted, which leads to a total spin number of S = 1 (0.5 + 0.5 as both unpaired electrons now have the same spin) and therefore to a multiplicity of M = 3, a triplet.

1.2.5 Absorption and Excitation [16,17,20]

As mentioned earlier, the orbital's energy is quantised and so is the energy gap between any two orbitals. An electron might be promoted from an orbital of lower energy to one with a higher one (typically an empty orbital) when the exact energy of the gap is applied to the electron and if the promotion follows the selection "rules". These rules are based on models, which approximate, but do not describe 100% accurately, reality, and therefore might be better understood as guidelines, that work most of the time. The spin selection rule states that the total electron spin must not change ($\Delta S = 0$) and that therefore the multiplicity (M = 2S + 1) must not change. So, excitation from singlet to triplet state and *vice versa* is spin forbidden. The orbital symmetry selection rule states, that a transition is more likely, the more similar the wave functions of the initial and the final state are. An example often given to explain this rule is the difference in probability for a π → π* transition, which occurs more likely because both molecular orbitals occupy the same region of space (which leads to a larger overlap of their wave functions) as opposed to n → π* transition, which are perpendicular to one another. Besides the more dominant π → π* and n → π* transition, σ → σ*, σ → π*, π → σ* and n → σ* transitions are theoretically possible.

In photochemistry, the energy to promote an electron comes from a photon, whose energy can be described as:

$$E = h * \nu$$

where h is Planck's constant and ν the frequency of the photon. If the energy of the photon matches the one of the gap, it may be absorbed by and its energy be added to the electron and therefore the molecule as a whole. We say the molecule is in another electronic - an excited - state for which the electronic ground state is called S_0 and the excited singlet states are called S_1, S_2, S_3, … whereas triplet states are called T_1, T_2, T_3, … respectively. Besides the excitation of electronic levels, molecules also have vibrational (dependent on the vibrational quantum number ν) and rotational levels, each of their levels are described by terms and each of them have selection rules for when excitation is allowed to happen from one level to another, which are not discussed here. Each electronic level houses several vibrational levels and each vibrational level houses several rotational levels. Adding those three terms additively gives a term to describe the energy state of a molecule as a whole. The Born-Oppenheimer approximation states, that because of the different magnitude of those three terms, they can approximately be treated individually. For example, excitation may occur from the ground state (S_0, ν_0) to an excited state (S_1, ν_3), conveniently ignoring rotational transitions as the photon's energy needed for rotational transitions is far lower (in the infrared region), whereas transitions of electronic states need photons from the UV/vis region. An electronic state can be visualised by Morse's empirical approach for the anharmonic oscillator - the Morse potential V(r):

$$V(r) = D_e * \left(1 - e^{-\beta(r - r_{equilibrium})}\right)^2$$

where D_e is the dissociation energy in [cm^{-1}], $r_{equilibrium}$ is the equilibrium distance in [cm] of those two atoms in the ground state and β [cm^{-1}] is defined according to the following equation:

$$\beta = \bar{\nu}_0 * \sqrt{\frac{2\pi^2 c\mu}{D_e h}}$$

where $\bar{\nu}_0$ is the wave number by assuming a harmonic oscillator, c is the velocity of light and h is Planck's constant. Furthermore, the vibrational energy levels (actually the vibrational term G, which is the vibrational energy divided by Planck's constant and the velocity of light) of an electronic level can be calculated and added as horizontal lines to the visualisation:

$$G(v) = \bar{\nu}_0 * \left(v + \frac{1}{2}\right) - \bar{\nu}_0 \chi_e * \left(v + \frac{1}{2}\right)^2$$

where χ_e is the anharmonicity constant.

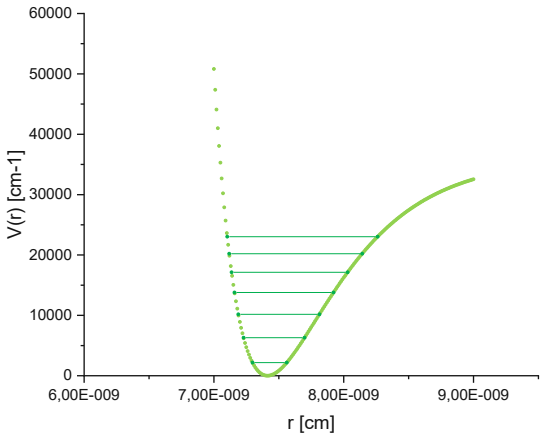

*Figure 4: Morse potential with De = 36000 cm^{-1}, β = 1.9*10^9 cm^{-1}, $r_{equilibrium}$ = 7.4*10^{-9} cm, μ = 8.4*10^{-28} kg, $\bar{\nu}_0$ = 4161 cm, χ_e = 0.03 in light green, and its vibrational levels in dark green.*

If several of those curves were to be applied within the same graphic it would soon become messy. Therefore, a simpler, more schematic way of portraying Morse's potential is done by drawing short horizontal lines in a kind of block-like structure. Each block of lines represents the various vibrational levels (indicated by the vibrational quantum number v) of one electronic state and several of those blocks are qualitatively sorted along the y-axis (E/hc) to indicate their energy gaps. To indicate a transition from one level to another, those two levels are connected with a vertical arrow. This vertical arrow is a consequence of the Frack-Condon principle, which states, that upon photon absorption the elementary particles need time to be accustomed to the new state and that electrons (compared to

protons and neutrons) are a lot faster in doing this due to their lower mass. In the time an electron needs to be promoted, the nuclei of the excited molecule are almost not moving or *de facto* fixated.

1.2.6 Jablonski diagram[16,17,20]

The simplified version of Morse's potential also gives the ability to qualitatively show in which ways the excited state can revert back to the ground state, which is summarised in the Jablonski diagram. The Jablonski diagram typically does, however, not display rotational energy levels.

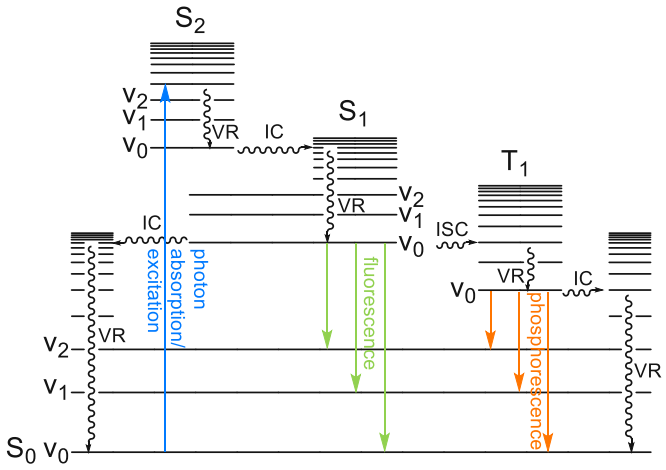

Figure 5: Jablonski diagram redrawn from literature.[17,23]

Vibrational relaxation (VR) occurs from higher vibrational levels to lower ones unless, of course, the excited state after absorption is already at the lowest vibrational level. It is mechanistically explained as a vibrating molecule, which, through collision with surrounding (solvent) molecules, gives off its vibrational energy either by exciting the collision partner or as heat. Kasha's rule states, that because of the relatively fast vibrational relaxation (as opposed to all other events), it is far more likely that vibrational relaxation is the first event happening after excitation and that all follow-up events start from the vibrational ground state (S_x, v_0) of any given electronically excited level. This is also true whenever a higher vibrational level is generated in any follow-up events such as the generation of other singlet or triplet states.

Internal conversion (IC) is a relaxation process, in which two Morse potential curves of different electronic states of the same multiplicity (of the same molecule) overlap in such a way, that two vibrational levels (one of each potential) are energetically close enough for the molecule to convert internally (hence the name) from a higher electronic, but vibrational ground state (e.g. S_{x+1}, v_0) to a lower electronic, but within that a higher vibrational level (e.g. S_x, $v_{y>0}$). This is possible due to the behaviour that the energy gap between electronic levels - in analogy to the energy gap of vibrational

levels in the anharmonic oscillator - gets smaller and smaller the higher the energy level is, ultimately causing them to overlap.

Intersystem crossing (ISC) is a spin-forbidden process, in which similarly to internal conversion, two potentials are overlapping. Here, however, one of the potentials is a triplet state, while the other one is the singlet state that is generated as mentioned in the processes above. While vibrational relaxation occurs, two vibrational levels, one of the singlet and one of the triplet state may be close enough in energy for a singlet-to-triplet transition to occur. The violation of the spin selection rule enabling intersystem crossing may occur due to spin-orbit coupling generally seen for heavy atoms (heavy atom effect).

Phosphorescence is a radiative deactivation process enabled by the spin-forbidden intersystem crossing, in which a singlet to triplet transition occurs. Once the triplet state reached its vibrational ground state *via* vibrational relaxation, a photon can be emitted that matches the energy gap of that triplet state and a lower electronic singlet state, which the molecule enters. If this singlet state is of higher vibrational levels, it will revert back to the electronic and vibrational ground state *via* vibrational relaxation. Fluorescence, on the other hand, is a less complex radiative deactivation, as no intersystem crossing occurs. Once the excited state enters its vibrational ground state a photon might be emitted in a similar way to phosphorescence, reverting the molecule back to its ground state.

1.2.7 Types of photochemical reactions[24]

So far, the Jablonski diagram just showed how a molecule is physically absorbing light and shortly after freeing itself of that excess energy, again by physical means. However, a molecule might not withstand the high energy of its excited state and break apart. Alternatively, a reaction might be triggered, which is where photochemistry starts. Generally, three types of photochemical reactions can be discriminated based on the activation pathway: Direct photoexcitation, photocatalysis and electron-donor-acceptor complex formation (or exciplex/charge-transfer complex formation). All of those have in common that the molecule that is going to react, needs to be activated first. The means of doing so, however, differ.

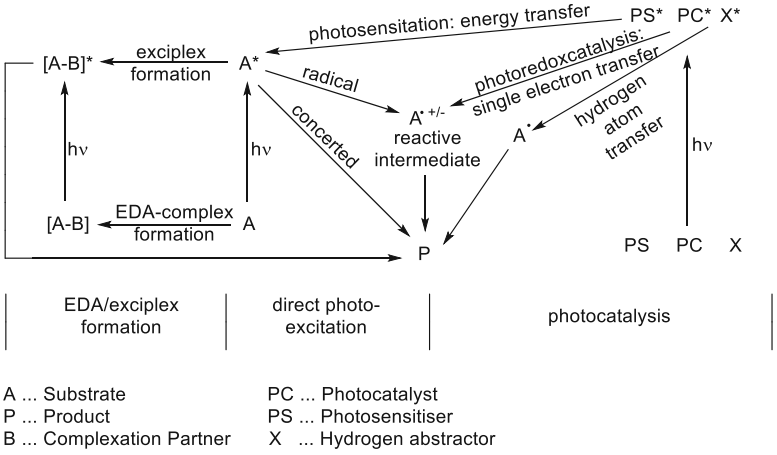

Figure 6: Pathways of the substrate (A) towards the product (P) via different activation strategies.

1.3 Direct photoexcitation[16,17]

The process of exciting a molecule simply by photon absorption directly without any additives, catalysts or photosensitisers is called direct photoexcitation. Once excited, a molecule can either go through a concerted reaction mechanism or it might form reactive intermediates depending on the excitable functional groups present.

As an example of a concerted mechanism, the [4+2] photocycloaddition of benzene (**5**) with N-methyl-1, 2, 3-triazoline-3, 5-dione (**6**) (Scheme 2) yields a valuable intermediate upon visible light irradiation. Compound 7 is crucial for various total syntheses[25] products, such as conduramin A, MK 7607 or 3*O*-desmethyl phomentrioloxin as the double bond formed in the cycloaddition can be further functionalised by e.g. epoxidation, dihydroxylation or hydroboration.

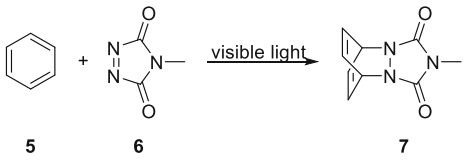

5 **6** **7**

Scheme 2: Example for a concerted, direct photoexcited reaction: [4+2]-cycloaddition.[25]

Photolysis happens in the simple case of σ-bonds breaking homolytically, leading to two radicals. The obtained radicals can further react, for example in photocatalysed polymerisations initiated by azobisisobutyronitrile (AIBN; **8**) (Scheme 3).[26]

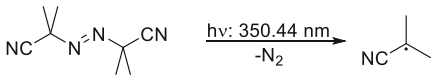

8 **9**

Scheme 3: Example for direct photoexcited photolysis.[26]

A set of famous reactions are the Norrish Type I and Type II reactions that are enabled by the (n→ π*) transition of a carbonyl group. The Norrish-Young cyclisation for example, which can only occur, if there is a hydrogen in γ-position to the carbonyl group, is one possible outcome of the Norrish Type II reactions and played an important role in the total synthesis of the antibiotic punctatin A.[27] Intermediate **10** was irradiated at 253.7 nm to trigger the (n → π*) transition of the carbonyl group, which leads to a diradical **11**, were one electron is in the π* orbital and therefore weakens the C=O double bond. Subsequently, one radical will rip out an electron from the C=O double bond, leading to a tertiary carbon radical on the ring, while the other one will snatch the γ-hydrogen by breaking its σ-bond homolytically. This results again in the formation of a tertiary carbon radical, but this time on the side chain, so that the new biradical **12** is formed. Both radicals, being in proximity and having no better option to be stabilised, will therefore recombine and form a four-membered ring **13** (Scheme 4).[27]

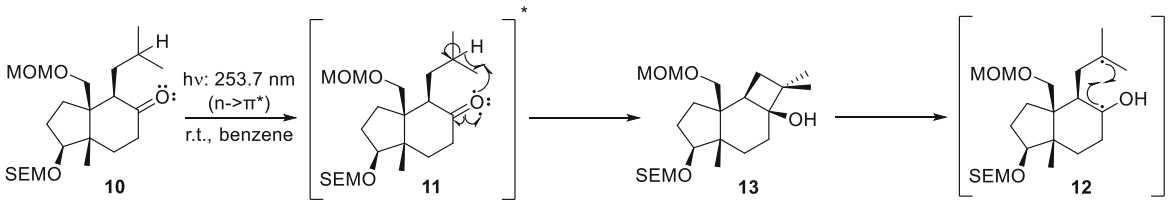

Scheme 4: Example for direct photoexcited (Norrish-Young) cyclisation.[27]

The possible formation of thermodynamically less stable products, for example in the case of isomerisation reactions is considered as one of the advantages of photochemistry. *E*/*Z*-isomerisations of azobenzenes **14** and **15** (Scheme 5), a model substance for photoswitches, are possible, since azobenzenes can be converted from *E* to *Z* isomer and *vice versa* and *via* either an (n → π*) or (π → π*) transition.[28]

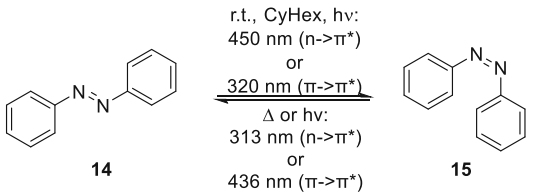

Scheme 5: Example for direct photoexcited isomerisation.[28]

Apart from cyclisation reactions, C-C bond formation is an interesting tool, for example in the case of the alkynylation to quaternary carbons with monosubstituted caesium oxalates **16** and substituted ethynylbenziodoxolanes **17** (Scheme 6). While the mechanism was not confirmed, it is clear that the oxalate needs to undergo a double photoelimination of CO_2 to provide an alkyl radical in order to form the product. As the oxalate was, however, not the light-absorbing species, the ethynylbenziodoxolane fulfils multiple roles: absorbing the light, activating (from the excited state) the oxalate and carrying the alkyne that is transferred. The reaction was mostly limited to tertiary radicals (from the oxalate part) possibly due to preventing rearrangements.[29]

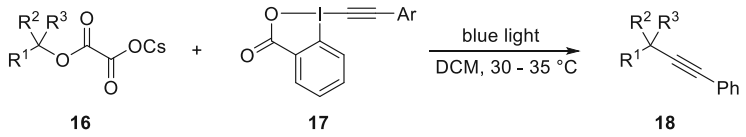

Scheme 6: Example for direct photoexcited C-C bond formation.[29]

1.3.1 Photosensitation, Photoredox Catalysis & Atom Transfer[30–32]

One of the major drawbacks of direct photoexcitation is that not all molecules host appropriate chromophores and that a desirable excited state might simply not form. They might be able to absorb UV light, which leads to photodegradation (breaking of σ-bonds), but that is in most cases an unwanted side reaction that needs to be avoided. For that reason, scientists developed several methods to circumvent these issues which can be discriminated based on activation by: energy transfer, single electron transfer (SET), or atom transfer.

The method based on energy transfer is called photosensitisation as a so-called photosensitiser (PS) is used, which absorbs light instead of the substrate to enter an electronically excited state (typically a triplet state *via* intersystem crossing) and passes its energy (energy transfer EnT) to the substrate and therefore excites it (Scheme 7, left). Photosensitisers are typically used to generate the more reactive singlet oxygen, to enable isomerisation reactions or to enable thermally forbidden cycloadditions. A good example is the intramolecular [2+2] cycloaddition published by Cibulka[33] *et al.* for which an alloxazine derivative **19** was fine-tuned in terms of absorption maxima and solubility, and further excited to its triplet state to sensitise various (non-conjugated) dienes **20** (Scheme 7). Interestingly, the (faster) *E*/*Z*-isomerisation occurred simultaneously, which did not seem to hinder the cycloaddition.

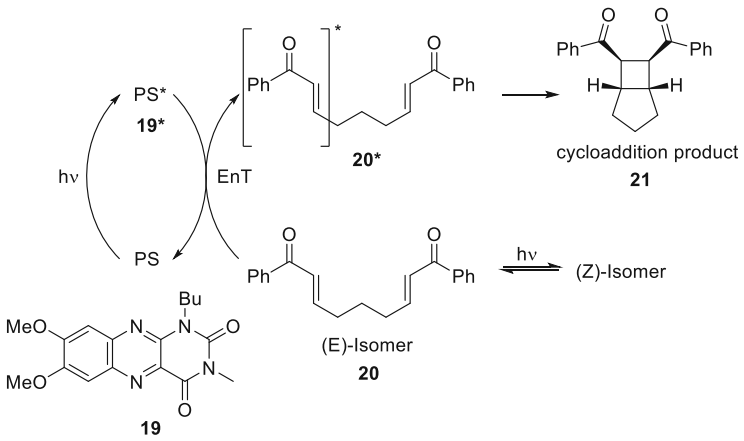

Scheme 7: Cycloaddition reaction by photosensitisation/energy transfer.

Similarly to photosensitisation, photocatalysis relies on excited photocatalysts (PC*) for substrate activation, which, unlike with energy transfer for PS, is triggered by SET. The SET depends on the redox properties of both the substrate and the PC. The whole process is, therefore, more specifically called photoredox catalysis as opposed to the broader term photocatalysis which eventually might also include photosensitisers and photocatalysts used in atom transfer reactions. Typically, the reductive potentials E_{Red} are used, which are written in the reductions' direction from the oxidised to the reduced form of a species Sp of oxidation state OxSt, like:

$$Sp^{OxSt}/Sp^{OxSt-z} = E_{Red}\,[V]$$

E_{Red} might be negative or positive. The higher the value of E_{Red} the more easily it is reduced, whereas the more negative it is, the more easily it is oxidised. To determine whether a redox reaction will take place one can use the change in Gibb's free energy[17]

$$\Delta G = -zFE$$

which is negative if E is positive; thus the reaction is spontaneous. The number of exchanged electrons is z (always positive), F the Faraday constant (96485 C/mol) and E the sum of the two reductive potentials.

In the simplest case, photo(-redox) catalysis can be subdivided into an "oxidative quenching" and a "reductive quenching" route (Scheme 8). Either mechanism might be extended with a co-catalytic cycle, which is then called synergistic photoredox catalysis.

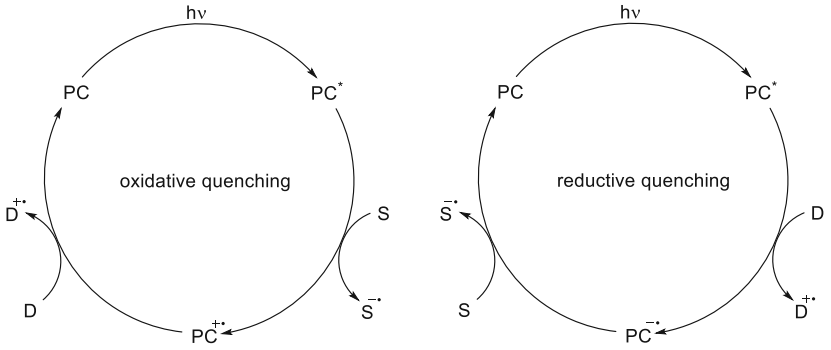

Scheme 8: Oxidative and reductive quenching in comparison

In the case of oxidative quenching, the photocatalyst (PC) harnesses the light's energy to enter an excited state (PC*), from where it transfers a single electron (SET process) to the substrate (S). The PC is later recovered by a subsequent reduction with a sacrificial donor (D). The opposite happens in the reductive quenching cycle: After excitation, PC* takes an electron from the donor first to then pass it on to the substrate. The aim of the photocatalyst is not necessarily to increase the reaction's speed, but to activate the target molecule.[32] The "catalysis" part indicates, that the PC is not needed in stoichiometric amounts; however, such reactions can still involve stoichiometrically used sacrificial reagents. Despite earlier development, it were the groups of MacMillan[34], Yoon[35] and Stephenson[36] that reignited the interest in photoredox catalysis. As an example of a reductive quenching, the catalytic cycle of a photoredox [2+2] cycloaddition can be seen in Scheme 9. The PC, a tris(2,2'-bipyridine)ruthenium(II) dichloride (**22**), absorbs a photon and gets excited. From there a SET from diisopropylethylamine (**23**) - a sacrificial donor - to the PC occurs, which leads to a subsequent SET from the PC to the diene substrate **Li$^+$-20**, affording the cycloaddition product **21**. Substrate and product are the same as for the example for photosensitisation (Scheme 7; **20**, **21**) showing that the same products might indeed be accessible by different photochemical activation modes.

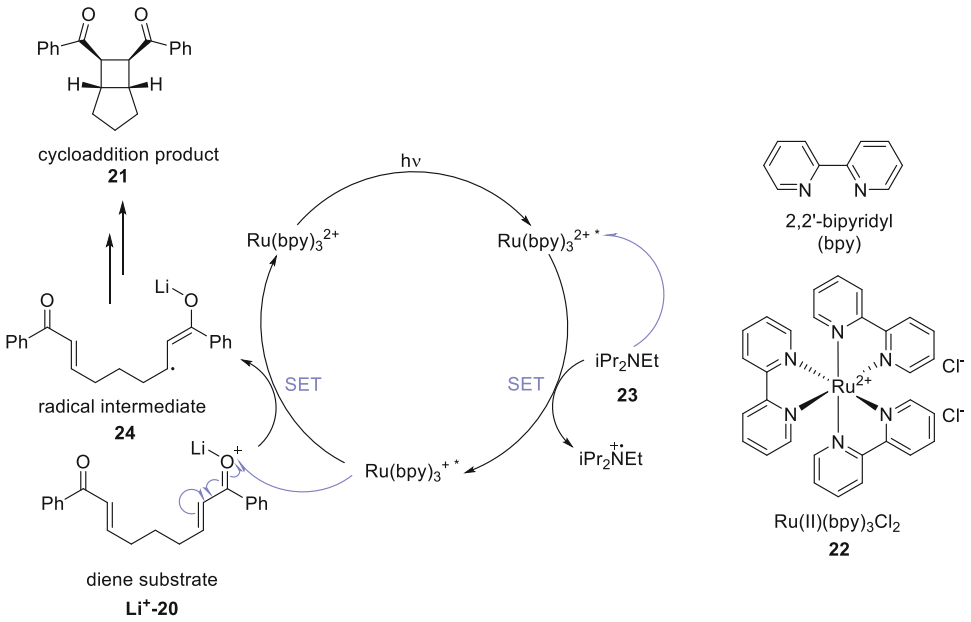

Scheme 9: Cycloaddition by reductive quenching photoredox catalysis.[35]

MacMillan's group reported an interesting example of asymmetric α-alkylation of aldehydes using Ru/enamine synergistic photoredox catalysis (Scheme 10). The reductive quenching of $Ru(bpy)_3^{2+}$ (**22**) by a chiral enamine species **30** afforded the Ru(I) species. This, in turn, initiated the homolytic cleavage of reagent **25**, and the resulting alkyl radical **26** was trapped by a ground-state enamine species **29**, affording the product **32**.

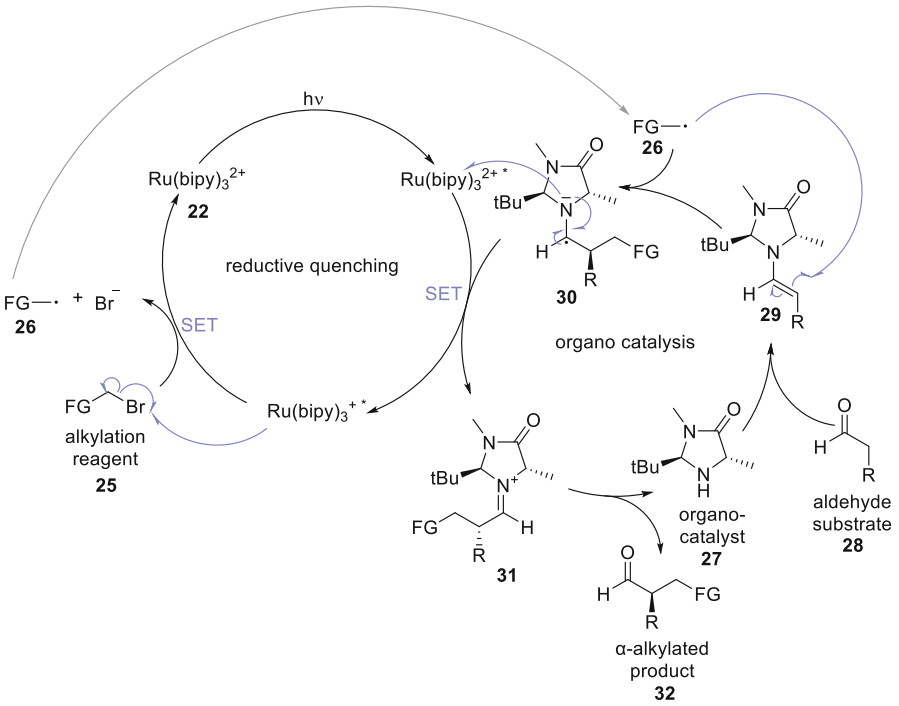

Scheme 10: α-Alkylation of aldehydes as an example of synergistic photoredox catalysis.[34]

Pioneered by Stephenson,[36] the field of hydrogen atom transfer (HAT) also provides a very efficient method for photochemical functionalisation. A HAT occurs between a hydrogen donor H-D and a hydrogen abstractor radical X.

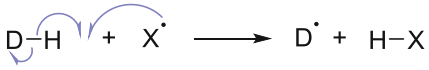

Scheme 11: Hydrogen atom transfer.

Depending on whether the PC is directly used as a hydrogen abstractor, one can talk about direct (dHAT) and indirect (iHAT) processes. One important example was published by Wu *et al*. using Eosin Y as a hydrogen abstractor for various sp^2-functionalisations of aldehydes, ethers and other "C-H" species.[37] Upon excitation, Eosin Y aromatises so that the two radicals initially generated are then locally separated. The alkoxyl radical is then able to abstract hydrogen of the donor - THF (**34**) in this case - which undergoes radical addition to the substrate. Meanwhile, the PC (eosin Y)-H becomes a mono radical and carries the hydrogen, which enables the PC to act as a hydrogen donor in a reverse HAT (RHAT) to the newly formed radical addition product **37**, therefore regenerating the PC and forming the final product **38** (Scheme 12).

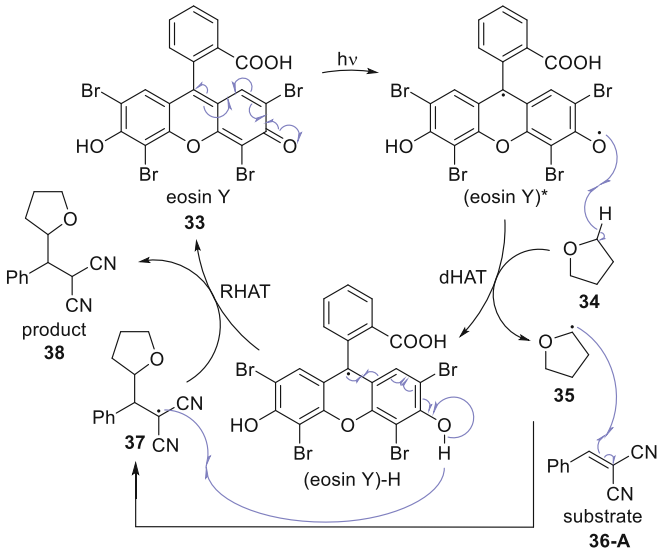

Scheme 12: Example of dHAT in an hydroalkylation reaction. [37]

1.3.2 Electron donor-acceptor complexes and exciplexes[24,38]

The third type of photochemical reactions is that of electron donor-acceptor (EDA) complexes and exciplexes, which are grouped together due to their similarity. EDA complexes rely on the formation of complexes from an electron-rich donor and an electron-poor acceptor molecule. The formed complex is able to absorb light in a different region than the donor or acceptor alone, which is usually

accompanied by a visible colour change upon the formation of the EDA complex. By absorption of light in this new absorption band, a single electron transfer (SET) from the donor to the acceptor can occur leading to a radical ion pair. From there, back electron transfer (BET) is highly likely due to the high reactivity of the radical ion pair, unless a leaving group (LG) is irreversibly cleaved to generate the final radical that participates in the following reactions.

While the assembly of the complex occurs first for EDA and the radical formation is triggered afterwards *via* light absorption, the opposite is true for exciplexes. In this case, the donor is excited first, and only when excited the complex formation with the acceptor is possible, which will then trigger radical formation (Scheme 13).

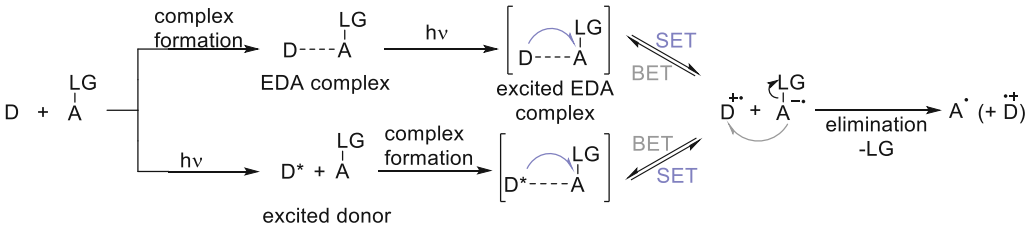

Scheme 13: Comparison of EDA complex and exciplex formation.

One of the most prominent examples of EDA complex formation used in organic synthesis is the α-alkylation/benzylation of aldehydes with brominated reactants from Melchiorre's group.[37] Scheme 14 shows the mechanism of one such reaction. The *in situ* formed enamine species **41** forms an EDA complex **43** with the extremely electron-poor brominated reagent **42**. Visible-light absorption of this complex generates the alkyl radical, which adds to the enamine, affording the benzylated product **46**.

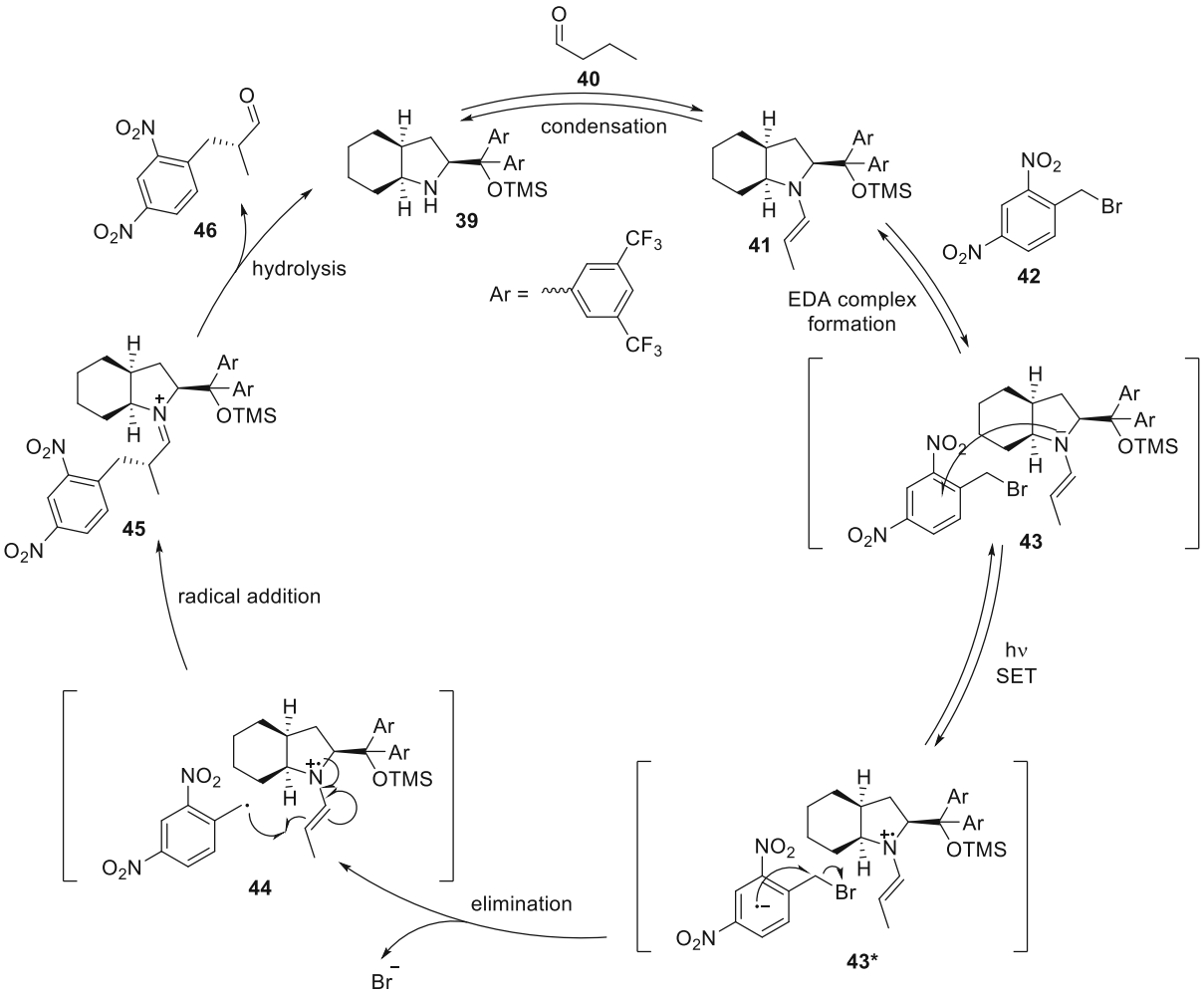

Scheme 14: Benzylation as an example of activation via EDA complex formation.[37]

1.4 Instrumentation and set-up[17,39,40]

Now that the basics of photochemistry were covered and its three groups of photochemical reactions were introduced, more practical questions can be asked. Specifically, how to set those reactions up in a way to obtain meaningful, reproducible results.

1.4.1 Wavelength and light sources

The most obvious thing to keep in mind is the wavelength-dependence of the absorbing species. As discussed earlier, the energy gap between different electronic and vibrational states is quantised; however, in organic molecules these transitions are so close that they start to "overlap". The absorption (or emission) spectrum therefore contains bands with one or more local maxima of which one will have been identified by analytical/methodological studies to trigger the photochemical reaction.

When planning a photochemical reaction, one needs to make sure that no back-reactions, side reactions or decomposition take place.

Keeping this in mind, light sources with a broader emission band can be used in exploratory experiments to test whether a photochemical reaction takes place or not, while light sources with a narrow emission band are used for selective activation, reducing the risk of triggered side reactions.

The continuous spectrum of the sun, whose intensity, based on the inverse-square law, is far too low for most photochemical reactions to finish in a reasonable time frame; thus, it needs to be simulated. Most "continuous" light sources consist of broad emission bands interrupted with low "baseline intensity" gaps. For example, the spectrum of the high-pressure mercury lamp[41] covers mostly the UV region with some dominant peaks in the violet and blue spectrum of visible light. On the other hand, apart from some peaks in the infrared region, the xenon lamps spectrum in the visible light region is roughly equally distributed. A mercury-xenon lamp[42] combines properties of both, the xenon and the mercury lamp: a stable baseline output in the visible spectrum as well as higher intensities in and at the border to the UV region. In any case, the intensity of the mercury, xenon or mercury-xenon lamp is too high and needs to be reduced with filters, by which undesired wavelengths can also be faded out. Other light sources with continuous emission spectra are the tungsten halogen lamp[43] (covering the visible, near-infrared and to some extent short wavelength infrared spectrum), deuterium lamps[44] (covering near and middle ultraviolet spectrum) and compact fluorescent lamps (CFLs), having their main emission bands in the visible light range[45] (487.7 nm, 546.5 nm, and a more continuous band from roughly 600 nm to 631.1 nm).

The low-pressure mercury lamp[46] is the more selective counterpart to its high-pressure variant and has a very strong emission peak at 253.7 nm amongst a few smaller ones. Light-emitting diodes (LEDs) are

a more practicable light source and are preferentially used in photochemical transformations. Although each LED peak is broader than that of any individual peak from the mercury/xenon lamps, the emission spectrum is limited to a much narrower wavelength region (+/− 10 nm) so they end up being more selective.[47] LEDs are available for various wavelengths, however, there is the issue of green-gap[48], which significantly reduces the efficiency of green and yellow LEDs. Similarly and specifically for the UV region, excimer lamps can emit within a narrow wavelength region depending on the materials used for the gas discharge lamp and can range from 108 nm (NeF) to 351 nm (XeF).[49] An example of an excimer lamp with 222 nm (KrCl) is shown in the bottom right graph of Figure 5.

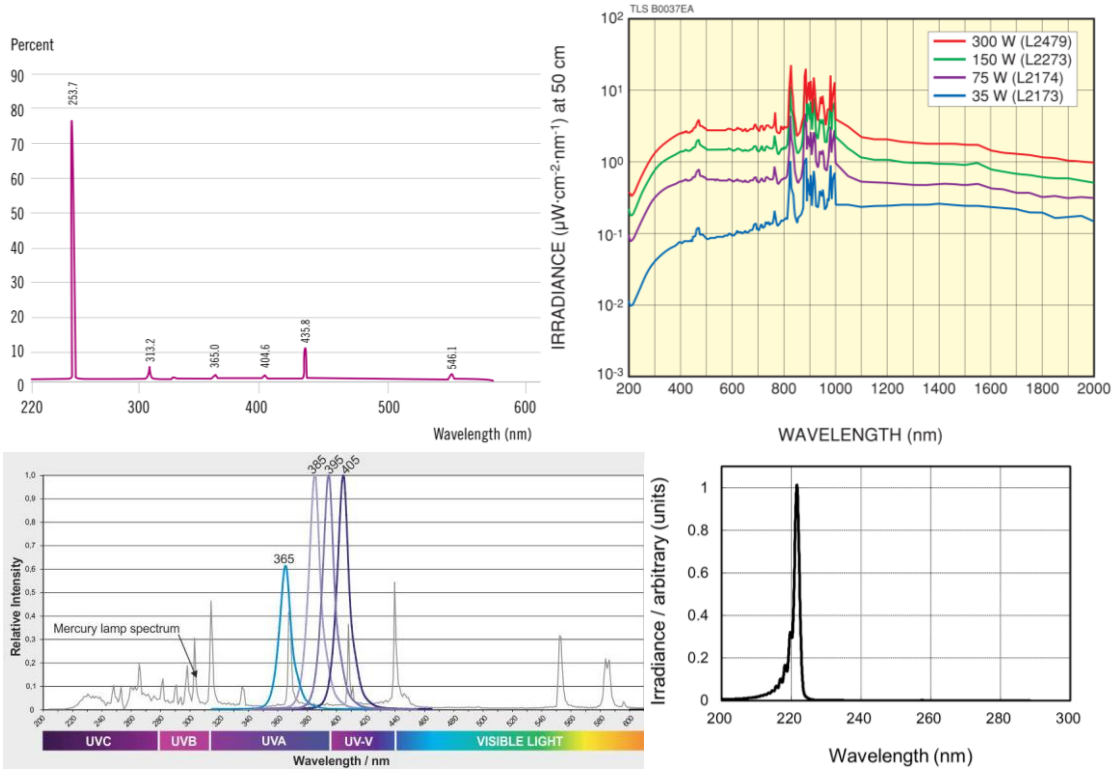

Figure 7: Examples of emission spectra of a low-pressure mercury lamp[46] (top left), xenon lamp[42] (top right), different LEDs[47] (bottom left) and a KrCl excimer lamp[48] (bottom right).

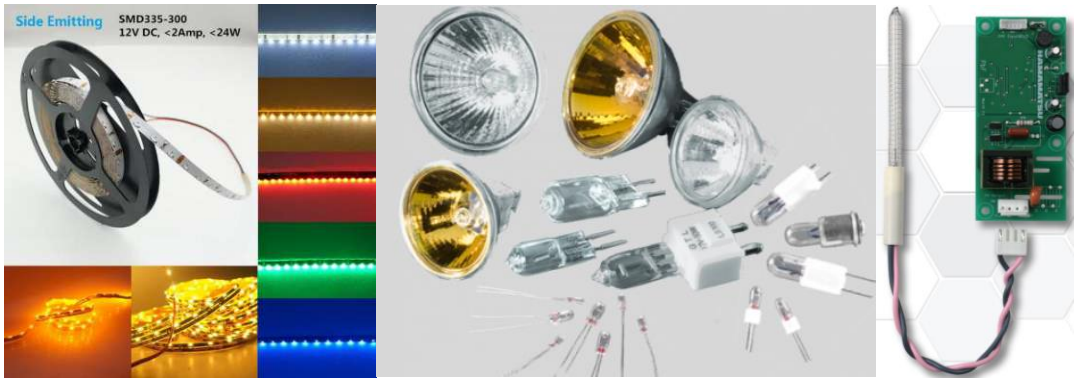

Figure 8: Different LED strips (left; picture taken from supplier: LEDLightsworld[50]), tungsten-halogen lamps in different sizes and shapes (middle; picture taken from supplier: InternationalLight[51]), and a small excimer lamp (right; picture taken from supplier's product catalogue[52]).

Apart from choosing the proper light source, the reaction vessel should be also properly chosen as it should be transparent to the chosen wavelength. For most photochemical transformations, simple borosilicate glassware is suitable: The transmittance of a typical DURAN® borosilicate glass is roughly 85 - 90% between 340 nm and 2000 nm.[53] Nevertheless, both borosilicate and "normal" silicate have significant light absorption in the far UV region, meaning that these transformations (<280 nm) always require quartz or light-transmitting polymer reaction vessels.

1.4.2 Light intensity

The light intensity is the next important factor: If the intensity drops to zero, no reaction takes place (Grotthuss-Draper law) and higher intensities (=more photons) can excite more molecules (Stark-Einstein law). It is possible to oversaturate the reaction mixture with photons: For example, if PCs are used, the excess energy of the photons might cause unwanted side reactions. The intensity (I) from a light source (of power S) depends on the distance (r) from the light source according to inverse-square law:

$$I = \frac{S}{4\pi r^2}$$

Borosilicate glass walls do not have 100% transmittance. The transmittance (T) is defined as the quotient of intensity (I) and the initial intensity (I_0). The initial intensity will be the intensity left over from the inverse-square law above.

$$T = \frac{I}{I_0}$$

The intensity is therefore:

$$I = T * I_0$$

Eventually, the intensity drop within a solution is described by Lambert-Beer's law:

$$A = \lg\left(\frac{1}{T}\right) = lg\left(\frac{I_0}{I}\right) = c * d * \varepsilon$$

Here, the absorption (A) equals the product of the concentration (c) of the solution, the distance (d) in centimetres the light travelled through the solution and the decadic molar extinction coefficient (ε). Figure 7 shows the intensity drop based on the distance the light travelled for a source of power S = 45 W, a concentration of c = 0.0099957 mol/L and a decadic molar extinction coefficient of $\varepsilon_{HE@460nm}$ = 49.22 L/mol*cm when the light source has a distance of r = 2 cm from the reaction vessel's walls.

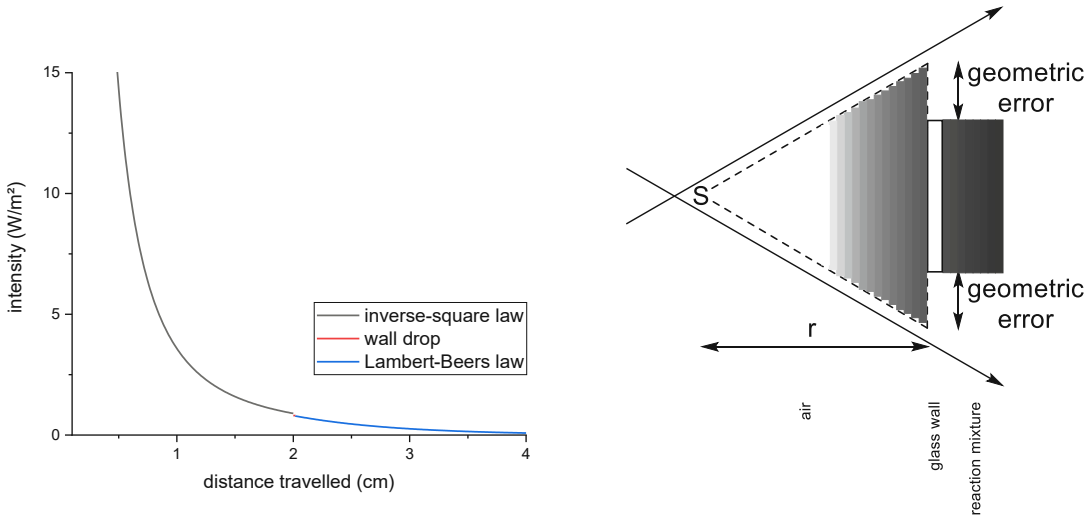

Figure 9: Intensity drop according to the inverse-square law, the "wall drop" due to transmittance and Lambert-Beer's law in solution over the distance travelled (left) and a visual representation, in which the brightness was decreased according to the left graph (brightness fixated for the first centimetre; each column represents 0.1cm).

1.4.3 Quantum yield[17]

Quantum yield is "*a measure of how efficiently the absorbed photons are utilized.*"[17] If a number of photons are absorbed, the respective excited molecules might either deactivate physically (leading to no reaction) or chemically (leading to a reaction).

Primary quantum yield is a measure of how likely the primary process of a reaction is compared to other deactivation processes and is defined as the number of bonds broken per photons absorbed and can therefore be at maximum equal to one.

$$\Phi_{prim.} = \frac{number\ of\ bonds\ broken}{number\ of\ photons\ absorbed}$$

The overall quantum yield on the other hand bases the conversion of the substrate on the absorbed photons by the substrate:

$$\Phi_{overall} = \frac{number\ of\ reactant\ molecules\ consumed}{number\ of\ photons\ absorbed\ by\ reactant}$$

Radical reactions proceeding *via* chain mechanism mostly have a quantum yield above one. Meanwhile, overall quantum yields below one might suggest that no chain mechanism is operative. Nevertheless, a quantum yield below one itself can also correspond to a reaction with a chain mechanism, whose photocatalytic activation is slow/inefficient.

1.4.4 Temperature

Irradiating the reaction mixture always results in heating. In order to prove that the reaction is only triggered photochemically and not *via* thermal activation, cooling is required to keep the temperature constant. Furthermore, lower temperatures reduce the possibility of thermal side reactions.

1.4.5 Impurities

As always, impurities that hinder or even quench a reaction need to be removed or avoided. In the case of photochemistry, where radical intermediates are often formed, this means that the diradical oxygen needs to be excluded and working under an inert atmosphere is recommended. Using anhydrous solvents to exclude water might be a good idea; however, they may still include oxygen, thus further pre-treatment with the freeze-pump-thaw technique might be necessary.

1.5 Introduction to Acylation and Hydroacylation

Acetylations, one of the most common forms of acylation, were known since at least the middle of the 19th century.[54] A typical acetylation example is given by the first synthesis of acetylsalicylic acid in 1853,[55] in which two functional groups, the nucleophilic alcohol group on the sodium salicylate (**47**) and the electrophilic carboxyl chloride group on the acetyl chloride (**48**), were reacted in a condensation reaction to yield sodium acetylsalicylate (**49**) (Scheme 15). It is worth mentioning, that Gerhardt was not able to isolate it, as just silver salicylate was obtained after work-up. Nevertheless, it serves as a first example of two polar groups reacting with each other.

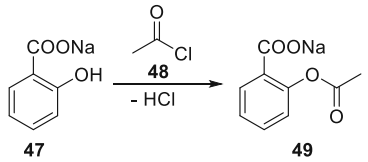

Scheme 15: Acetylation: First documented attempt to synthesise acetylsalicylic acid.[55]

Friedel and Crafts were[55] able to perform an acylation reaction in 1877 in which the aromatic substrate did not need any functional group. The activation of the reagent benzoyl chloride (**50**) with aluminium chloride was strong enough for the electrophilic aromatic substitution to take place (Scheme 16).

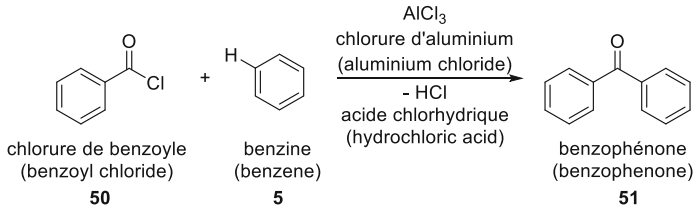

Scheme 16: Friedel-Crafts acylation.[55]

Three types of hydroacylations can be distinguished: Free radical hydroacylation, metal-catalysed hydroacylation and organocatalyzed hydroacylation.[56]

The first hydroacylations were a series of free radical hydroacylations, which were performed in 1948.[57] Scheme 17 shows the reaction of 1-octene (**52**) and heptanal (**53**), which were reacted under inert atmosphere at 70 °C (due to the lamps heating) to yield 23% of 7-pentadecanone (**54**).

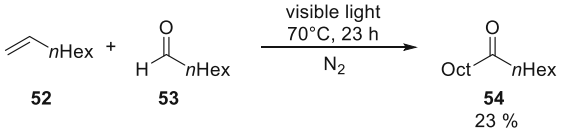

Scheme 17: Radical hydroacylation: Photochemical example from the first set of hydroacylations.[57]

24 years later, in 1972, the metal-catalysed hydroacylation was reported by the group of Sakai,[58] who used Wilkinson's catalyst (**55**) for an intramolecular cyclisation of γ,δ-unsaturated aldehydes **56** towards cyclopentanone derivatives **57** with up to 34% yield.

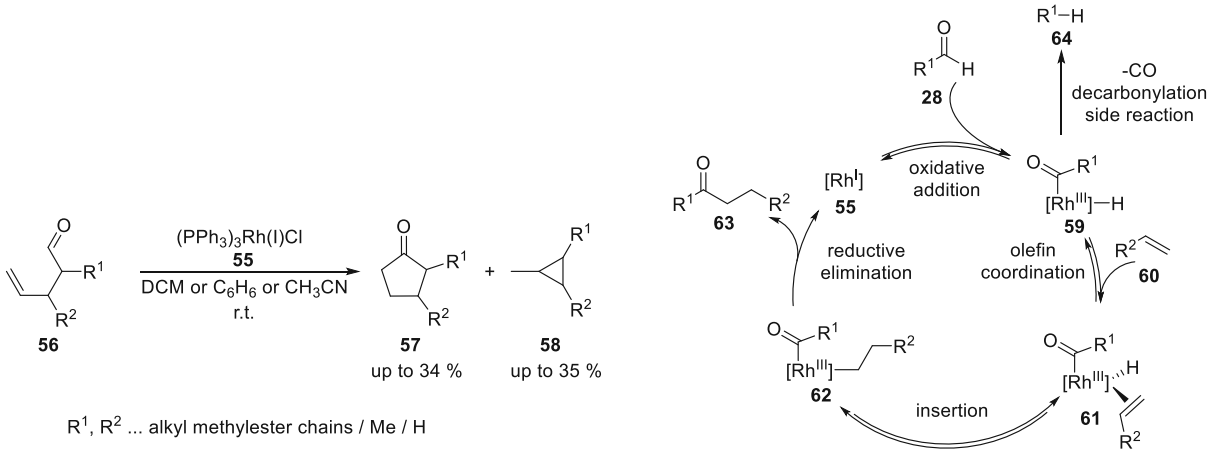

Scheme 18: First metal catalysed hydroacylation reactions with the reaction scheme (left) and mechanism (right).[58]

The mechanism starts with the oxidative addition of aldehyde **28** / **56** to the catalyst **55**, followed by the coordination of alkene substrate **60** / **56**, which then inserts between the Rh-H bond. The cycle is completed with the reductive elimination of the acyl group with the alkyl group from **62** to yield the ketone product **63**. Decarbonylation to alkane **64** can occur as a side reaction after oxidative addition. As to be expected, the catalyst evolved by using different strategies and ligands to prevent decarbonylation, to improve regio- and stereoselectivity and to control intra- *vs.* intermolecular reaction pathway.[59] Additionally, methods with other transition metals than rhodium were developed.[60]

As for the first organocatalytic hydroacylation in 1976, Stetter[61] reported a thiamine NHC-catalysed, modified benzoin-condensation strategy, which enabled the hydroacylation with aldehyde species (Scheme 19).

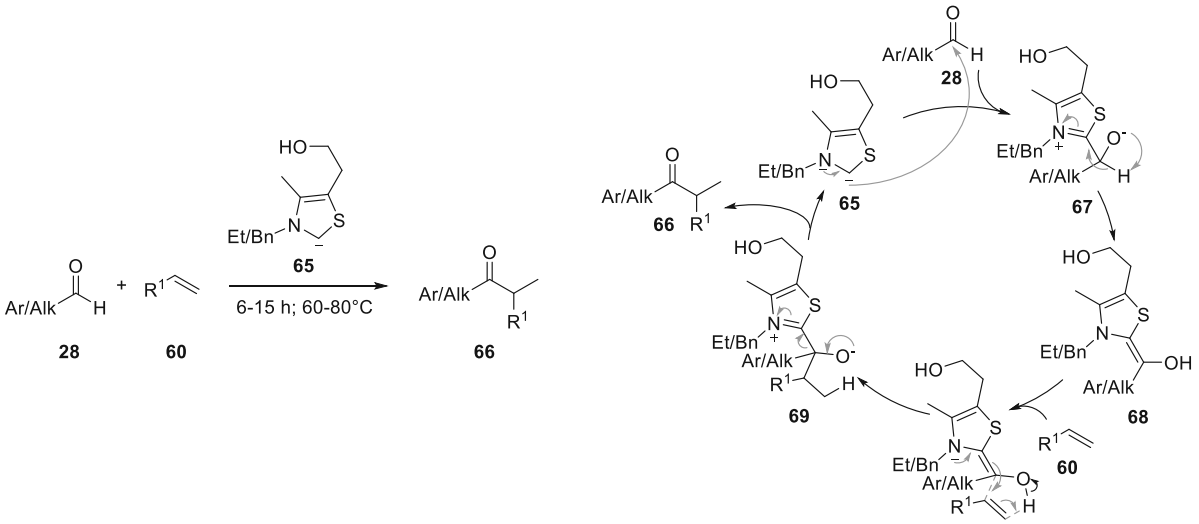

Scheme 19: Stetter reaction: First organocatalytic hydroacylation with the reaction scheme (left) and the mechanism (right).

Even though the catalyst has evolved over time, mechanistically the core principle remains the same.[62] In the first step the NHC **65** attacks the carbonyl **28** upon which the generated negatively charged oxygen abstracts the (formerly) aldehyde hydrogen and a carbene (stabilised *via* the ylidene-form **68**) is re-generated. If the alkene substrate **60** is in proximity, the nitrogen can activate the ylidene to attack the double bond, which in turn takes the O-H hydrogen, leaving the oxygen on intermediate **69** negatively charged. A subsequent elimination step regenerates the catalyst **65** and sets the product **66** free.

1.6 Free Radical Hydroacylations

The first intramolecular radical hydroacylation was reported in 1972 by Čeković, who used AIBN to activate tributyl tin hydride as tributyl tin radical, which in turn abstracts the chloride from the citronelloyl chloride (**70**) to trigger the cyclisation reaction. For product formation, the hydrogen of another tributyl tin hydride is abstracted and the cycle begins again (Scheme 20). Menthone (**71**) was obtained in 43% yield and the decarboxylation by-product **72** in 27% yield.[63] The principle of Čekovićs synthesis - the *in situ* generation of acyl radicals from R-C(O)-X precursors - can be adapted as in the case of using seleno esters (X = SPh).

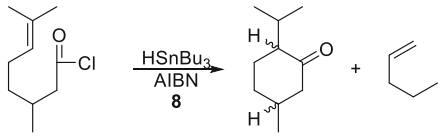

70 **71** 43% **72** 27%

Scheme 20: First intramolecular radical hydroacylation.[63]

Bachi and Bosch adapted the seleno carbonate part in 1986[64] for an intramolecular hydroesterification, and soon later Boger and Mathvink followed up with the intra-[65] and intermolecular[66] hydroacylation. From a 2022 point of view, both methods suffer from the same disadvantage: the stoichiometric use of toxic tin reagents. Nevertheless, such procedures resulted in improved yields of the intermolecular hydroacylation to 60-70% (still dependent on electron-poor alkenes) and the intramolecular one to 70-90%. At the same time (1988) a similar reaction was published by Delduc, Tailhan and Zard. This procedure relied on *O*-ethyl xanthogenates on the substrate (X = S-C(S)-OEt) for a photochemical degradation to acyl radicals and yields up to 70% cyclised product;[67] however, because of decarbonylation reactions this method also resulted in the formation of alkyl radicals.

In 1984, Gottschalk and Neckers[68] performed a hydroacylation/cyclisation reaction using a new photoinitiator (*tert*-butyl-*p*-benzoylperbenzoate). They showed that the radical intermediate **76** can be further utilised synthetically (cyclisation to **77**) after acyl addition to a double bond before hydrogen abstraction from the next aldehyde gives the product **78** (Scheme 21).

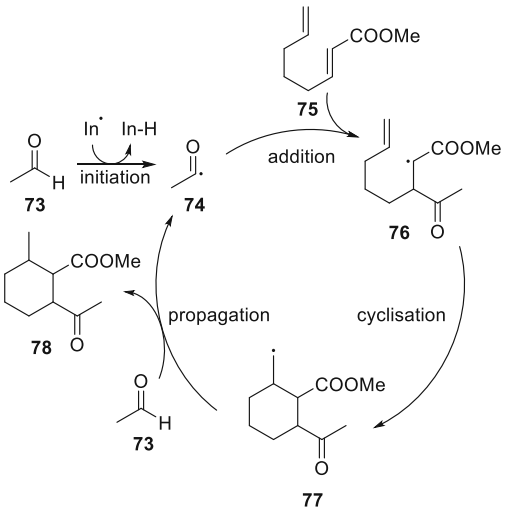

Scheme 21: Combining hydroacylation with a cyclisation reaction.

One of the major breakthroughs was the adaptation of polarity-reversal catalysis, from hydrosilylation[69] to hydroacylation[70] in 1996 by Dang and Roberts. A general mechanism can be seen in Scheme 22. After thermal or photochemical cleavage of a proper initiator the generated initiator radical (In*) can abstract a hydrogen atom from the polarity-reversal catalyst (PRC-H), therefore initiating the radical chain addition and generating the PRC radical, which will then abstract aldehyde hydrogen **28**. The generated acyl radical **79** will add to the substrate's **80** multiple bond, leaving a radical (generally) on the higher substituted side of the former alkene **81**. After the abstraction of hydrogen from PRC-H product **82** is formed and the catalyst regenerated. As seen in the upper part of Scheme 22, an alternative initiation route exists.

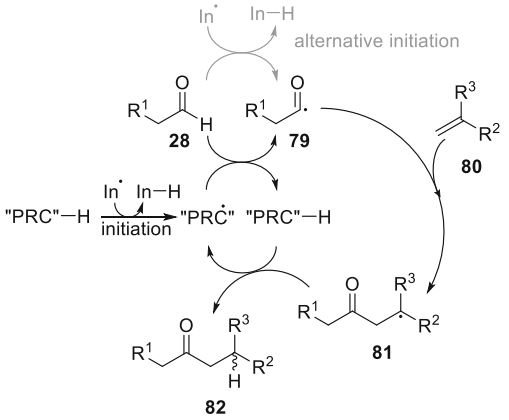

Scheme 22: General mechanism of PRC-catalysed hydroacylation.

Interestingly, Roberts' reaction works - by design - best with electron-rich alkene substrates, something that was not possible until then. He later (1998[71]) found a workaround by using different thiol catalysts for electron-rich, electron-poor and to be cyclised alkenes, leading to good yields. Furthermore, in 1999[72] he published a review to explain polarity-reversal catalysis, focusing on the core problem with radical chain addition reactions for hydroacylation, i.e. the hydrogen abstraction of the aldehyde-

alkene-adduct radical **81** from the next aldehyde **28.** The reason is that both the acyl radical **79** formed from hydrogen abstraction and the adduct radical **81** are nucleophilic. To use an analogy, a comparable problem would be observed when performing an acid-base reaction by using a strong acid with a very weak base. A very slow reaction, if one at all, would be expected. So, having one nucleophilic radical generate another nucleophilic radical creates a mismatch scenario due to polarity effects. The same is obviously true for electrophilic radicals. A favourable match would be obtained by a nucleophilic radical generating an electrophilic one and *vice versa*. Their solution to this problem was to use electrophilic thiol radicals as a hydrogen shuttle from the aldehyde to the adduct. Because the mismatch scenarios reaction was so slow, using two fast reaction steps – hydrogen from aldehyde **28** to thiol radical (PRC*) and then from thiol (PRC-H) to adduct radical **81** – resulted in an overall faster reaction and higher yields.

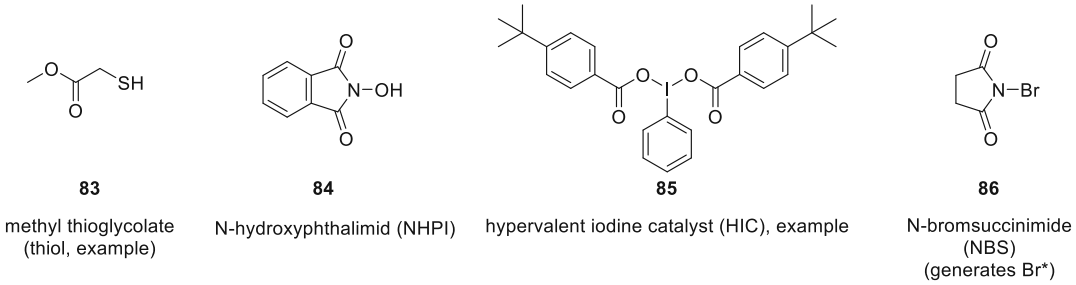

Figure 10: Examples of different kinds of polarity reversal catalysts.

Since the first application of thiols, other polarity-reversal catalysts including *N*-hydroxyphthalimide (**84**),[73] hypervalent iodine (III)-species (HIC) like **85**,[74] *N*-bromosuccinimide[75] and phenylglyoxals[76] were reported as effective initiators for PRC reactions. Despite some nuanced mechanistic differences, they work similarly enough to justify not showing the whole individual mechanisms for each; however, the alternative activation route for hypervalent iodine and for phenylglyoxal/water is shown below in Scheme 23 and Scheme 24.

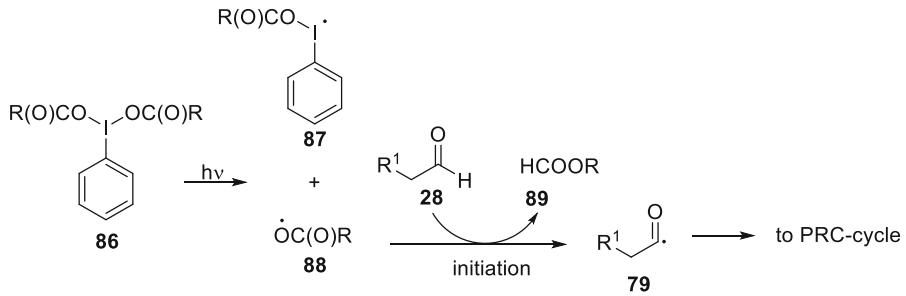

Scheme 23: Initiation route with HIC.

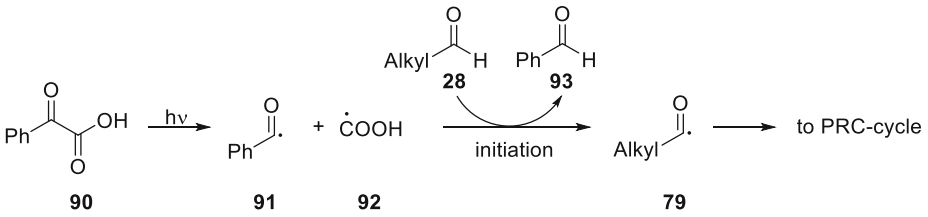

Scheme 24: Initiation route with phenylglyoxal/water.

For the HIC route (Scheme 23), the iodine-oxygen bond is cleaved photolytically and the so-formed ester radical **88** initiates the reaction while the other one serves as PRC. In the case of phenylglyoxal/water (Scheme 24), phenylglyoxal (**90**) is also cleaved homolytically to generate two radicals. The benzoyl radical (**91**) will counter-intuitively (since the benzoyl radical is the more stabilised one) abstract the aldehyde hydrogen from the aliphatic aldehydes **28** and therefore initiate the reaction. Following the alternative initiation in Scheme 22, the adduct radical **81** will abstract hydrogen from water after addition to the alkene **80**, thus generating hydroxyl radicals, which serve as PRC.

An example of hydroacylations that are not limited to carbon-carbon multiple bonds is given in Scheme 25. Zhang and co-workers found a method to perform a hydroacylation on an azo-compund in 2010.[77] The concept was limited to strong electron-withdrawing, azodicarboxylate-type substrates. Interestingly, the reaction was performed solely with water as solvent at room temperature and yields up to 97%; however, the reaction may take between 3 h and up to 360 h depending on R_1.

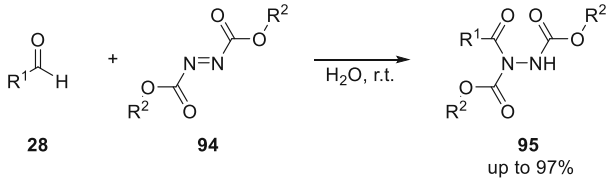

Scheme 25: Hydroacylation of a nitrogen double bond.

2 Aim of the thesis

This thesis aimed to use 4-acyl Hantzsch ester derivatives as radical reservoirs for hydroacylation of electron-withdrawing substrates, preferentially in a photocatalyst- and additive-free fashion. In order to understand the aim of this thesis, we need to take a look at some recent publications, which go beyond free radical hydroacylation: In 2019 there were two publications reported, which each dealt with benzothiazoline as both an alkyl radical and an acyl radical generating compound. In both cases, electron-poor benzylidenemalononitrile and derivatives were used as substrates. However, the method of how a catalytic cycle was sustained and how the alkyl/acyl radical was generated differed.

Akiyama and co-workers[78] utilised tris(2,2'-bipyridine)ruthenium(II) dichloride (**22**) as a photoredox catalyst (Scheme 26). The reductive quenching of the PC initiated the aromatisation of the benzothiazoline species **97** to **98**, releasing the alkyl/acyl radical **99**, which was then added to an electron-poor double bond **36** to afford the product **102**.

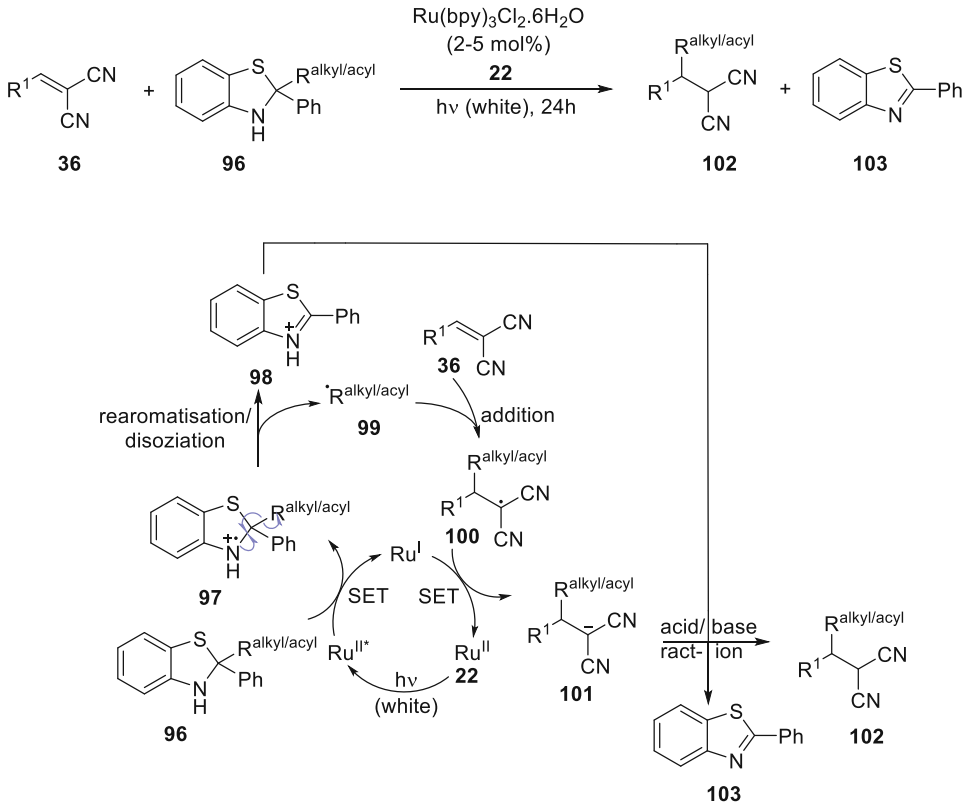

Scheme 26: Reaction scheme (top) and mechanism (bottom) of the photoredox catalysed hydroalkylation/hydroacylation utilising benzothiazoline.[78]

On the other hand, Zhu and co-workers[79] used hydroxybenziodoxolone (**105**), which underwent condensation with the acyl-carrying benzothiazoline **104** to generate a photolabile nitrogen-iodine bond (species **106**). After homolytic cleavage, the unstable benzothiazoline radical **107** expelled the acyl radical **79** - again due to the aromatisation as the driving force - which was added to the benzylidenemalononitrile substrate **36**. The radical adduct **109** abstracted a hydrogen atom from the

next acyl-carrying benzothiazoline **104** to both form the product **110** and propagate a new iteration of the radical chain addition reaction (Scheme 27).

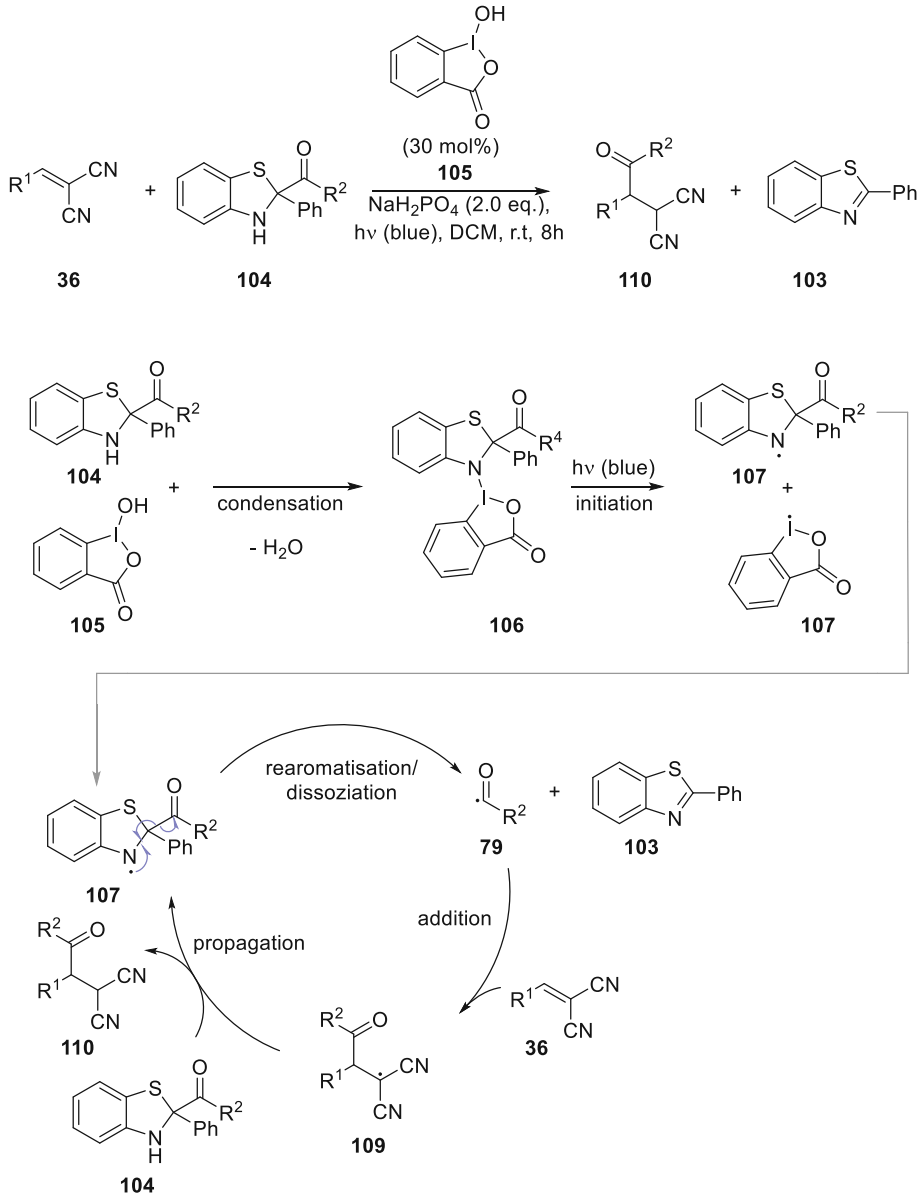

Scheme 27: Reaction scheme (top) and mechanism (bottom) of the hydroxybenziodoxolone catalysed hydroacylation utilising benzothiazoline.

As such, these methods required either a photocatalyst or a stoichiometrically used reagent for the hydroacylation to take place. Apart from benzothiazolines, so-called Hantzsch esters (HE) (2,6-dimethyl-3,5-dicarboxylethylester-1,4-dihydropyridine) work by the same principle, *i.e.* the aromatisation as driving force to split an alkyl/acyl radical. Originally used as a functional mimic of NADH as a hydride donor, Hantzsch esters were often used as reagent in asymmetric transfer hydrogenations.[80] Moreover, 4-substituted HE species turned out to be also potent alkylating reagents.[81] More interestingly, in 2017 Melchiorre *et al.*[82] published a nickel-catalysed coupling reaction between the expelled alkyl radical from alkyl-HE and an aryl bromide (Scheme 28). Despite

their proposed mechanism, in which the nickel catalyst **113** was used to oxidise the excited benzyl-HE **112** to generate the alkyl radical, they also showed in a control experiment (Scheme 29) that benzyl-HE **115** expels the alkyl radical directly upon light irradiation even in the absence of catalyst leading to the aromatised Hantzsch pyridine (**116**, HPyr) by-product, toluene (**117**) and dibenzyl (**118**), which are all expected products from benzyl radicals.

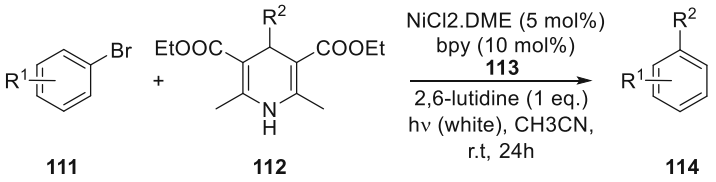

Scheme 28: Nickel-catalysed coupling reaction utilising alkyl-HE. [82]

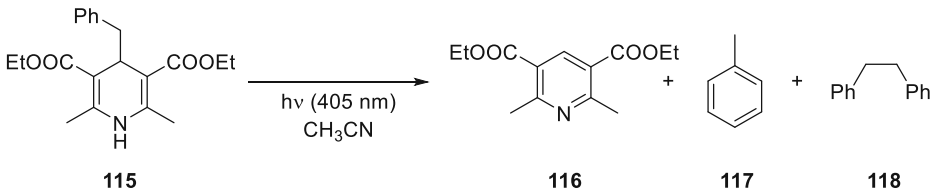

Scheme 29: Direct photoexcitation of benzyl-HE. [82]

Knowing that HEs can be used to generate alkyl radicals *via* direct photoexcitation, it is only a small step towards generating acyl radicals in a similar manner. This thesis aims to establish an alternative hydroacylation strategy for the functionalization of electron-poor double bonds (like in Scheme 30). By using HEs instead of benzothiazolines, one might have the advantage that neither additional additive (base or other reagents), nor catalyst is needed.

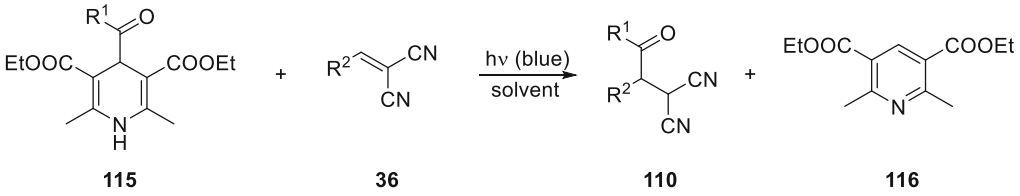

Scheme 30: Direct photoexcited hydroacylation of electron-poor Michael acceptors.

3 Results and discussion

3.1 Preparation of benzylidenemalononitrile substrates

The corresponding benzylidenemalononitrile substrates **36-{A, L}** were prepared *via* a straightforward Knoevenagel-condensation, in accordance with Foucaud *et al*. [83]

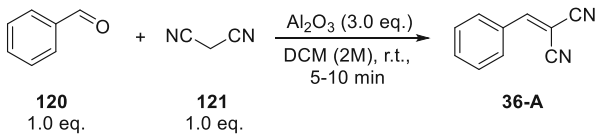

Scheme 31: Knoevenagel-condensation to benzylidenemalononitrile. [83]

Using this method, a pool of substrates bearing functional groups with different steric and electronic properties has been prepared (Figure 9).

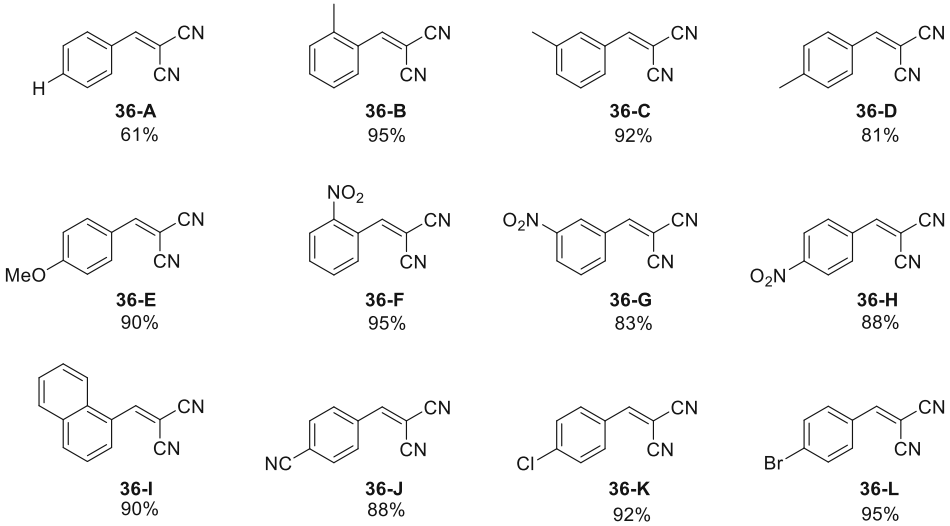

Figure 11: Synthesised and available substrates for following up photoreactions.

Trying to synthesise a saturated substrate analogue **125**, following the above procedure did not yield the desired product because aldol condensation dominated instead. Changing to a different procedure from Woo *et al.*[84] (Scheme 32) also gave just aldol condensation.

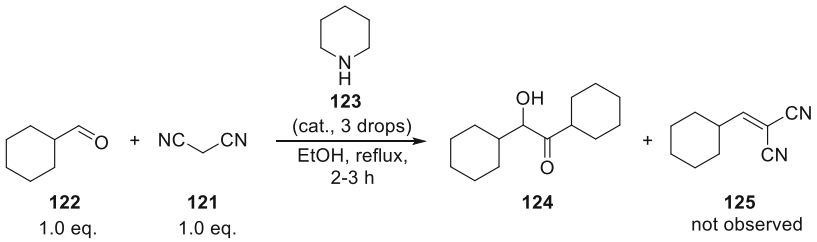

Scheme 32:A failed attempt to synthesise 1,2-dicyano-2-cyclohexylethylene following a procedure of Woo et al. [84]

3.2 Preparation of Hantzsch esters

The 4-acyl-Hantzsch esters were prepared according to Melchiorre *et al* in 2019.[85] As such, a one-pot reaction of glyoxal **127** as the "pre-acyl group" with ethyl acetoacetate (**128**) and ethyl-3-aminocrotonate (**129**) readily afforded the 4-acyl HEs under solvent-free conditions (Scheme 34). Despite the rather straightforward Hantzsch ester synthesis itself, most glyoxals are not commercially available and needed to be prepared beforehand (Scheme 33).

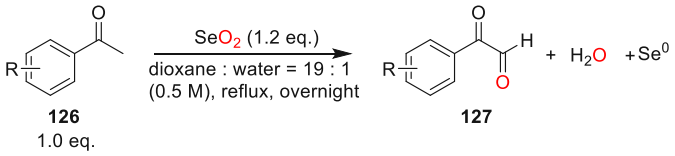

Scheme 33: Phenylglyoxal synthesis from acetophenones according to Melchiorre and co-workers. [85]

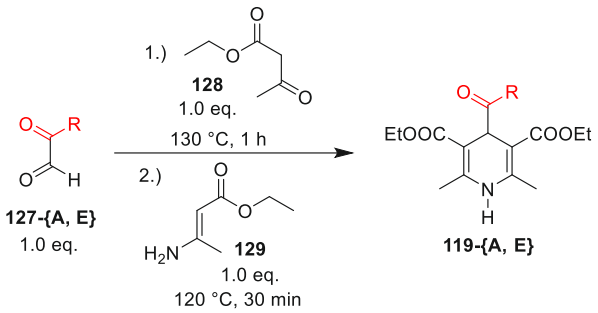

Scheme 34: HE synthesis according to Melchiorre and co-workers. [85]

Several difficulties were encountered during the glyoxal synthesis. First, glyoxals started to decompose after exposure to air, which is not a problem for the synthesis itself, as argon was used as inert gas. However, elemental selenium needs to be removed, which, according to the literature, was done by simply filtrating the solution over celite quickly. Still, red decomposition product was found inside the filtrate and on top; moreover, the filtration was not effective enough as a little bit of black selenium dust found its way to the filtrate. Analyses of the decomposition product were attempted, but discarded due to the negligible solubility in water, in most common available organic solvents or in acids, suggesting that minor polymerisation could have taken place. In order to overcome these issues, the glyoxals were alternatively purified *via* recrystallization; however, this provided no improvements. Eventually, another procedure from Wu *et al.* [86] was adopted; however, no glyoxal product was formed (Scheme 35).

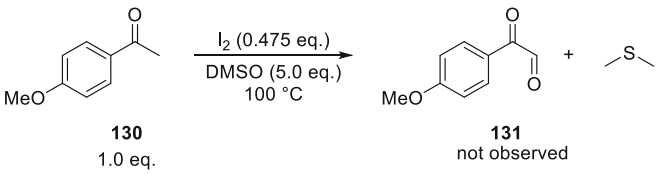

*Scheme 35: Failed attempt for the synthesis of glyoxal **131** following the procedure of Wu et al.*[86]

Concluding from these issues, the initially used SeO_2-based syntheses were repeated; however, the work-up and purification part was largely reduced and the crude glyoxals were used for subsequent Hantzsch ester synthesis without any purifications. The so-obtained Hantzsch esters were purified by crystallisation and/or by column chromatography. Figure 10 shows the overall yield for different acyl-Hantzsch esters obtained with this method.

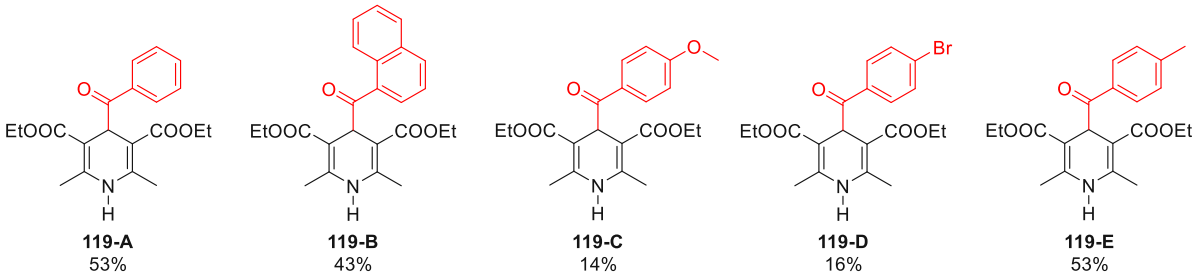

Figure 12: Synthesised acyl-HE reagents.

With the acylated Hantzsch esters at hand, we also aimed for preparing 4-alkyl Hantzsch esters according to the literature[34]:

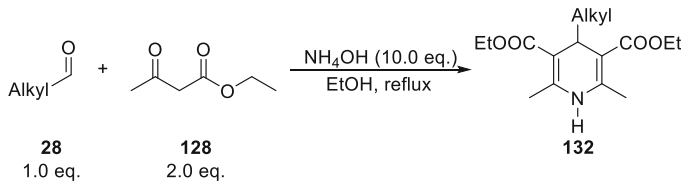

Scheme 36: Procedure for alkyl-HE synthesis.[34]

Unfortunately, when using hexanal or heptanal (“Alkyl” = hexyl or pentyl), no product formation was observed; however, phenylacetaldehyde (“Alkyl” = benzyl) gave 29% yield of benzylated Hantzsch ester.

3.3 Optimisation

We were initially interested in the direct hydrobenzoylation of benzylidenemalononitrile (Scheme 37). Based on prior findings from our lab, it was first verified that the reaction proceeds favourably under standard blue light irradiation at 460 nm.

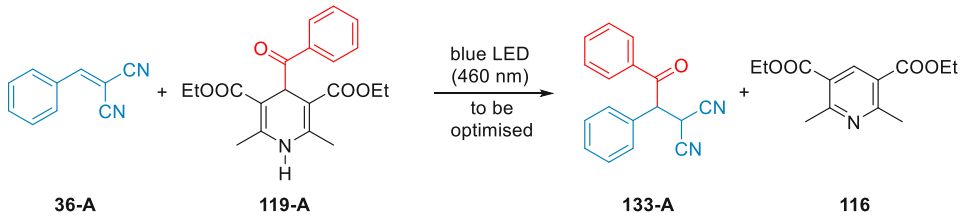

*Scheme 37: Reaction of substrate **36-A** with Hantzsch ester **119-A** used as "standard reaction" for optimisation.*

Next, it was investigated whether freeze-pump-thawed (fpt) solvent was necessary or if simply anhydrous solvent was sufficient, while the technical grade solvent was used as a control. Freeze-pump-thaw is a process that consists of first freezing an (anhydrous) solvent under an inert atmosphere, then applying a vacuum and finally letting it thaw slowly while still under a vacuum to provide a degassed solvent. While working under an argon atmosphere was indeed found to be beneficial, no fpt needed to be applied (Figure 11, left graph). Meanwhile, several different solvents were identified as suitable for the reaction, and toluene and acetonitrile worked best (Figure 11, right graph). Gratifyingly, a small increase in the HE loading from 1.1 eq. (Figure 11, right graph, blue) to 1.2 eq. (Figure 11, right graph, orange) resulted in almost full conversion.

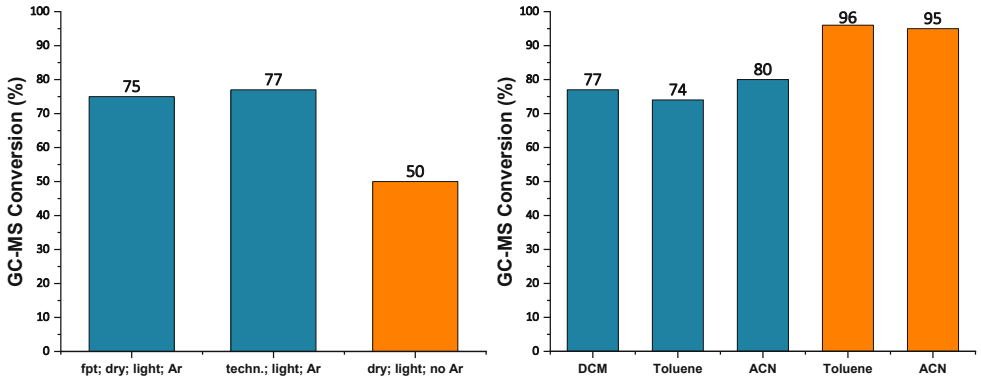

Figure 13: Using different solvent qualities (left graph, blue columns), a non-inert atmosphere control (left graph, orange column) and different solvents (right graph) as well as different HE loadings (right graph: blue columns [1.1 eq.] vs orange columns [1.2 eq.]).

Finally, the reaction time was considered, as shown in Figure 12, where the GC-MS conversion is shown as a function of reaction time. While the reaction with the unsubstituted substrate (blue) was basically done within 3-4 h, using a different substrate like 1-naphthylmethylidenemalononitrile (orange) can take substantially longer and required up to 16 h (data point not shown due to scaling of the graph). Therefore, all further reactions were performed for exactly 16 h.

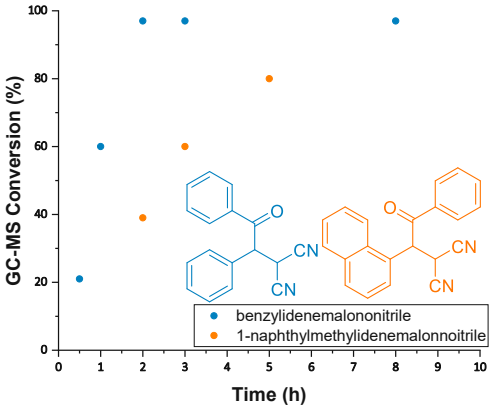

Figure 14: Comparison of reaction rates of the phenyl and 1-naphthyl substituted photoproduct.

To sum up the optimisation, all further experiments were performed at blue light irradiation (460 nm peak) for 16 h, in acetonitrile, using 1.2 equivalents of Hantzsch ester (**119-{A, E}**).

3.4 Hydroacylation reactions

3.4.1 Saturated photoproducts

With the optimized reaction conditions in hand, we aimed for investigating the scope and limitations of this process at first by using different benzylidenemalononitrile-type substrates (Scheme 38).

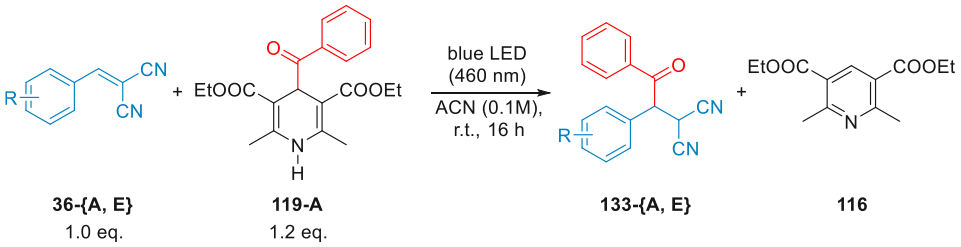

Scheme 38: Synthesis towards saturated photoproducts.

Following the reaction scheme above, the photoreactions between different benzylidenemalononitrile substrates (**36-{A, E}**) and benzoyl-Hantzsch ester **119-A** were conducted on a 2 × 0.2 mmol scale. After verifying the presence of the product by GC-MS, the combined reactions (0.4 mmol in total) were purified *via* column chromatography. In cases where mixed fractions were obtained due to decomposed HE species, the products could be further purified by simple Pasteur filtration with DCM. Following this procedure, a set of different hydroacylated products with different substituents could be obtained in good to excellent yields; meanwhile, the introduction of nitro-substituents resulted in decomposition during the photoreaction (Figure 13).

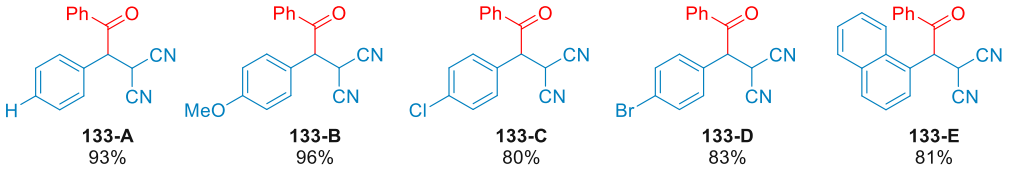

Figure 15: First set of obtained saturated photoproducts.

The reaction was not limited to electron-poor Knoevenagel-like acceptors, as photoreactions with cyclopent-2-en-1-on (**134**) or cyclohex-2-en-1-on (**136**) provided the products in 68% and 63% yield respectively:

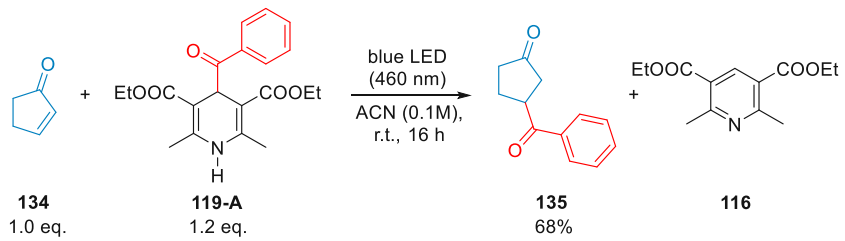

Scheme 39: Photobenzoylation of cyclopent-2-en-1-on.

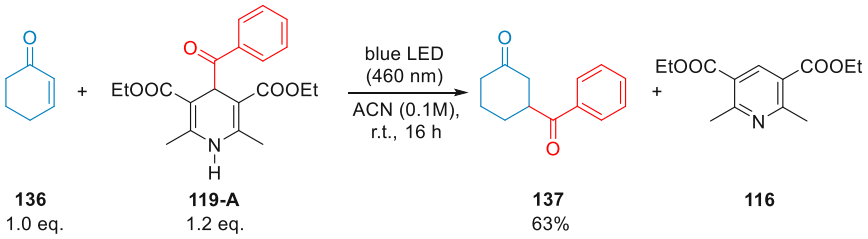

Scheme 40:Photobenzoylation of cyclohex-2-en-1-on.

Apart from screening substrates with different steric and electronic properties, different Hantzsch esters were also investigated together with a co-worker in our lab. As one can see from Figure 14, this method was suitable for transferring different acyl moieties, and the corresponding hydroacylated products were obtained in general excellent yields of 80 - 86%.

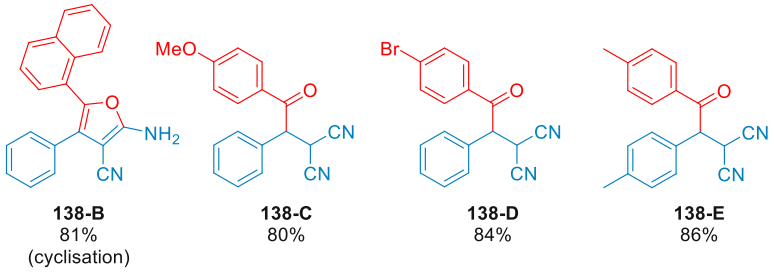

Figure 16: Hydroacylation products (including one cyclisation) using different acyl-HEs.

3.4.2 Towards furane-formation

When using the 4-CN-substituted substrate **36-J**, a cyclisation occurred. Similar cyclisations have been reported by Akiyama *et al.*[78] In order to figure out whether this eventually occurs during or only after the photoreaction (e.g. upon isolation on the stationary phase) the GC-MS and NMR spectra were compared to those of the "standard reaction" as seen in Figure 15 and Figure 16.

As for the standard reaction using benzylidenemalonitrile (substrate **36-A**, Figure 15), one can find traces of remaining substrates (zoomed in for visibility, m/z = 153.91) as well as the 4-unsubstituted Hantzsch pyridine (**116**, m/z = 250.94). For the product, two hydrogens are eliminated under GC-MS conditions at high temperature to form a double bond, as indicated by the dashed line. This elimination might lead to a more stable molecule, as essentially 3 isolated conjugated systems are combined into one big conjugated one, ultimately resulting in a peak with M-2 mass (m/z = 257.90). Additionally, the ^{1}H NMR spectrum showed that the saturated hydroacylation product **133-A** was formed, confirming that this conjugation only occurs in the GC-MS (Figure 15).

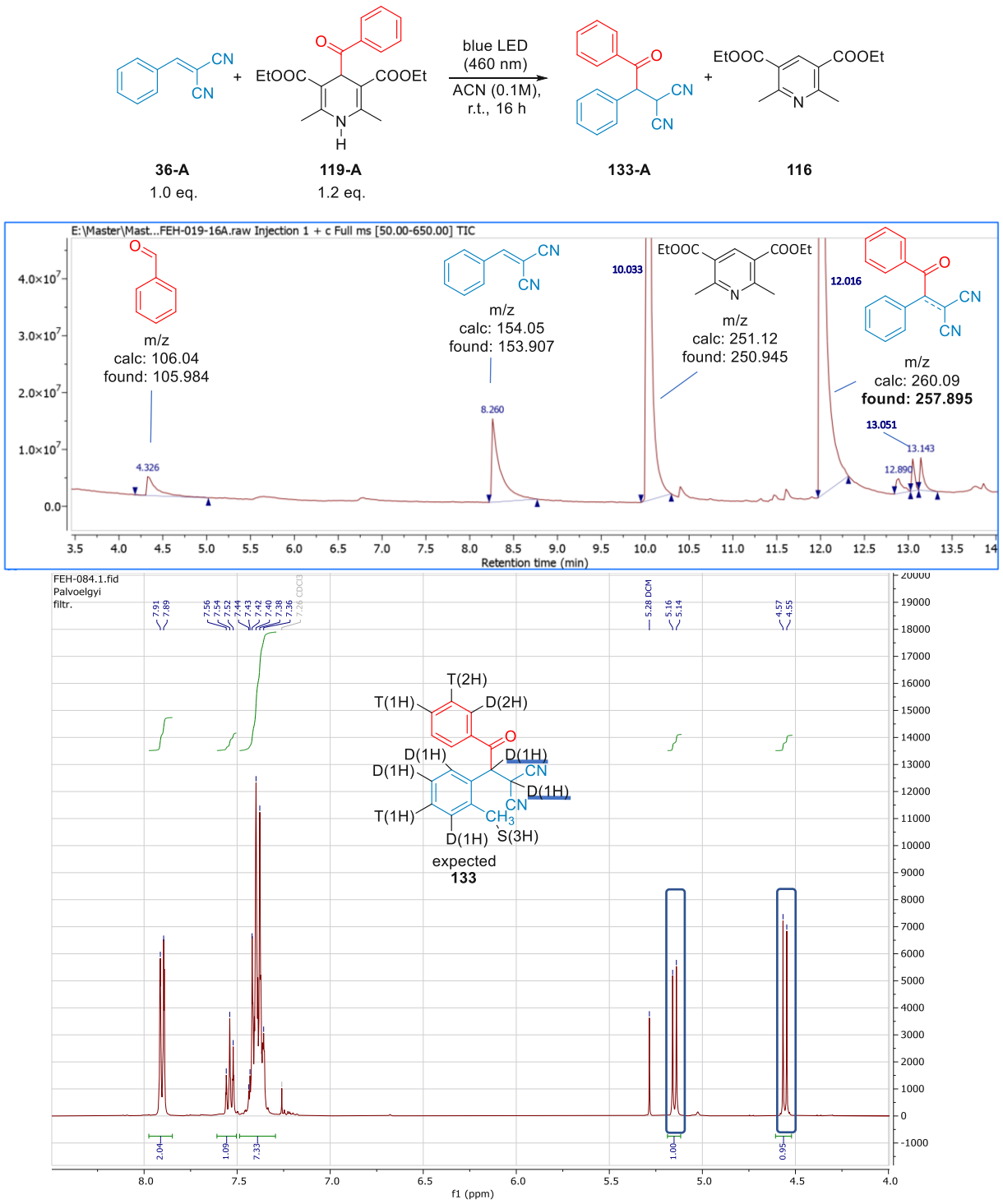

Figure 17: Showing the standard reaction (top), its crude GC-MS (middle) and ^{1}H NMR of the purified product (bottom).

For the photoreaction of the 4-CN species **36-J**, one can observe that there is only one peak matching with the M-2 mass (m/z = 282.87); which - in analogy to the above-discussed - suggests the formation of the saturated product. Nevertheless, after chromatographic purification, the corresponding ^{1}H NMR spectrum perfectly fits to the furane derivative **145-J**, showing no peaks in the region of 4.5 - 5.5 ppm (Figure 16, bottom). This suggests that the compound readily underwent cyclisation upon isolation.[37,87]

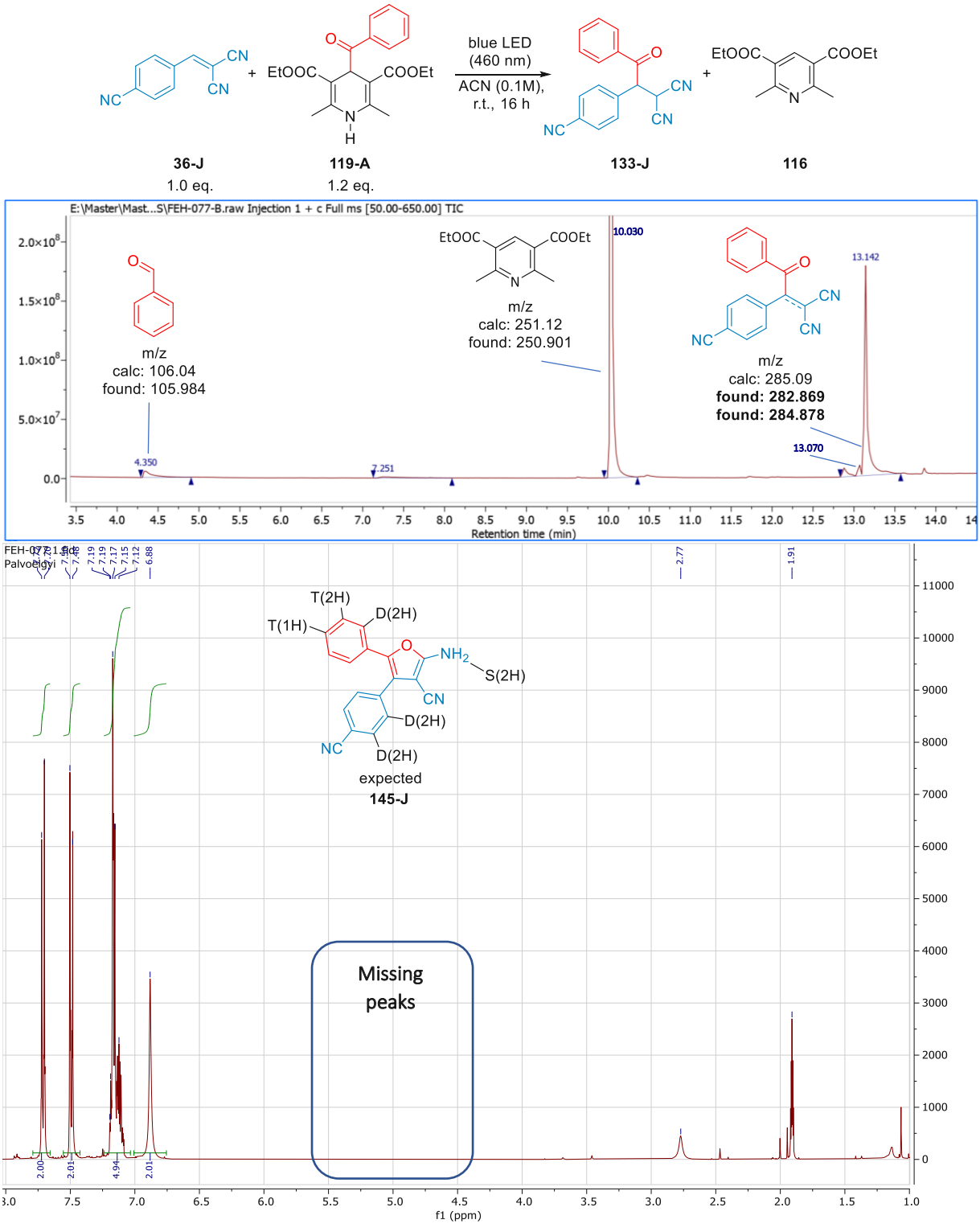

Figure 18: Showing the reaction scheme for the 4-CN substrate scheme (top), its crude GC-MS (middle) and ^{1}H NMR of the purified product (bottom).

The cyclisation should take place as follows (Scheme 41):

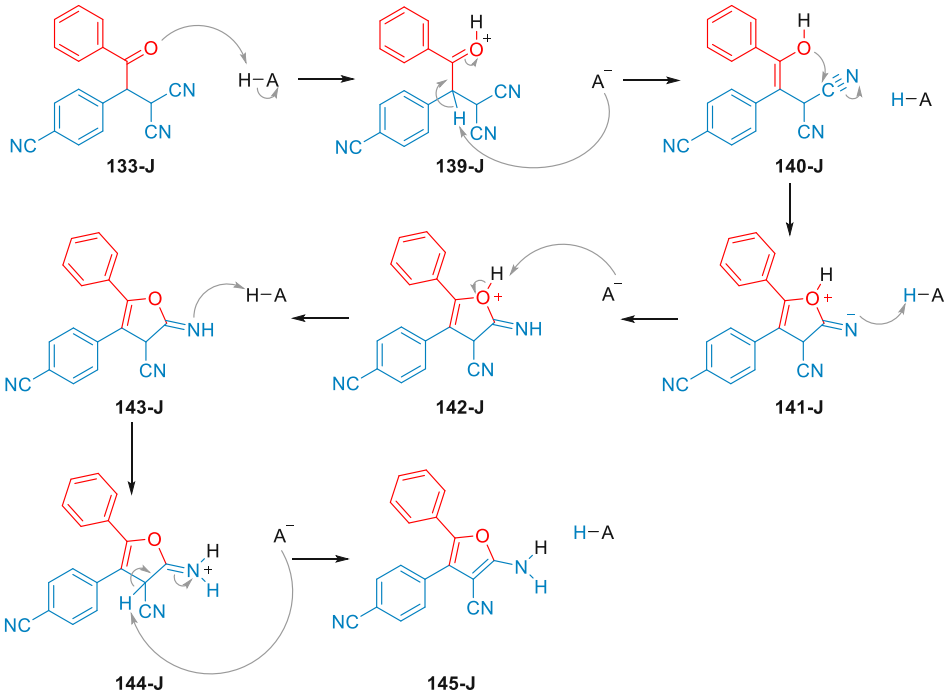

Scheme 41: Cyclisation mechanism by acidic catalysis, resulting in furane formation.

3.4.3 Synthesis of formal alkenylation products

Saturated photoproducts were detected as their unsaturated counterpart *via* GC-MS, which implies that they should be easily oxidised. Inspired by this, we aimed for mimicking this synthetically by investigating a one-pot further derivatization method. In order to do so, a simple oxidation strategy has been applied. After the photoreaction, DDQ (2,3-dichloro-5,6-dicyano-1,5-benzoquinone) was added to the crude mixture and after 2 h stirring at room temperature, purification by column chromatography readily afforded the corresponding unsaturated products in good to excellent yields (Scheme 42).

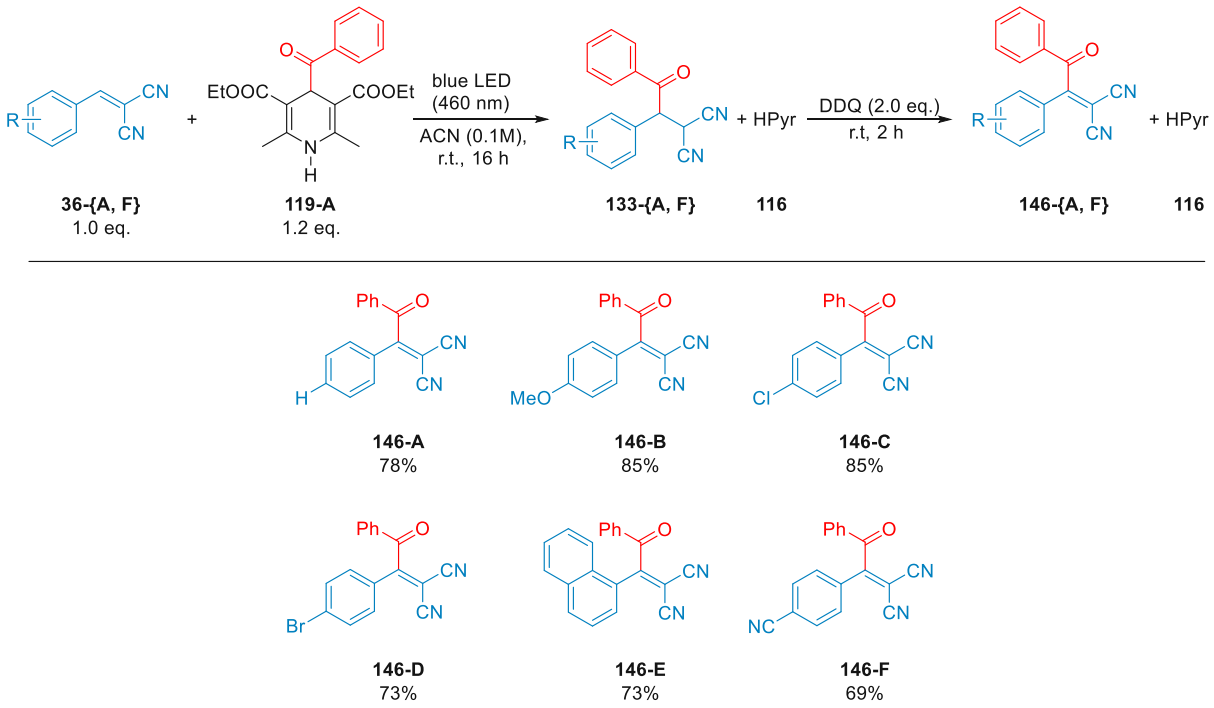

Scheme 42: Reaction scheme of the hydroacylation and following-up oxidation to formal alkenylation products (top) and isolated products (bottom).

3.4.4 Trial for silylation

The intermediate of furane formation is thought to be an enole; which raises the question of whether the enole can be quenched with, for example, tetrabutyldimethylsilyl chloride (TBDMS-Cl). Unfortunately, TLC spots before and after imidazole addition as well as after TBDMS-Cl addition were identical.

Weighting TBDMS-Cl into a small vial and adding NET_3 as a stronger base before adding both to the reaction mixture gave the same results, from which it can be concluded, that either no reaction takes place (imidazole too weak of a base) or that the intramolecular furane formation (almost identical Rf value) is too fast compared to the intermolecular S_N2 reaction. In either case, **147-A** was not detected.

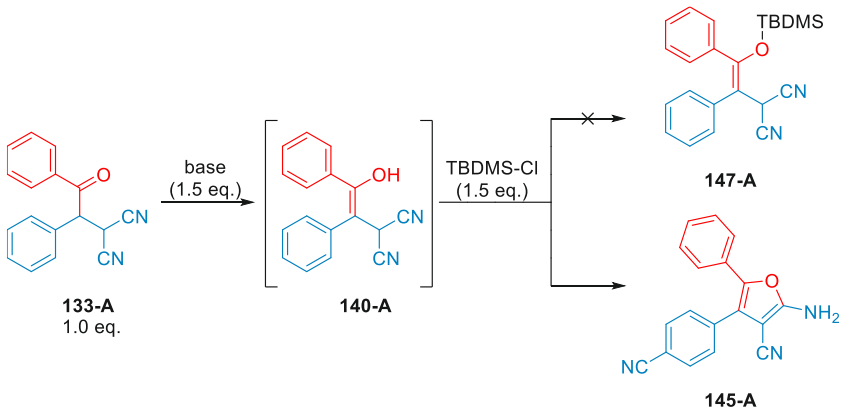

Scheme 43: Trial for silylation via enolisation.

3.5 Mechanistic considerations

In order to gain more insight into the reaction, a series of control experiments were carried out for the hydroacylation of **36-A**. A typical sign of a radical process is that a reaction is readily inhibited by the exclusion of light at room temperature. When performing the reaction in darkness, no product formation was observed (Scheme 44).

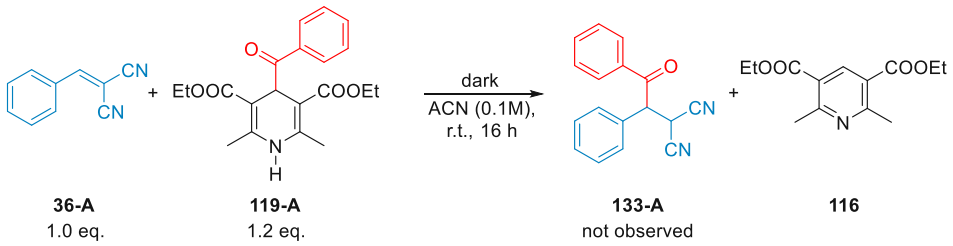

Scheme 44: Hydroacylation control experiment in darkness yields no product.

Similarly, no conversion could be observed when irradiating the reaction in the presence of 1.5 eq. TEMPO (2,2,6,6-tetramethylpiperidin-1-yl)oxyl, Scheme 45). Meanwhile, some of the corresponding TEMPO-adduct-related fragments like 2,2,6,6-tetramethylpiperidine (3.980 min) and benzoic acid (6.141 min) were found in the GC-MS (Figure 17).

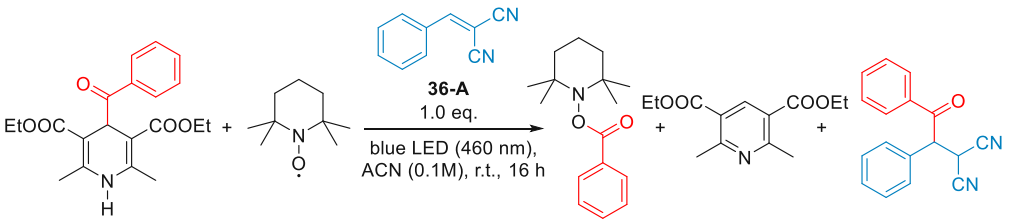

Scheme 45: Hydroacylation control experiment with radical scavenger TEMPO yields no product.

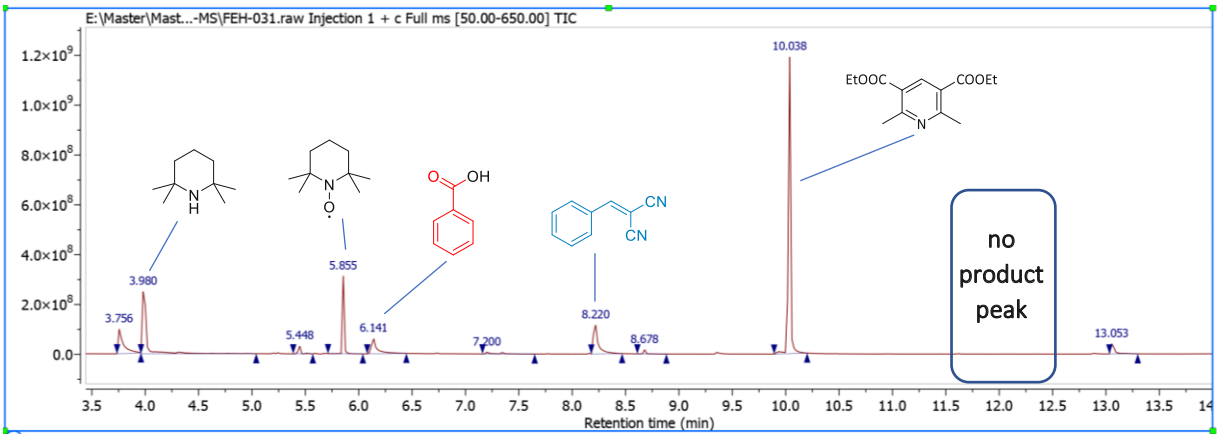

Figure 19: GC part of a GC-MS measurement for the TEMPO control reaction showing no product peak.

Apart from GC-MS analysis - under which the TEMPO-benzoyl-adduct seemed to be rather unstable - the TEMPO-adduct was also analysed by ^{1}H NMR. In this case, a “blank” reaction was carried out using only TEMPO and the benzoyl-HE. The spectrum showed full consumption of the Hantzsch ester; the peaks of the de-benzoylated species and the TEMPO-adduct could be clearly assigned. This further proved that the reaction indeed proceeded *via* the formation of a benzoyl radical.

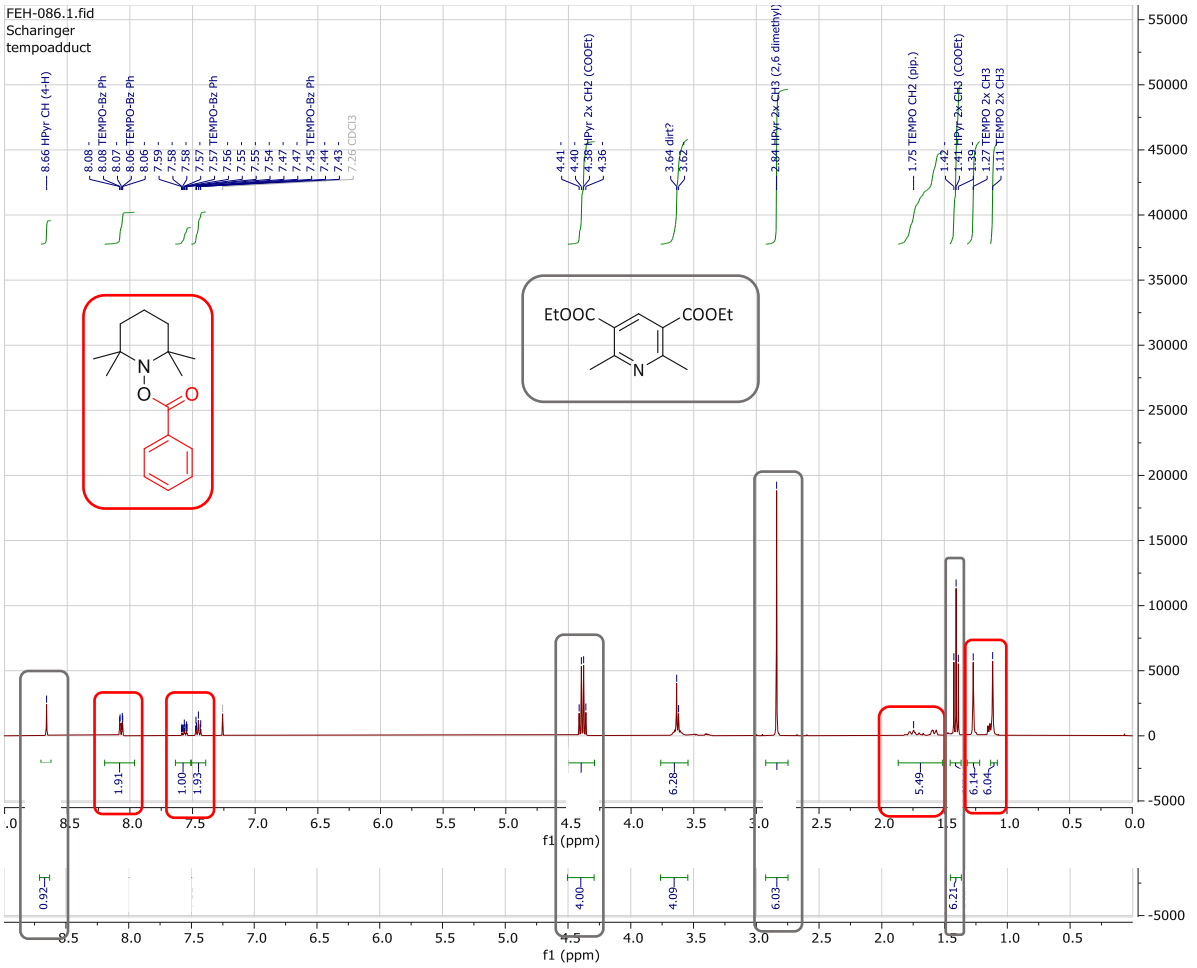

Figure 20: ^{1}H NMR of a mixture of benzoyl-TEMPO-adduct and HPyr (double x-axis is used for the visibility of integration).

To further prove that the reaction only takes place while irradiated at 460 nm, a light-on/light-off kinetic experiment was performed (Figure 19, next page). Every 15 min, the light was alternatingly switched on and off and a sample was taken for GC-MS to determine the conversion. Indeed, only marginal reactivity could be observed during the light-off periods, indicating that no long-living radicals are present to contribute to the product formation, therefore essentially excluding the option for a radical chain mechanism.

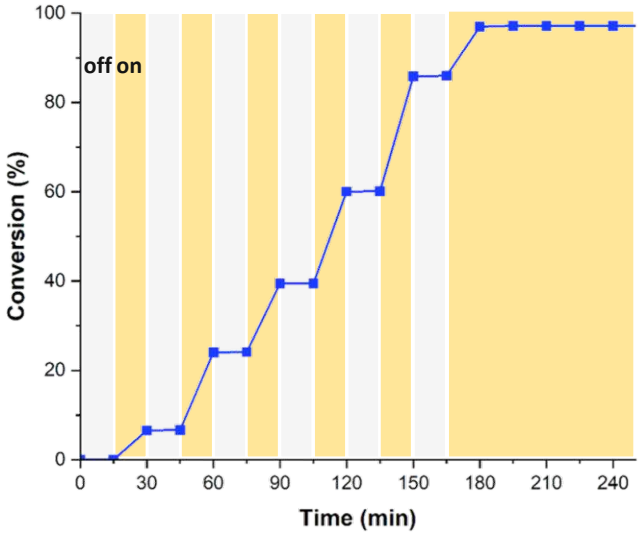

Figure 21: The Light-on, light-off experiment's conversion as a function of time.

To investigate the exact photochemical activation mode (direct photoexcitation, photocatalysis, EDA complex/exciplex formation), UV-VIS measurements were carried out. Photocatalysis can be ruled out as no photocatalyst, photosensitiser, etc. was added to the reaction, which raises the question of whether EDA complex formation might play a role. If so, a difference in absorbance between the separated and the combined reagents should be noticeable. Figure 20 shows that this is not the case, because the absorption spectrum of a benzoyl-Hantzsch ester (HE-Bz, **119-A**) solution and that of a 1:1 mixture of HE-Bz and benzylidenemalononitrile substrate are *de facto* identical and no additional absorption bands appear. This indicates that no EDA complex is formed, which leaves direct photoexcitation as the only remaining activation mode.

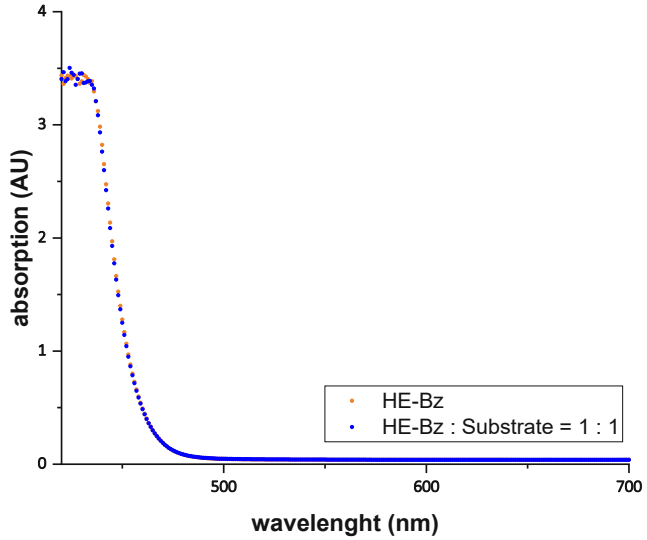

Figure 22: UV-VIS measurement of HE-Bz (orange dots) and a 1:1 mixture of HE-Bz with benzylidenemalononitrile substrate (blue dots) in comparison.

Taking all these considerations into account, the reaction proceeds *via* direct photoexcitation (Scheme 46). The visible-light excitation of the Hantzsch ester **119** results in the generation of acyl

radical **91**, which undergoes a radical conjugate addition with the electron-poor substrate **36**, which is then followed by a hydrogen atom transfer (HAT) step from either the positively charged HPyr radical **150** or the ground-state Hantzsch ester species **119** to afford the hydroacylation product **133**.

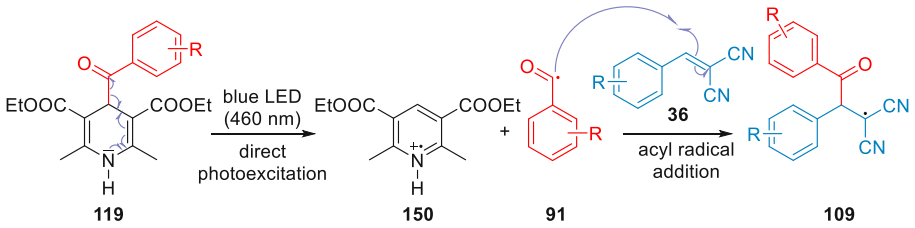

*Scheme 46: Activation of Hantzsch ester **119** by irradiation of blue light and release of a benzoyl radical **91**, which adds to the electron-poor substrate **36**.*

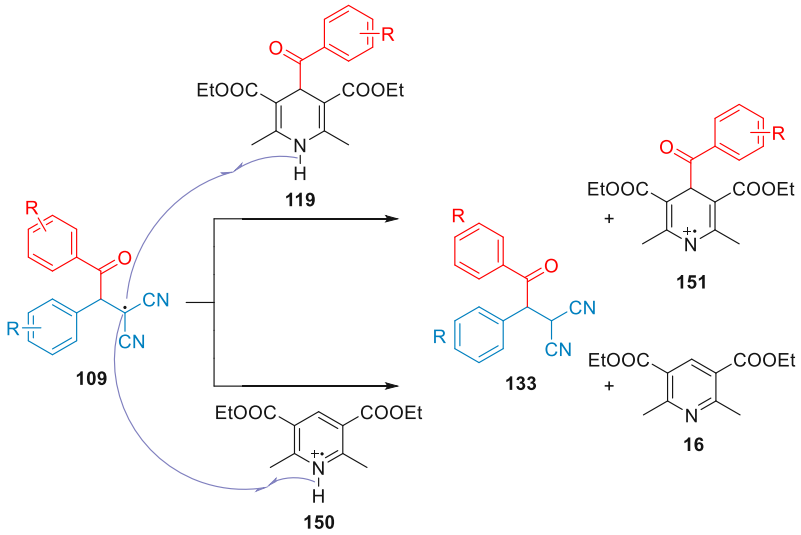

Scheme 47: Mechanism of direct photoexcitation and successive hydroacylation of benzylidenemalononitrile substrate.

The Stern-Volmer equation compares the unimolecular fluorescence quantum yield Φ_f of the photoreaction in the absence of a quencher with the quantum yield while a quencher is present ${}^{Q}\Phi_f$ and it predicts a linear relationship based on[16,17]:

$$\frac{\Phi_f}{{}^{Q}\Phi_f} = 1 + K_Q[Q]$$

Where [Q] is the concentration of the quencher added, and K_Q Stern-Volmer quenching constant. "*Since fluorescence intensity and fluorescence lifetime are both proportional to the fluorescence quantum yield, plots of $I_f/{}^{Q}I_f$ and $\tau_0/{}^{Q}\tau$ against [Q] are also linear with slope K_Q and intercept 1.*"[17] In the case of the hydroacylation of substrate **36-A**, there is a linear relationship between the fluorescence intensity of the Hantzsch ester reagent **119-A** with the increasing concentrations of quencher

(substrate **36-A**) (Figure 21.) This indicates a bimolecular, photochemical process between the substrate and expelled benzoyl radical.

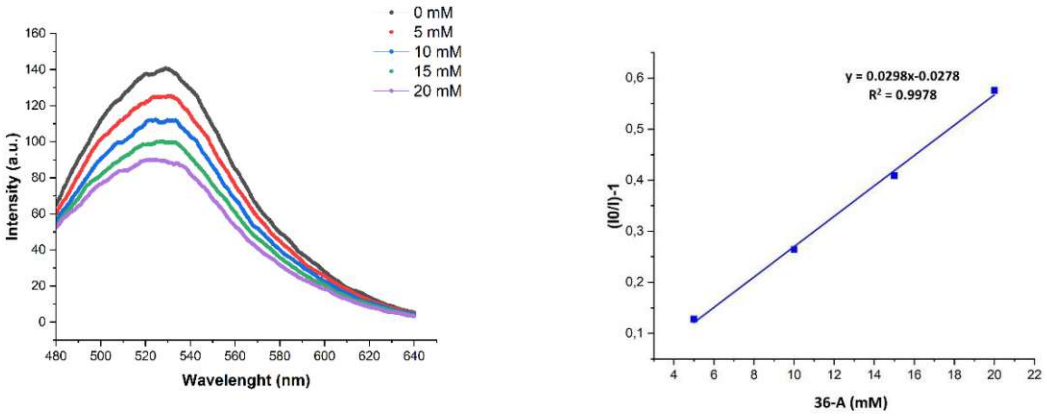

Figure 23: Stacked fluorescence emission spectra of HE (0.15 m) with increasing concentration of benzylidenemalononitrile (0 – 20 mM) at an excitation wavelength of λ_{max} = 365 nm (left) and the corresponding Stern-Volmer-plot (right).

4 Summary

In this work, it has been shown that the direct photoexcited hydroacylation using Hantzsch ester at visible blue light irradiation (λ_{max} = 460nm) works in the absence of a base, (photo)catalyst or other additive. The strategy was applicable for various Michael-acceptors and enones in good to excellent yields; furthermore, it also enabled one-pot further derivatizations: a simple oxidation with DDQ readily afforded the corresponding unsaturated, formal alkenylation products. Treatment with Et_3N led to cyclization to the furane analogues. Detailed mechanistic examinations supported the hypothesis of a non-chain radical process, and strongly indicated, that the reaction proceeds *via* direct photoexcitation of the Hantzsch-ester species.

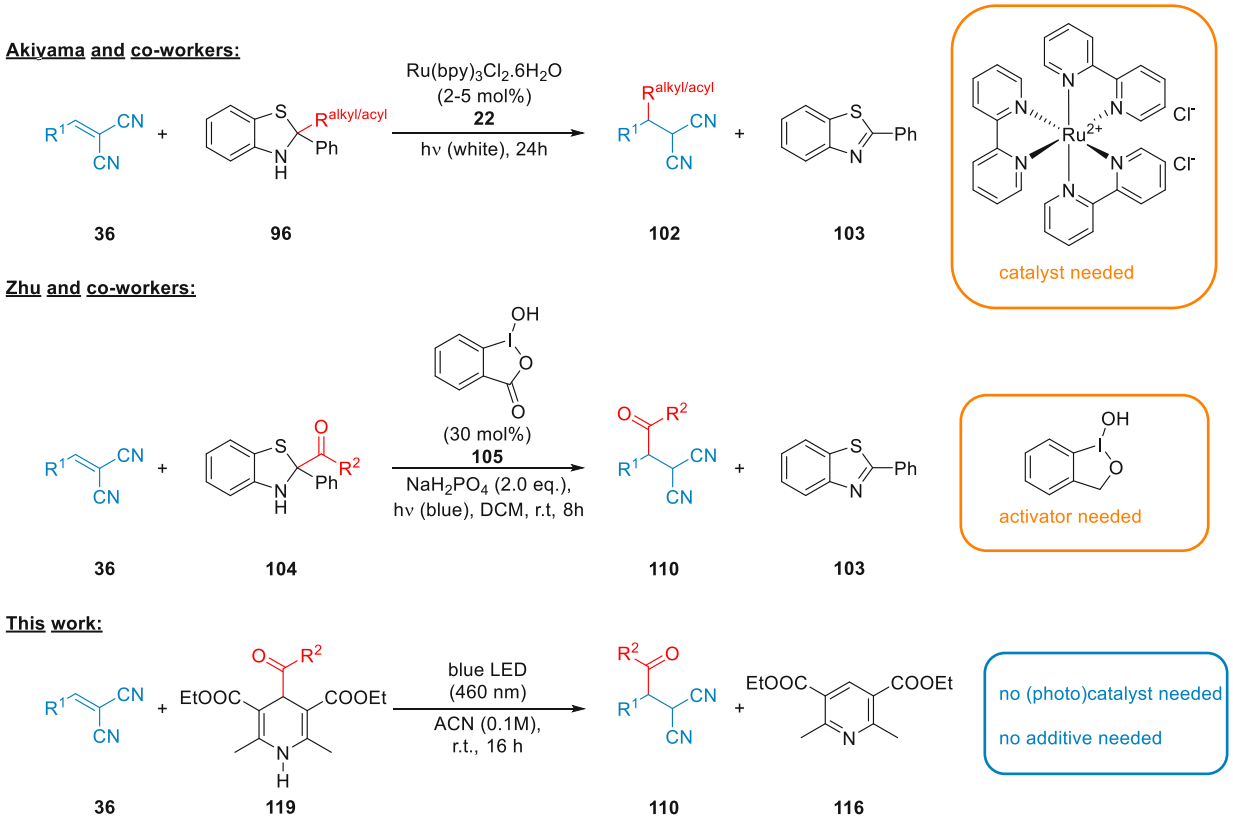

5 Experimental part

5.1 Materials & methods

Column chromatography was performed on standard manual glass columns using Merck (40-63 µm) silica gel with pre-distilled solvents (PE: petroleum ether, EtOAc: ethyl acetate).

For TLC analysis, precoated aluminium-backed plates were purchased from Merck (silica gel 60 F_{254}). UV active compounds were detected at 254 nm. Non-UV active compounds have been detected using either vanillin staining (5% vanillin in EtOH + H_2SO_4) or by Henessian's staining solutions (15% aq. Sulphuric acid saturated with ceric sulfate).

^{1}H and ^{13}C NMR spectra were recorded on a Bruker Advance UltraShield 400 MHz spectrometer and chemical shifts are reported in ppm using TMS (tetramethylsilane) as an internal standard. Coupling constants (*J*) are given in Hz. GC-MS measurements have been performed on a Thermo Scientific DSQ II on BGB5 column (30 m), equipped with a quadrupole MS detector DSQ II. HR-MS analysis was performed using an HTC PAL system autosampler, an Agilent 1100/1200 HPLC with binary pumps and column, column thermostat and Agilent 6230 AJS ESI-TOF mass spectrometer.

Infrared spectra were recorded on a Perkin-Elmer Spectrum 65 FT IR spectrometer equipped with a specac MK II Golden Gate Single Reflection ATR unit.

UV-VIS spectra have been recorded in 1 cm path-length quartz cuvettes on a Shimadzu UV/VIS 1800 spectrometer.

Fluorescence measurements were carried out on a PerkinElmer LS 55 luminescence spectrometer.

5.2 The photochemical setup

All photoreactions were performed in a custom-made photoreactor (Figure 22, next page). 3.6 m of a flexible blue LED strip (34.5 W, a total of 48 W, 12 V, 4.0 A, 120 LEDs/m, λ_{max} = 460 nm) was coiled into a 3D-printed cylindric case (diameter × height 10 cm × 14 cm, ABS polymer). A cylindric lid was used, providing a uniform irradiation environment for the Schenk tubes at a distance of 2 cm from the light source. A computer fan (40 × 10 mm, 6800 rpm) was integrated into the reactor lid, maintaining a temperature not higher than 28 ˚C.

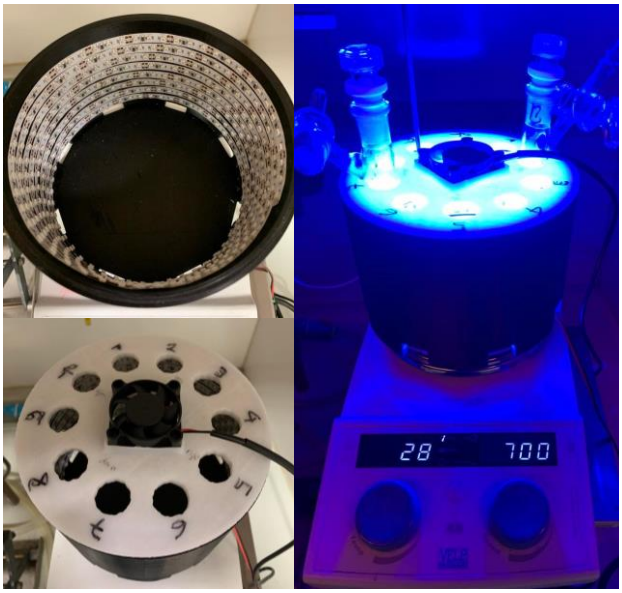

Figure 24: The inside of the photoreactor showing the LED strips (left, top), the photoreactor's top lid with cooling fan (left, bottom) and the photoreactor in action (right).

5.3 Synthesis of malononitrile substrates

General Procedure:

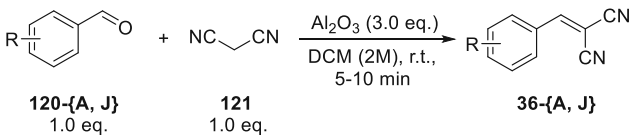

Scheme 48: Knoevenagel condensation to benzylidenemalonitrile derivatives. [83]

The malononitrile substrates **36-{A, J}** were prepared *via* Knoevenagel condensation according to literature[83]: Solid (not molten) malononitrile (**121**, 20.00 mmol, 1.32 g, 1.0 eq., CAS: 109-77-3) was weighed into a 50 mL round bottom flask. After the addition of the corresponding liquid benzaldehyde **120-{A, J}** derivative (20.00 mmol, 1.0 eq.), DCM (2M) was added, and aluminium oxide (60 mmol, 3.0 eq.) was poured as desiccant into the stirred reaction mixture. After 5 – 10 min (control *via* TLC), the reaction mixture was filtered through celite to remove the aluminium oxide. The purity was checked *via* ^{1}H NMR; and if necessary, the crude products were subjected to crystallisation from EtOH.

5.3.1 Benzylidenemalononitrile (36-A, CAS: 2700-22-3)

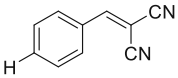

Following the general procedure, benzaldehyde (2.0 mL, 19.60 mmol, 1.0 eq.; CAS: 100-52-7), malononitrile (1.29 g, 19.60 mmol, 1.0 eq., CAS: 109-77-3) and aluminium oxide (6.00 g, 3.0 eq.) were used in DCM (2M) to give the crude product, which after crystallisation from EtOH (ca. 3 mL) yielded benzylidenemalononitrile (**36-A**) as a colourless solid (1.93 g, 62%).

^{1}H NMR (400 MHz, $CDCl_3$): δ = 7.88 – 7.81 (m, 2H), 7.71 (s, 1H), 7.61 – 7.52 (m, 1H), 7.52 – 7.43 (m, 2H). (corresponds to literature[88,89]).

5.3.2 2-(2-Methylbenzylidene)malononitrile (36-B, CAS: 2698-44-4)

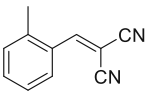

Following the general procedure, 2-methylbenzaldehyde (2.40 g, 20.00 mmol, 1.0 eq., CAS: 529-20-4), malononitrile (1.32 g, 20.00 mmol, 1.0 eq., CAS: 109-77-3) and aluminium oxide (6.00 g, 3.0 eq.) were used in DCM (2M) to give the product (**36-B**) as a colourless solid (3.09 g, 92%) without the need of further purification.

^{1}H NMR (400 MHz, $CDCl_3$): δ = 8.09 (d, *J* = 11.5 Hz, 2H), 7.50 (t, *J* = 7.5 Hz, 1H), 7.41 – 7.28 (m, 2H), 2.45 (s, 3H). (corresponds to literature[88]).

5.3.3 2-(3-Methylbenzylidene)malononitrile (36-C, CAS: 15728-26-4)

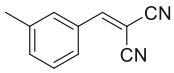

Following the general procedure, 3-methylbenzaldehyde (2.40 g, 20.00 mmol, 1.0 eq., CAS: 620-23-5), malononitrile (1.32 g, 20.00 mmol, 1.0 eq., CAS: 109-77-3) and aluminium oxide (6.00 g, 3.0 eq.) were used in DCM (2M) to give the product (**36-C**) as a colourless solid (3.22 g, 96%) without the need of further purification.

^{1}H NMR (400 MHz, $CDCl_3$) δ = 7.74 (s, 2H), 7.69 (tq, *J* = 1.4, 0.8 Hz, 1H), 7.44 (s, 2H), 2.43 (s, 3H). (corresponds to literature[90]).

5.3.4 2-(4-Methylbenzylidene)malononitrile (36-D, CAS: 2826-25-7)

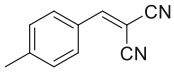

Following the general procedure, 4-methylbenzaldehyde (2.40 g, 20.00 mmol, 1.0 eq., CAS: 104-87-0), malononitrile (1.32 g, 20.00 mmol, 1.0 eq., CAS: 109-77-3) and aluminium oxide (6.00 g, 3.0 eq.) were used in DCM (2M) to give the product (**36-D**) as colourless solid (2.75 g, 81%) without the need of further purification.

^{1}H NMR (400 MHz, $CDCl_3$): δ = 7.81 (d, *J* = 8.5 Hz, 2H), 7.72 (s, 1H), 7.34 (d, *J* = 8.1 Hz, 2H), 2.46 (s, 3H). (corresponds to literature[88]).

5.3.5 2-(4-Methoxybenzylidene)malononitrile (36-E, CAS: 2826-26-8)

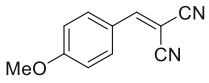

Following the general procedure, 4-methoxybenzaldehyde (2.72 g, 20.00 mmol, 1.0 eq., CAS: 123-11-5), malononitrile (1.32 g, 20.00 mmol, 1.0 eq., 109-77-3) and aluminium oxide (6.00 g, 3.0 eq.) were used in DCM (2M) to give the product (**36-E**) as a light-yellow solid (3.32 g, 90%) without the need of further purification.

^{1}H NMR (400 MHz, $CDCl_3$) δ = 7.91 (d, *J* = 8.6 Hz, 2H), 7.65 (s, 1H), 7.01 (d, *J* = 9.0 Hz, 2H), 3.91 (s, 3H). (corresponds to literature[88–90]).

5.3.6 2-(2-Nitrobenzylidene)malononitrile (36-F, CAS: 2826-30-4)

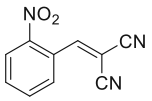

Following the general procedure, 2-nitrobenzaldehyde (3.02 g, 20.00 mmol, 1.0 eq., CAS: 552-89-6), malononitrile (1.32 g, 20.00 mmol, 1.0 eq., CAS: 109-77-3) and aluminium oxide (6.00 g, 3.0 eq.) were used in DCM (2M) to give the product (**36-F**) as a colourless solid (3.42 g, 92%) without the need of further purification.

^{1}H NMR (400 MHz, $CDCl_3$): δ = 8.45 (s, 1H), 8.36 (dd, *J* = 8.2, 1.4 Hz, 1H), 7.92 – 7.85 (m, 1H), 7.85 – 7.77 (m, 2H). (corresponds to literature[89]).

5.3.7 2-(3-Nitrobenzylidene)malononitrile (36-G, CAS: 2826-32-6)

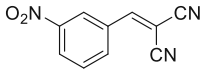

Following the general procedure, 3-nitrobenzaldehyde (3.02 g, 20.00 mmol, 1.0 eq., CAS: 99-61-6 malononitrile (1.32 g, 20.00 mmol, 1.0 eq., CAS: 109-77-3) and aluminium oxide (6.00 g, 3.0 eq.) were used in DCM (2M) to give the product (**36-G**) as a colourless solid (3.09 g, 83%) without the need of further purification.

^{1}H NMR (400 MHz, $CDCl_3$): δ = 8.66 (t, *J* = 2.0 Hz, 1H), 8.47 (ddd, *J* = 8.3, 2.2, 1.1 Hz, 1H), 8.32 (dt, *J* = 7.8, 0.9 Hz, 1H), 7.89 (s, 1H), 7.79 (t, *J* = 8.1 Hz, 1H). (corresponds to literature[89]).

5.3.8 1-Naphthylmethylidenemalononitrile (36-I, CAS: 2972-83-0)

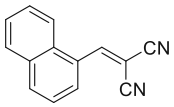

Following the general procedure, 1-naphthaldehyde (3.12 g, 20.00 mmol, 1.0 eq., CAS: 66-77-3), malononitrile (1.32 g, 20.00 mmol, 1.0 eq., CAS: 109-77-3) and aluminium oxide (6.00 g, 3.0 eq.) were used in DCM (2M) to give the product (**36-I**) as a yellow solid (3.69 g, 90%) without the need of further purification.

^{1}H NMR (400 MHz, $CDCl_3$): δ = 8.66 (s, 1H), 8.28 (d, *J* = 7.4 Hz, 1H), 8.11 (d, *J* = 8.4 Hz, 1H), 7.96 (dd, *J* = 8.2, 1.4 Hz, 2H), 7.73 – 7.59 (m, 3H). (corresponds to literature[89,90]).

5.3.9 2-(4-Cyanobenzylidene)malononitrile (36-J, CAS: 36937-92-5)

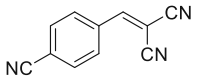

Following the general procedure, 4-cyanobenzaldehyde (2.62 g, 20.0 mmol, 1.0 eq., CAS: 105-07-7 malononitrile (1.32 g, 20.0 mmol, 1.0 eq., CAS: 109-77-3) and aluminium oxide (6.00 g, 3.0 eq.) were used in DCM (2M) to give the product (**36-J**) as a colourless solid (3.17 g, 88%) without the need of further purification.

^{1}H NMR (400 MHz, $CDCl_3$): δ = 8.03 – 7.96 (m, 2H), 7.87 – 7.80 (m, 3H). (corresponds to literature[90]).

5.4 Synthesis of Hantzsch esters

5.4.1 Glyoxal synthesis

For the synthesis of benzoyl-HE **119-A**, phenylglyoxal monohydrate was purchased from Sigma-Aldrich. All other glyoxals were prepared *via* Riley oxidation. [85]

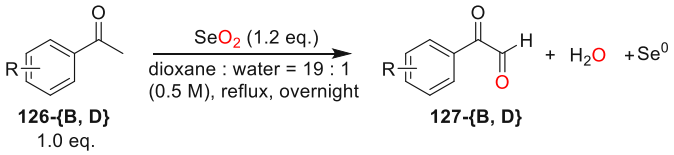

Scheme 49: Phenylglyoxal synthesis from acetophenones according to Melchiorre and co-workers. [85]

Selenium dioxide (12.00 mmol, 1.33 g, 1.2 eq.) was weighted into a round bottom flask. The corresponding acetophenone derivative (**126-{B, D}**, 10.00 mmol, 1.0 eq.) was added (if solid) and the flask was set under an inert atmosphere. Then, acetophenone derivative (if liquid) and a solvent mixture of 1,4-dioxane and water (0.5M, 19:1) were added and the reaction mixture was stirred under reflux overnight (*ca.* 16 h). The reaction mixture turned greenish-yellowish, and black, elemental selenium precipitated out. The conversion was checked by TLC analysis. The reaction mixture was filtered through celite and the filtrate was concentrated under reduced pressure. The crude glyoxals **127-{B, D}** were used without further purification.

5.4.2 Hantzsch ester synthesis

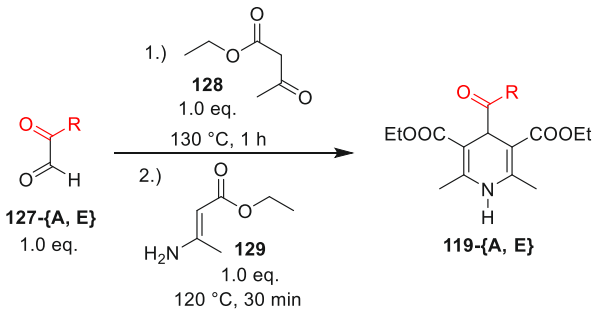

Scheme 50: HE synthesis according to Melchiorre and co-workers. [85]

A one-pot reaction was carried out as described in the literature[85]:

The corresponding glyoxal (**127-{A, D}**, 25.00 mmol, 1.0 eq.) and ethyl acetoacetate (**128**, 25.00 mmol, 1.0 eq., 3.16 mL) were added to a one-neck round bottom flask, and it was heated to 130 °C for 15-30 minutes. As the Knoevenagel condensation was finished (*TLC control*), the reaction mixture was cooled to 80 °C. Ethyl-3-aminocrotonate (**129**, 25.00 mmol, 1.0 eq.) was added in smaller portions (strongly exothermic reaction!), and the reaction mixture was stirred at 120 °C for another

10 - 25 minutes. Then, the mixture was cooled to room temperature, and the small amount of remaining water was removed by co-evaporation with toluene *in vacuo*. The crude product was dissolved in a hot cyclohexane/ethyl acetate mixture (4:1, 6-7× crude mass). After stirring for 15 minutes, it was cooled to room temperature, and then to 0 °C. The yellow precipitate was filtered off, washed with a cold cyclohexane/ethylacetate mixture (4:1, V/V), and dried under a high vacuum. The crude products were optionally purified by column chromatography (SiO_2, PE/EE = 7/1 to 3/1), followed by recrystallization from cyclohexane/ethyl acetate mixture (4:1, V/V).

5.4.2.1 Diethyl-4-benzoyl-2,6-dimethyl-1,4-dihydropyridine-3,-5-dicarboxylate / „Benzoyl Hantzsch ester" (119-A, CAS: n.a.)

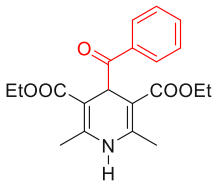

Commercially available phenylglyoxal monohydrate (**127-A**, 2.00 g, 13.15 mmol, 1.0 eq., CAS: 1074-12-0) and ethyl acetoacetate (**128**, 1.70 g, 13.15 mmol, 1.0 eq., CAS: 141-97-9) were used, which was further reacted with ethyl-3-aminobut-2-enoate (**129**, 1.70 g, 13.15 mmol, 1.0 eq., CAS: 626-34-6). Crystallisation as described above afforded the product **119-A** as a bright yellow solid (2.49 g, 53%).

^{1}H NMR (400 MHz, $CDCl_3$) δ = 8.24 – 8.10 (m, 2H), 7.57 – 7.49 (m, 1H), 7.49 – 7.40 (m, 2H), 6.75 (s, 1H), 5.72 (s, 1H), 4.07 – 3.85 (m, 4H), 2.29 (s, 6H), 1.03 (t, *J* = 7.1 Hz, 6H). (corresponds to literature[91]).

5.4.2.2 Diethyl-4-(1-naphthoyl)-2,6-dimethyl-1,4-dihydropyridine-3,5-dicarboxylate / „Napthoyl Hantzsch ester" (119-B, CAS: n.a.)

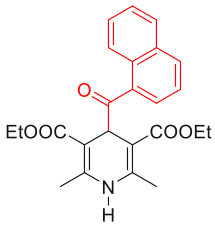

1-Naphthyl glyoxal (**127-A**, CAS: 63464-85-7) was prepared *via* Riley oxidation from 1-acetonaphthone (**126-B**, 1.5 mL, 10.00 mmol, 1.0 eq., CAS: 941-98-0) using selenium(IV) oxide (1.33 g, 12.00 mmol, 1.2 eq., CAS: 7446-08-4) as the oxidant yielding colourless solid glyoxal product (572.2 mg, 31%), which was subjected to Hantzsch ester synthesis according above procedure using ethyl acetoacetate (**128**, 358 µL, 2.83 mmol, 1.0 eq., CAS: 141-97-9) and ethyl-3-aminobut-2-enoate (**129**, 365.5 mg, 2.83 mmol, 1.0 eq., CAS: 626-34-6). The crude product was purified by column chromatography (71.9 g SiO_2, isocratic PE:EE = 4:1) to yield yellow naphthoyl Hantzsch ester as **119-B** a yellow solid (496.8 mg, 43%).

^{1}H NMR (400 MHz, $CDCl_3$) δ = 8.15 – 8.03 (m, 1H), 7.95 – 7.75 (m, 3H), 7.54 – 7.41 (m, 3H), 6.05 (s, 1H), 5.64 (s, 1H), 3.83 (ddq, *J* = 69.6, 10.8, 7.1 Hz, 4H), 2.38 (s, 6H), 0.95 (t, *J* = 7.1 Hz, 6H). (corresponds to literature[91]).

5.4.2.3 Diethyl-4-(4-methoxybenzoyl)-2,6-dimethyl-1,4-dihydropyridine-3,5-dicarboxylate / „Methoxy benzoyl Hantzsch ester“ (119-C, CAS: n.a.)

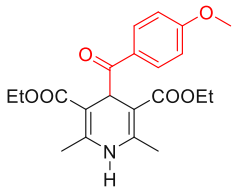

4-Methoxyphenylglyoxal (**127-C**, CAS: 1076-95-5) was prepared *via* Riley oxidation from 1-(4-methoxyphenyl)ethanone (**126-C**, 1.50 g, 10.00 mmol, 1.0 eq., CAS: 100-06-1) and selenium(IV) oxide (1.33 g, 12.00 mmol, 1.2 eq., CAS: 7446-08-4). Without isolation or purification, the crude glyoxal was used according to the above procedure using ethyl acetoacetate (**128**, 1.30 g, 10.00 mmol, 1.0 eq., CAS: 141-97-9) and ethyl-3-aminobut-2-enoate (**129**, 1.29 g, 10.00 mmol, 1.0 eq., CAS: 626-34-6). Crystallisation as described above afforded the product **119-C** as olive-coloured crystals (560.0 mg, 14%).

^{1}H NMR (400 MHz, $CDCl_3$) δ = 8.16 (d, *J* = 8.9 Hz, 2H), 6.92 (d, *J* = 9.0 Hz, 2H), 6.88 (s, 1H), 5.69 (s, 1H), 4.00 (qd, *J* = 10.9, 7.2 Hz, 4H), 3.86 (s, 3H), 2.28 (s, 6H), 1.07 (t, *J* = 7.1 Hz, 6H). (corresponds to literature[91]).

5.4.2.4 Diethyl-4-(4-bromobenzoyl)-2,6-dimethyl-1,4-dihydropyridine-3,5-dicarboxylate / „bromo benzoyl Hantzsch ester“ (119-D, CAS: n.a.)

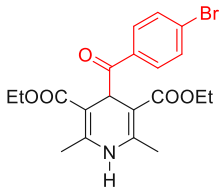

4-Bromophenylglyoxal (**127-D**, CAS: 5195-29-9) was prepared *via* Riley oxidation from 4-bromoacetophenone (**126-D**, 4.98 g, 25.00 mmol, 1.0 eq., CAS: 99-90-1) and selenium(IV) oxide (3.34 g, 30.00 mmol, 1.2 eq., CAS: 7446-08-4). The crude product was reacted with ethyl acetoacetate (**128**, 2.5 mL, 20.00 mmol, 1.0 eq., CAS: 141-97-9) and ethyl-3-aminobut-2-enoate (**129**, 2.58 g, 20.00 mmol, 1.0 eq., CAS: 626-34-6). Column chromatography and recrystallization afforded the product **119-D** as a bright yellow solid (1.43 g; 16%).

^{1}H NMR (400 MHz, CDCl3) δ = 8.16 – 7.95 (m, 2H), 7.68 – 7.48 (m, 2H), 7.09 (s, 1H), 5.65 (s, 1H), 3.98 (qq, *J* = 10.8, 7.1 Hz, 4H), 2.25 (s, 6H), 1.04 (t, *J* = 7.1 Hz, 6H). (corresponds to literature[91]).

5.4.2.5 Diethyl-2,6-dimethyl-4-(4-methylbenzoyl)-1,4-dihydropyridine-3,5-dicarboxylate / „Methyl benzoyl Hantzsch ester“ (119-E, CAS: n.a.)

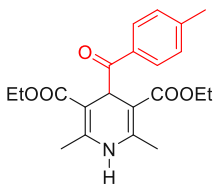

4-Methylphenylglyoxal (**127-E**, CAS: 1075-47-4) was prepared *via* Riley oxidation from 4-methylacetophenone (**126-E**, 3.355 mL, 25.00 mmol, 1.0 eq., CAS: 122-00-9) and selenium(IV) oxide (3.34 g, 30.00 mmol, 1.2 eq., CAS: 7446-08-4). The crude product was reacted with ethyl acetoacetate (**128**, 3.16 mL, 25.00 mmol, 1.0 eq., CAS: 141-97-9) and ethyl-3-aminobut-2-enoate (**129**, 3.23 g, 25.00 mmol, 1.0 eq., CAS: 626-34-6).

Column chromatography and subsequent recrystallization afforded the product **119-E** as a yellow powder (2.98 g, 53%).

^{1}H NMR (400 MHz, $CDCl_3$) δ = 8.06 (d, *J* = 8.4 Hz, 2H), 7.38 (s, 1H), 7.23 (d, *J* = 7.8 Hz, 2H), 5.72 (s, 1H), 4.07 – 3.89 (m, 4H), 2.39 (s, 3H), 2.25 (s, 6H), 1.05 (t, *J* = 7.1 Hz, 6H). (corresponds to literature[91]).

5.5 Synthesis of saturated photoproducts

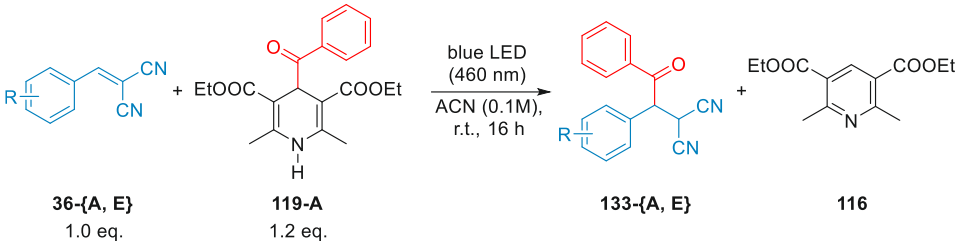

Scheme 51: Synthesis towards saturated photoproducts.

Into an 8 mL Schlenk tube, Hantzsch ester (**119-A**, 0.24 mmol, 1.2 eq.) and substrate (**36-{A-E}**, 0.20 mmol, 1.0 eq.) were added. The Schlenk tube was then evacuated and filled with argon, and acetonitrile (2 mL, 0.1 M) was added *via a* syringe under argon counterflow. The tubes were sealed and placed into a custom-made photoreactor. The reaction mixtures were stirred under blue light irradiation (λ_{max} = 460 nm) for 16 hours. The conversion was determined by GC-MS analysis. Two parallel runs were merged, the solvent was removed *in vacuo* and the crude products were purified by column chromatography (PE/EE or PE/acetone mixtures as mobile phase) providing the products. If the Hantzsch ester residue still resulted in product contamination after column chromatography, it was further removed by means of short-path Pasteur-column eluting with DCM (ca. 25 mL for 0.4 mmol scale).

5.5.1 2-(2-Oxo-1,2-diphenylethyl)malononitrile (133-A, CAS: 312307-43-0)

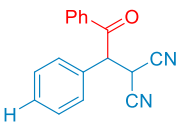

According to the general procedure. Column chromatography (14.1 g SiO_2, dry-loading, isocratic: PE/acetone = 10/1) and subsequent Pasteur filtration with DCM yielded product **133-A** as a light yellow oil (98.0 mg, 94%).

^{1}H NMR (400 MHz, $CDCl_3$) δ = 7.95 – 7.87 (m, 2H), 7.54 (t, *J* = 7.5 Hz, 1H), 7.39 (q, *J* = 8.4 Hz, 7H), 5.15 (d, *J* = 8.2 Hz, 1H), 4.56 (d, *J* = 8.1 Hz, 1H). (corresponds to literature[79,92]).

5.5.2 2-(1-(4-Methoxyphenyl)-2-oxo-2-phenylethyl)malononitrile (133-B, CAS: n.a.)

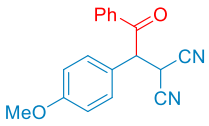

According to the general procedure. Column chromatography (12.8 g SiO_2, dry-loading, PE/acetone = 9/1) and subsequent Pasteur filtration with DCM yielded the product **133-B** as a light yellow solid (117.5 mg, 96%).

^{1}H NMR (400 MHz, $CDCl_3$) δ = 7.82 (dd, *J* = 8.5, 1.3 Hz, 2H), 7.47 (t, *J* = 7.4 Hz, 1H), 7.39 – 7.30 (m, 2H), 7.24 – 7.15 (m, 2H), 6.92 – 6.80 (m, 2H), 5.00 (d, *J* = 8.3 Hz, 1H), 4.43 (d, *J* = 8.3 Hz, 1H), 3.70 (s, 3H). (corresponds to literature[79]).

5.5.3 2-(1-(4-Chlorophenyl)-2-oxo-2-phenyl)malononitrile (133-C, CAS: n.a.)

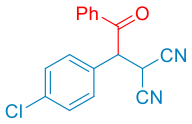

According to the general procedure. Column chromatography (13.1 g SiO_2, dry-loading, PE/acetone = 12/1) and subsequent Pasteur filtration with DCM yielded the product **133-C** as a light yellow oil (94.2 mg, 80%).

^{1}H NMR (400 MHz, $CDCl_3$) δ = 7.91 – 7.82 (m, 2H), 7.60 – 7.53 (m, 1H), 7.45 – 7.35 (m, 4H), 7.34 – 7.27 (m, 2H), 5.14 (d, *J* = 7.9 Hz, 1H), 4.55 (d, *J* = 7.9 Hz, 1H). (corresponds to literature[79]).

5.5.4 2-(1-(4-Bromophenyl)-2-oxo-2-phenyl)malononitrile (133-D, CAS: n.a.)

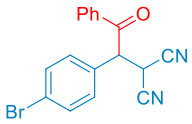

According to the general procedure. Column chromatography (13.6 g SiO_2, dry-loading, PE/acetone = 12/1) and subsequent Pasteur filtration with DCM yielded the product **133-D** as a light yellow oil (112.3 mg, 83%).

^{1}H NMR (400 MHz, $CDCl_3$) δ = 7.84 – 7.74 (m, 2H), 7.50 – 7.43 (m, 3H), 7.38 – 7.28 (m, 2H), 7.19 – 7.11 (m, 2H), 5.03 (d, *J* = 8.0 Hz, 1H), 4.45 (d, *J* = 8.0 Hz, 1H). (corresponds to literature[79]).

5.5.5 2-(1-(Naphthen-1-yl)-2-oxo-2-phenylethyl)malononitrile (133-E, CAS: n.a.)

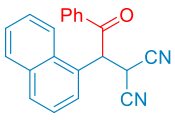

According to the general procedure. Column chromatography (13.4 g SiO_2, dry-loading, PE/acetone = 12/1 to 6:1) and subsequent Pasteur filtration with DCM yielded product **133-E** (100.8 mg, 81%).

^{1}H NMR (400 MHz, $CDCl_3$) δ = 8.32 (d, *J* = 8.6 Hz, 1H), 7.98 (d, *J* = 8.2 Hz, 1H), 7.90 (d, *J* = 8.3 Hz, 1H), 7.86 – 7.73 (m, 3H), 7.65 (t, *J* = 7.6 Hz, 1H), 7.53 – 7.37 (m, 2H), 7.37 – 7.20 (m, 3H), 5.95 (d, *J* = 7.7 Hz, 1H), 4.63 (d, *J* = 7.6 Hz, 1H). (corresponds to literature[79]).

5.5.6 3-Benzoylcyclopentan-1-one (135, CAS: 92516-43-3)

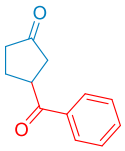

According to the general procedure, but with substrate **134**. Column chromatography (13.4 g SiO_2, dry-loading, PE/acetone = 12/1 to 6:1) and subsequent Pasteur filtration with DCM yielded product **135** (85%).

^{1}H NMR (400 MHz, $CDCl_3$) δ = 8.06 – 7.91 (m, 2H), 7.65 – 7.54 (m, 1H), 7.54 – 7.42 (m, 2H), 4.20 – 4.05 (m, 1H), 2.68 (dd, *J* = 18.6, 8.0 Hz, 1H), 2.51 – 2.08 (m, 5H). (corresponds to literature[93]).

5.5.7 3-Benzoylcyclohexanone (137, CAS: 58753-28-9)

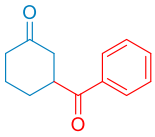

According to the general procedure, but with substrate **136**. Column chromatography (13.4 g SiO_2, dry-loading, PE/acetone = 12/1 to 6:1) and subsequent Pasteur filtration with DCM yielded product **137** (80%).

^{1}H NMR (400 MHz, $CDCl_3$) δ = 8.02 – 7.88 (m, 2H), 7.65 – 7.53 (m, 1H), 7.53 – 7.41 (m, 2H), 3.91 – 3.74 (m, 1H), 2.81 – 2.63 (m, 1H), 2.56 – 2.32 (m, 3H), 2.20 – 2.00 (m, 2H), 1.96 – 1.73 (m, 2H). (corresponds to literature[94]).

5.6 Synthesis of formal alkenylation-type photoproducts

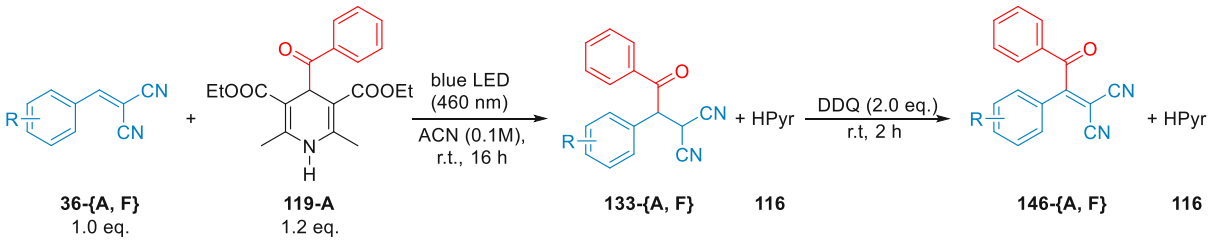

36-{A, F} 1.0 eq. | **119-A** 1.2 eq. | **133-{A, F}** | **116** | **146-{A, F}** | **116**

Scheme 52: Reaction scheme of the hydroacylation and following-up oxidation to formal alkenylation products.

Into an 8 mL Schlenk tube, Hantzsch ester (**119-A**, 0.24 mmol, 1.2 eq.) and substrate (**36-{A-E}**, 0.20 mmol, 1.0 eq.) were added. The Schlenk tube was then evacuated and back-filled with argon, and acetonitrile (2 mL, 0.1 M) was added *via* a syringe under argon counterflow. The tubes were sealed and placed into a custom-made photoreactor. The reaction mixtures were stirred under blue light irradiation (λ_{max} = 460 nm) for 16 hours. The tubes were removed from the photoreactor, DDQ (0.4 mmol, 2.0 eq., CAS: 84-58-2) was added and the reaction mixtures were stirred at 25 °C for another 3 hours (*TLC indicated full conversions*). Two parallel runs were merged, the solvent was removed *in vacuo* and the crude products were purified by column chromatography (PE/EE or PE/acetone mixtures as mobile phase) providing the products.

If the Hantzsch ester residue still resulted in product contamination after column chromatography, it was further removed by means of short-path Pasteur-column eluting with DCM (ca. 25 mL for 0.4 mmol scale).

5.6.1 2-(2-Oxo-1,2-diphenylethylidene)malononitrile (146-A, CAS: 23195-86-0)

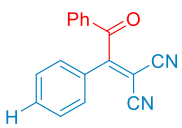

According to the general procedure. Column chromatography (13.3 g SiO_2, dry-loading, PE/acetone = 9/1) yielded product **146-A** as a colourless solid (80.1 mg, 78%). ^{1}H NMR (400 MHz, $CDCl_3$) δ = 7.89 (dd, *J* = 8.4, 1.3 Hz, 2H), 7.82 – 7.72 (m, 2H), 7.72 – 7.65 (m, 1H), 7.65 – 7.57 (m, 1H), 7.53 (td, *J* = 7.9, 7.3, 1.8 Hz, 4H). (corresponds to literature[79]).

5.6.2 2-(1-(4-Methoxyphenyl)-2-oxo-2-phenylidene)malononitrile (146-B, CAS: n.a.)

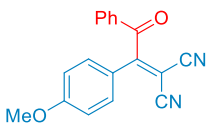

According to the general procedure. Column chromatography (15.5 g SiO_2, dry-loading, PE/acetone = 9:1) yielded product **146-B** as a colourless solid (98.0 mg, 85%).

^{1}H NMR (400 MHz, CDCl3) δ = 7.94 – 7.85 (m, 2H), 7.83 – 7.76 (m, 2H), 7.71 – 7.61 (m, 1H), 7.56 – 7.46 (m, 2H), 7.03 – 6.94 (m, 2H), 3.86 (s, 3H). (corresponds to literature[79]).

5.6.3 2-(1-(4-Chlorophenyl)-2-oxo-2-phenylidene)malononitrile (146-C, CAS: n.a.)

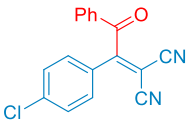

According to the general procedure. Column chromatography (13.2 g SiO_2, dry-loading, PE/acetone = 12/1 to 8/1) yielded the product **146-C** as a colourless solid (61.03 mg, 85%).

^{1}H NMR (400 MHz, $CDCl_3$) δ = 7.87 (dd, *J* = 8.4, 1.4 Hz, 2H), 7.79 – 7.63 (m, 3H), 7.60 – 7.45 (m, 4H). (corresponds to literature[79]).

5.6.4 2-(1-(4-Bromophenyl)-2-oxo-2-phenylidene)malononitrile (146-D, CAS: n.a.)

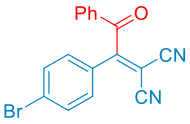

According to the general procedure. Column chromatography (13.6 g SiO_2, dry-loading, PE/acetone = 12/1) yielded the product **146-D** as a colourless solid (98.8 mg, 73%).

^{1}H NMR (400 MHz, $CDCl_3$) δ = 7.87 (dt, *J* = 8.5, 1.5 Hz, 2H), 7.73 – 7.58 (m, 5H), 7.57 – 7.48 (m, 2H). (corresponds to literature[79]).

5.6.5 (2-(1-(Naphthalen-1-yl)-2-oxo-2-phenylethylidene)malononitrile (146-E, CAS: n.a.)

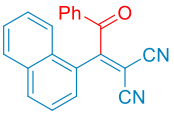

According to the general procedure. Column chromatography (13.2 g SiO_2, dry-loading, PE/acetone = 9/1), and subsequent Pasteur filtration with DCM yielded the product **146-E** as a pale yellow solid (89.7 mg, 73%).

^{1}H NMR (400 MHz, $CDCl_3$) δ = 8.04 (t, *J* = 8.0 Hz, 2H), 7.99 – 7.85 (m, 3H), 7.75 (d, *J* = 7.1 Hz, 1H), 7.72 – 7.64 (m, 1H), 7.64 – 7.51 (m, 3H), 7.45 (t, *J* = 7.9 Hz, 2H). ^{13}C NMR (101 MHz, CDCl3) δ = 190.43, 172.52, 135.52, 133.93, 133.35, 129.79, 129.40, 129.32, 128.92, 128.54, 127.93, 127.41, 125.11, 124.41, 111.37, 111.12, 90.39. IR ATR (ν_{max}/cm^{-1}) 3057, 2235, 1661, 1256, 801, 678. HRMS (ESI) Cald for C21H13N2O $[M + H]^+$ 309.1028, Found 309.1022.

5.6.6 2-(1-(4-Cyanophenyl)-2-oxo-2-phenylethylidene)malononitrile (146-F, CAS: n.a.)

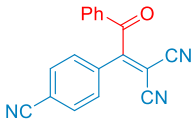

According to the general procedure. Column chromatography (15 g SiO_2, dry-loading, PE/acetone = 12/1 to 6/1) yielded the product **146-F** as a colourless solid (78.0 mg, 69%).

^{1}H NMR (400 MHz, $CDCl_3$) δ = 7.96 – 7.77 (m, 6H), 7.72 (t, *J* = 7.5 Hz, 1H), 7.55 (t, *J* = 7.9 Hz, 2H). ^{13}C NMR (101 MHz, CDCl3) δ = 189.75, 169.19, 136.35, 134.21, 133.34, 132.74, 130.02, 129.77, 128.90, 117.15, 116.91, 110.54, 87.23. IR ATR (ν_{max}/cm^{-1}) 3104, 3065, 2240, 2231, 1672, 1229, 836, 690. HRMS (ESI) Cald for C18H10N3O $[M + H]^+$ 284.0824, Found 284.0421.

5.7 Furane formation

5.7.1 2-Amino-5-(naphthalene-1-yl)-4-phenylfuran-3-carbonitrile (146-Ab, CAS: n.a.)

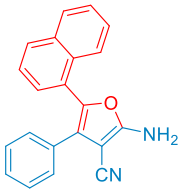

According to the general procedure for saturated hydroacylation product, but with Diethyl-4-(1-naphthoyl)-2,6-dimethyl-1,4-dihydropyridine-3,5-dicarboxylate ("1-naphthyl-Hantzsch ester", **119-B**, 0.24 mmol, 1.2 eq.) and benzylidene malononitrile (**36-A**, 0.2 mmol, 1.0 eq.). Column chromatography (15 g SiO_2, liquid-loading, PE/EE = 10/1) yielded the product (**146-Ab**) as a colourless solid (47.6 mg, 38%).

^{1}H NMR (400 MHz, acetone-d6) δ = 7.89 – 7.64 (m, 3H), 7.45 – 7.23 (m, 4H), 7.20 – 7.00 (m, 5H), 6.75 (s, 2H). ^{13}C NMR (101 MHz, acetone-d6) δ = 164.23, 138.03, 134.00, 131.86, 131.34, 129.45, 129.29, 128.47, 128.42, 128.20, 127.63, 126.56, 126.18, 125.65, 125.31, 123.51, 69.20. IR ATR (ν_{max}/cm^{-1}) 3454, 3323, 2210, 1450, 1204, 1072, 780, 698. HRMS (ESI) Cald for C21H14N2ONa $[M + Na]^+$ 333.1004, Found 333.1010.

5.7.2 2-Amino-4-(4-cyanophenyl)-5-phenylfuran-3-carbonitrile (146-J, CAS: n.a.)

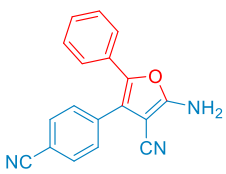

According to the general procedure for saturated hydroacylation products. Column chromatography (13.8 g SiO_2, dry-loading, PE/acetone = 9/1 to 6/1) yielded the product **146-J** as a colourless solid (77%).

^{1}H NMR (400 MHz, $CDCl_3$) δ = 7.71 (d, *J* = 8.7 Hz, 2H), 7.49 (d, *J* = 8.7 Hz, 2H)-CH-*CH-CR*), 7.24 – 7.03 (m, 5H), 6.88 (s, 2H). ^{13}C NMR (101 MHz acetone-d6) δ = 163.54, 139.08, 136.56, 132.70, 129.99, 129.24, 128.68, 127.73, 125.36, 120.27, 118.26, 114.18, 111.76, 70.40. IR ATR

(ν_{max}/cm^{-1}) 3465, 3331, 3193, 2918, 2234, 2198, 1597, 1450, 1204, 1065, 698. HRMS (ESI) Cald for C18H11N3ONa $[M + Na]^+$ 308.0800, Found 308.0793.

5.8 Silylation trials

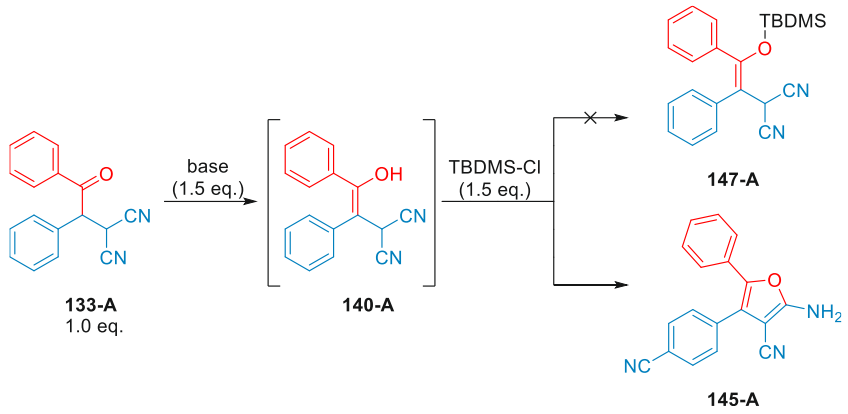

Scheme 53: Trial for silylation via enolisation.

After hydroacylation of substrate **36-A** (0.10 mmol, 1.0 eq.) with acyl-HE **119-A** (0.12 mmol, 1.2 eq.) to hydroacylation product **133-A**, the solvent (ACN) of the crude reaction mixture was removed *in vacuo* and replaced with 1 mL anhydrous DCM. Imidazole (0.15mmol) was added and the reaction mixture was stirred for 1h.

6 Appendix

6.1 List of figures and schemes

Scheme 1: Photochemically triggered aromatisation and enol formation followed by acetylation[11,12]. 1
Figure 1: Schematic representation of photoisomerisations (redrawn from literature[19]). 3
Figure 2: Representation (program: Graphing calculator 3D) of the squared angular part (not the actual orbitals) of the wave functions for s, p, and d orbitals, which are arbitrarily scaled for better representation. 5
Figure 3: Schematic representation of HOMO, LUMO, SOMO and SUMO is a recreation from literature[17] (giving formaldehyde as an example). 6
Figure 4: Morse potential with De = 36000 cm^{-1}, $\beta = 1.9*10^{9}$ cm^{-1}, $r_{equilibrium} = 7.4*10^{-9}$ cm, $\mu = 8.4*10^{-28}$ kg, $\nu 0$ = 4161 cm, χe = 0.03 in light green, and its vibrational levels in dark green. 8
Figure 5: Jablonski diagram redrawn from literature.[17,23] 9
Figure 6: Pathways of the substrate (A) towards the product (P) via different activation strategies. 11
Scheme 2: Example for a concerted, direct photoexcited reaction: [4+2]-cycloaddition.[25] 12
Scheme 3: Example for direct photoexcited photolysis.[26] 12
Scheme 4: Example for direct photoexcited (Norrish-Young) cyclisation.[27] 13
Scheme 5: Example for direct photoexcited isomerisation.[28] 13
Scheme 6: Example for direct photoexcited C-C bond formation.[29] 13
Scheme 7: Cycloaddition reaction by photosensitisation/energy transfer. 14
Scheme 8: Oxidative and reductive quenching in comparison 15
Scheme 9: Cycloaddition by reductive quenching photoredox catalysis.[35] 16
Scheme 10: α-Alkylation of aldehydes as an example of synergistic photoredox catalysis.[34] 16
Scheme 11: Hydrogen atom transfer. 17
Scheme 12: Example of dHAT in an hydroalkylation reaction.[37] 17
Scheme 13: Comparison of EDA complex and exciplex formation. 18
Scheme 14: Benzylation as an example of activation via EDA complex formation.[37] 19
Figure 7: Examples of emission spectra of a low-pressure mercury lamp[46] (top left), xenon lamp[42] (top right), different LEDs[47] (bottom left) and a KrCl excimer lamp[48] (bottom right). 21
Figure 8: Different LED strips (left; picture taken from supplier: LEDLightsworld[50]), tungsten-halogen lamps in different sizes and shapes (middle; picture taken from supplier: InternationalLight[51]), and a small excimer lamp (right; picture taken from supplier's product catalogue[52]). 21
Figure 9: Intensity drop according to the inverse-square law, the "wall drop" due to transmittance and Lambert-Beer's law in solution over the distance travelled (left) and a visual representation, in which the brightness was decreased according to the left graph (brightness fixated for the first centimetre; each column represents 0.1cm). 23
Scheme 15: Acetylation: First documented attempt to synthesise acetylsalicylic acid.[55] 25
Scheme 16: Friedel-Crafts acylation.[55] 25
Scheme 17: Radical hydroacylation: Photochemical example from the first set of hydroacylations.[57] 25
Scheme 18: First metal catalysed hydroacylation reactions with the reaction scheme (left) and mechanism (right).[58] 26
Scheme 19: Stetter reaction: First organocatalytic hydroacylation with the reaction scheme (left) and the mechanism (right). 27
Scheme 20: First intramolecular radical hydroacylation.[63] 28
Scheme 21: Combining hydroacylation with a cyclisation reaction. 29
Scheme 22: General mechanism of PRC-catalysed hydroacylation. 29
Figure 10: Examples of different kinds of polarity reversal catalysts. 30
Scheme 23: Initiation route with HIC. 30
Scheme 24: Initiation route with phenylglyoxal/water. 31
Scheme 25: Hydroacylation of a nitrogen double bond. 31

Scheme 26: Reaction scheme (top) and mechanism (bottom) of the photoredox catalysed hydroalkylation/hydroacylation utilising benzothiazoline.[78] 32
Scheme 27: Reaction scheme (top) and mechanism (bottom) of the hydroxybenziodoxolone catalysed hydroacylation utilising benzothiazoline. 33
Scheme 28: Nickel-catalysed coupling reaction utilising alkyl-HE. [82] 34
Scheme 29: Direct photoexcitation of benzyl-HE. [82] 34
Scheme 30: Direct photoexcited hydroacylation of electron-poor Michael acceptors. 34
Scheme 31: Knoevenagel-condensation to benzylidenemalononitrile. [83] 35
Figure 11: Synthesised and available substrates for following up photoreactions. 35
Scheme 32:A failed attempt to synthesise 1,2-dicyano-2-cyclohexylethylene following a procedure of Woo et al. [84] 35
Scheme 33: Phenylglyoxal synthesis from acetophenones according to Melchiorre and co-workers. [85] 36
Scheme 34: HE synthesis according to Melchiorre and co-workers. [85] 36
*Scheme 35: Failed attempt for the synthesis of glyoxal **131** following the procedure of Wu et al.*[86] 36
Figure 12: Synthesised acyl-HE reagents. 37
Scheme 36: Procedure for alkyl-HE synthesis.[34] 37
*Scheme 37: Reaction of substrate **36-A** with Hantzsch ester **119-A** used as "standard reaction" for optimisation.* 38
Figure 13: Using different solvent qualities (left graph, blue columns), a non-inert atmosphere control (left graph, orange column) and different solvents (right graph) as well as different HE loadings (right graph: blue columns [1.1 eq.] vs orange columns [1.2 eq.]). 38
Figure 14: Comparison of reaction rates of the phenyl and 1-naphthyl substituted photoproduct. 39
Scheme 38: Synthesis towards saturated photoproducts. 40
Figure 15: First set of obtained saturated photoproducts. 40
Scheme 39: Photobenzoylation of cyclopent-2-en-1-on. 40
Scheme 40:Photobenzoylation of cyclohex-2-en-1-on. 41
Figure 16: Hydroacylation products (including one cyclisation) using different acyl-HEs. 41
Figure 17: Showing the standard reaction (top), its crude GC-MS (middle) and ^{1}H NMR of the purified product (bottom). 43
Figure 18: Showing the reaction scheme for the 4-CN substrate scheme (top), its crude GC-MS (middle) and ^{1}H NMR of the purified product (bottom). 44
Scheme 41: Cyclisation mechanism by acidic catalysis, resulting in furane formation. 45
Scheme 42: Reaction scheme of the hydroacylation and following-up oxidation to formal alkenylation products (top) and isolated products (bottom). 46
Scheme 43: Trial for silylation via enolisation. 47
Scheme 44: Hydroacylation control experiment in darkness yields no product. 47
Scheme 45: Hydroacylation control experiment with radical scavenger TEMPO yields no product. 48
Figure 19: GC part of a GC-MS measurement for the TEMPO control reaction showing no product peak. 48
Figure 20: ^{1}H NMR of a mixture of benzoyl-TEMPO-adduct and HPyr (double x-axis is used for the visibility of integration). 49
Figure 21: The Light-on, light-off experiment's conversion as a function of time. 50
Figure 22: UV-VIS measurement of HE-Bz (orange dots) and a 1:1 mixture of HE-Bz with benzylidenemalononitrile substrate (blue dots) in comparison. 50
*Scheme 46: Activation of Hantzsch ester **119** by irradiation of blue light and release of a benzoyl radical **91**, which adds to the electron-poor substrate **36**.* 51
Scheme 47: Mechanism of direct photoexcitation and successive hydroacylation of benzylidenemalononitrile substrate. 51
Figure 23: Stacked fluorescence emission spectra of HE (0.15 m) with increasing concentration of benzylidenemalononitrile (0 – 20 mM) at an excitation wavelength of λ_{max} = 365 nm (left) and the corresponding Stern-Volmer-plot (right). 52
Figure 24: The inside of the photoreactor showing the LED strips (left, top), the photoreactor's top lid with cooling fan (left, bottom) and the photoreactor in action (right). 55
Scheme 48: Knoevenagel condensation to benzylidenemalonitrile derivatives. [83] 56

Scheme 49: Phenylglyoxal synthesis from acetophenones according to Melchiorre and co-workers. [85] 59
Scheme 50: HE synthesis according to Melchiorre and co-workers. [85] 59
Scheme 51: Synthesis towards saturated photoproducts. 62
Scheme 52: Reaction scheme of the hydroacylation and following-up oxidation to formal alkenylation products. 65
Scheme 53: Trial for silylation via enolisation. 69

7 Literature

1. Roth, H. D. The Beginnings of Organic Photochemistry. *Angew. Chemie Int. Ed. English* **28**, 1193–1207 (1989).
2. Schulze, J. H. Scotophorus pro Phosphoro inventvs - seu experimentum curiosum de effectu radiorum solarium. *Ioannes Christophovs Fr. Bibl. Novis. Obs. Ac Recens.* **5**, 234–240 (1719).
3. Roth, P., Egetenmeier, P. & Soentgen, J. Scotophorus pro Phosphoro inventvs - seu experimentum curiosum de effectu radiorum solarium // Die Entdeckung eines 'Dunkelbringers' anstelle eines 'Lichtbringers' - Oder ein interessantes Experiment über die Wirkung der Sonnenstrahlen. 1–28 (2015).
4. Leggo, W. A. & Desbarats, G. E. Improvement in photo-electrotype. (1865).
5. Morvan, A. G. Improvement in electro-photo damaskening and enameling. (1870).
6. Edwards, E. Improvement in photo-mechanical printing. (1872).
7. Trommsdorff, H. Ueber Santonin. *Ann. der Pharm.* **XI**, 190–207 (1834).
8. Fritzsche, J. C. Ueber die festen Kohlenwasserstoffe des Steinkohlentheers. *Chem. Zentralblatt* **12**, 449–456 (1867).
9. Liebermann, C. T. Ueber Polythymochinon. *Berichte der Dtsch. Chem. Gesellschaft* **10**, 2177–2179 (1877).
10. Jannasch, P. Ueber Trimethylbenzol. *Justus Liebigs Ann. Chem.* **176**, 283–290 (1875).
11. Klinger, H. Ueber das Isobenzil und die Einwirkung des Sonnenlichts auf organische Substanzen. *Berichte der Dtsch. Chem. Gesellschaft* **19**, 1862–1870 (1886).
12. Klinger, H. Ueber die Einwirkung des Sonnenlichts auf organische Verbindungen. *Justus Liebigs Ann. Chem.* **249**, 137–146 (1888).
13. Johnston, S. F. *A History of Light and Colour Measurement*. (Institute of Physics Publishing, 2001). doi:10.1201/9781420034776.
14. Michelson, A. A. On the application of interference methods to spectroscopic measurements. *London, Edinburgh, Dublin Philos. Mag. J. Sci.* **34**, 280–299 (1892).
15. Walsh, A. The application of atomic absorption spectra to chemical analysis. *Spectrochim. Acta* **7**, 108–117 (1955).
16. Dinda, B. *Essentials of Pericyclic and Photochemical Reactions*. vol. 93 (Springer International Publishing AG, 2017).
17. Wardle, B. *Principles and Applications of Photochemistry*. (John Wiley & Sons, Ltd, Publication, 2009).
18. Adamson, A. W. Properties of Excited States. *J. Chem. Educ.* **60**, 797–802 (1983).
19. Tausch, M. *Chemie mit Licht - Innovative Didaktik für Studium und Unterricht*. *Chemie mit Licht* (Springer-Verlag GmbH Deutschland, 2019).
20. Wedler, G. & Freund, H.-J. *Lehrbuch der Physiaklischen Chemie*. (WILEY-VCH Verlag GmbH & Co. KGaA, 2012).
21. Kaiser, W. & Garrett, C. G. B. Two-Photon Excitation in CaF2:Eu2+. *Phys. Rev. Lett.* **7**, 229–232 (1961).
22. Verma, P. & Truhlar, D. G. Status and Challenges of Density Functional Theory. *Trends Chem.* **2**, 302–318 (2020).
23. Blog - What is a Jablonski Diagram (Perrin-Jablonski Diagram)? *Edinburgh Instruments* https://www.edinst.com/blog/jablonski-diagram-2/.
24. Sumida, Y. & Ohmiya, H. Direct excitation strategy for radical generation in organic synthesis. *Chem. Soc. Rev.* **50**, 6320–6332 (2021).
25. Zhang, Z., Zhou, Y. & Liang, X. Total synthesis of natural products using photocycloaddition reactions of arenes. *Org. Biomol. Chem.* **18**, 5558–5566 (2020).
26. Zhao, Q. L. *et al.* Photoinduced ICAR ATRP of Methyl Methacrylate with AIBN as Photoinitiator. *J. Polym. Res.* **21**, (2014).
27. Majhi, S. Applications of Norrish type I and II reactions in the total synthesis of natural products:

a review. *Photochem. Photobiol. Sci.* **20**, 1357–1378 (2021).
28. Merritt, I. C. D., Jacquemin, D. & Vacher, M. cis -> trans photoisomerisation of azobenzene: a fresh theoretical look. *Phys. Chem. Chem. Phys.* **23**, 19155–19165 (2021).
29. Amos, S. G. E., Cavalli, D., Le Vaillant, F. & Waser, J. Direct Photoexcitation of Ethynylbenziodoxolones: An Alternative to Photocatalysis for Alkynylation Reactions. *Angew. Chemie Int. Ed.* **60**, 23827–23834 (2021).
30. Amos, S. G. E., Garreau, M., Buzzetti, L. & Waser, J. Photocatalysis with organic dyes: facile access to reactive intermediates for synthesis. *Beilstein J. Org. Chem.* **16**, 1163–1187 (2020).
31. Shaw, M. H., Twilton, J. & MacMillan, D. W. C. Photoredox Catalysis in Organic Chemistry. *J. Org. Chem.* **81**, 6898–6926 (2016).
32. Brimioulle, R., Lenhart, D., Maturi, M. M. & Bach, T. Enantioselective Catalysis of Photochemical Reactions. *Angew. Chemie Int. Ed.* **54**, 3872–3890 (2015).
33. Mojr, V. *et al.* Tailoring flavins for visible light photocatalysis: organocatalytic [2+2] cycloadditions mediated by a flavin derivative and visible light. *Chem. Commun.* **51**, 12036–12039 (2015).
34. Nicewicz, D. A. & MacMillan, D. W. C. Merging Photoredox Catalysis with Organocatalysis: The Direct Asymmetric Alkylation of Aldehydes. *Science* **322**, 77–80 (2008).
35. Ischay, M. A., Anzovino, M. E., Du, J. & Yoon, T. P. Efficient Visible Light Photocatalysis of [2+2] Enone Cycloadditions. *J. Am. Chem. Soc.* **130**, 12886–12887 (2008).
36. Narayanam, J. M. R., Tucker, J. W. & Stephenson, C. R. J. Electron-Transfer Photoredox Catalysis: Development of a Tin-Free Reductive Dehalogenation Reaction. *J. Am. Chem. Soc.* **131**, 8756–8757 (2009).
37. Xuan-Zi, F. *et al.* Eosin Y as a Direct Hydrogen-Atom Transfer Photocatalyst for the Functionalization of C-H Bonds. *Angew. Chem. Int. Ed.* **57**, 8514–8518 (2018).
38. Tasnim, T., Ayodele, M. J. & Pitre, S. P. Recent Advances in Employing Catalytic Donors and Acceptors in Electron Donor-Acceptor Complex Photochemistry. *J. Org. Chem.* **87**, 10555–10563 (2022).
39. Buglioni, L., Raymenants, F., Slattery, A., Zondag, S. D. A. & Noël, T. Technological Innovations in Photochemistry for Organic Synthesis : Flow Chemistry, High-Throughput Experimentation, Scale-up, and Photoelectrochemistry. *Chem. Rev.* **122**, 2752–2906 (2022).
40. Buzzetti, L., Crisenza, G. E. M. & Melchiorre, P. Mechanistic Studies in Photocatalysis Angewandte. *Angew. Chemie Int. Ed.* **58**, 3730–3747 (2019).
41. Heraeus. Amba UV curing lamps.
42. HAMAMATSU. SUPER-QUIET XENON LAMP SUPER-QUIET MERCURY-XENON LAMP.
43. High power Tungsten-Halogen Light Source - ASBN-W-050 / ASBN-W075 - ASBN-W100 / ASBN-W150 - Operation Manual. https://www.spectralproducts.com/pdf/SP-ASBN-HPTH_wAdjPowerBd.pdf.
44. Spectral Products. Deep UV Deuterium Light Source - ASBN-D130 - Operation Manual. https://www.spectralproducts.com/pdf/SP-ASBN-D130.pdf.
45. Spectrum of Fluorescent Light. http://www.bealecorner.org/best/measure/cf-spectrum/.
46. Heraeus. High-quality light sources for analytical instruments.
47. PHOTOELECTRONICS. UV LED emission spectrum. https://www.photoelcuring.com/en/technologies/uv-led/emission-spectrum/.
48. Fukui, T. *et al.* Exploratory clinical trial on the safety and bactericidal effect of 222-nm ultraviolet C irradiation in healthy humans. *PLoS One* **15**, 1–13 (2020).
49. rp-photonics. Excimer Lamps. https://www.rp-photonics.com/excimer_lamps.html.
50. LEDLIGHTSWORLD. 12V MD335-300 Side View Flexible LED Strips 60 LEDs Per Meter 8mm Wide FPCB LED Tape. https://ledlightsworld.com/collections/flexible-led-strips/products/12v-dc-smd335-300-side-view-flexible-led-strips-60-leds-per-meter?variant=17870807760986.
51. InternationlLight. Tungsten Halogen & Gas Filled Lamps. https://internationallight.com/applications/tungsten-halogen-gas-filled-lamps.
52. HAMAMATSU. EX-PEN, Excimer Lamp Light Source.

53. SCHOTT. Schott Technische Gläser - Physikalische und chemische Eigenschaften. http://www.jb-electronics.de/downloads/elektronik/nixies/eigenbau/schott_technical_glasses.pdf.
54. Wurtz, M. A. Recherches sur les éthers cyaniques et leurs dérivés. *comptes rendus des séances l'académie des Sci.* **27**, 241–243 (1848).
55. Gerhardt, C. Untersuchungen über die wasserfreien organischen Säuren. *Justus Liebigs Ann. Chem.* **87**, 149–179 (1853).
56. Willis, M. C. Hydroacylation of Alkenes, Alkynes, and Allenes. in *Comprehensive Organic Synthesis* (eds. Knochel, P. et al.) vol. 4 961–994 (Elsevier Ltd., 2014).
57. Kharasch, M. S., Urry, W. H. & Kuderna, B. M. REACTIONS OF ATOMS AND FREE RADICALS IN SOLUTION. XX. THE ADDITION OF ALDEHYDES TO OLEFINS. *J. Org. Chem.* **14**, 248–253 (1949).
58. Sakai, K., Ide, J., Oda, O. & Nakamura, N. SYNTHETIC STUDIES ON PROSTANOIDS 1 SYNTHESIS OF METHYL 9-OXOPROSTANONE. *Tetrahedron Lett.* **13**, 1287–1290 (1972).
59. Guo, R. & Zhang, G. Recent Advances in Intermolecular Hydroacylation of Alkenes with Aldehydes through Rhodium Catalysis. *Synlett* **29**, 1801–1806 (2018).
60. Ghosh, A., Johnson, K. F., Vickerman, K. L., Walker, J. A. & Stanley, L. M. Recent advances in transition metal-catalysed hydroacylation of alkenes and alkynes. *Org. Chem. Front.* **3**, 639–644 (2016).
61. Stetter, H. Die katalysierte Addition von Aldehyden an aktivierte Doppelbindungen - Ein neues Syntheseprinzip. *Angew. Chemie* **88**, 695–704 (1976).
62. Thalakottuka, D. D. & Gandhi, T. NHC-Organocatalysed Hydroacylation of Unactivated or Weakly Activated C-C Multiple Bonds and Ketones. *Asian J. Org. Chem.* **11**, e202200080 (1-17) (2022).
63. Zivorad, C. Intramolecular cyclization of unsaturated acyl chlorides by tributyltin hydride. *Tetrahedron Lett.* **13**, 749–752 (1972).
64. Bachi, M. D. & Bosch, E. Synthesis of alpha-alkylidene-gamma-lactones by intramolecular addition of alkoxycarbonyl free-radicals to acetylenes. *Tetrahedron Lett.* **27**, 641–644 (1986).
65. Boger, D. L. & Mathvink, R. J. Acyl Radicals: Functionalized Free Radicals for Intramolecular Cyclization Reactions. *J. Org. Chem.* **53**, 3377–3379 (1988).
66. Boger, D. L. & Mathvink, R. J. Phenyl Selenoesters as Effective Precursors of Acyl Radicals for Use in Intermolecular Alkene Addition Reactions. *J. Org. Chem.* **54**, 1777–1779 (1989).
67. Delduc, P., Tailhan, C. & Zard, S. A Convenient Source of Alkyl and Acyl Radicals. *Chem. Commun.* 308–310 (1988).
68. Gottschalk, P. & Neckers, D. C. Low Temperature Free-Radical Reactions Initiated with tertButyl p-Benzoylperbenzoate. Selective Acyl Radical Additions to Substituted Olefins. *J. Org. Chem.* **50**, 3498–3502 (1985).
69. Dang, H. S. & Roberts, B. P. Polarity-Reversal Catalysis by Thiols of Radical-Chain Hydrosilylation of Alkenes. *Tetrahedron Lett.* **36**, 2875–2878 (1995).
70. Dang, H.-S. & Roberts, B. P. Homolytic aldol reactions: thiol-catalysed radical-chain addition of aldehydes to enol esters and to silyl enol ethers. *Chem. Commun.* 2201–2202 (1996).
71. Dang, H. S. & Roberts, B. P. Radical-chain addition of aldehydes to alkenes catalysed by thiols. *J. Chem. Soc. Perkin Trans. 1* 67–75 (1998) doi:10.1039/a704878e.
72. Roberts, B. P. Polarity-reversal catalysis of hydrogen-atom abstraction reactions: concepts and applications in organic chemistry. *Chem. Soc. Rev.* **28**, 25–35 (1999).
73. Tsujimoto, S., Iwahama, T., Sakaguchi, S. & Ishii, Y. The radical-chain addition of aldehydes to alkenes by the use of N-hydroxyphthalimide (NHPI) as a polarity-reversal catalyst. *Chem. Commun.* 2352–2353 (2001).
74. Moteki, S. A., Usui, A., Selvakumar, S., Zhang, T. & Maruoka, K. Metal-Free C-H Bond Activation of Branched Aldehydes with a Hypervalent Iodine (III) Catalyst under Visible-Light Photolysis: Successful Trapping with Electron-Deficient Olefins. *Angew. Chemie Int. Ed.* **53**, 11060–11064 (2014).
75. Wang, H. *et al.* Bromine radical as a visible-light-mediated polarity-reversal catalyst. *iScience*

24, article 102693 (p.1-44) (2021).
76. Voutyritsa, E. & Kokotos, C. G. Green Metal-Free Photochemical Hydroacylation of Unactivated Olefins. *Angew. Chemie Int. Ed.* **59**, 1735–1741 (2020).
77. Zhang, Q., Parker, E., Headley, A. D. & Ni, B. A practical and highly efficient hydroacylation reaction of azodicarboxylates with aldehydes in water. *Synlett* 2453–2456 (2010).
78. Uchikura, T. *et al.* Benzothiazolines as radical transfer reagents: Hydroalkylation and hydroacylation of alkenes by radical generation under photoirradiation conditions. *Chem. Commun.* **55**, 11171–11174 (2019).
79. Li, L., Guo, S., Wang, Q. & Zhu, J. Acyl Radicals from Benzothiazolines: Synthons for Alkylation, Alkenylation, and Alkynylation Reactions. *Org. Lett.* **21**, 5462–5466 (2019).
80. Berenguer-Murcia, A. & Fernandez-Lafuente, R. New Trends in the Recycling of NAD(P)H for the Design of Sustainable Asymmetric Reductions Catalyzed by Dehydrogenases. *Curr. Org. Chem.* **14**, 1000–1021 (2010).
81. Li, G. *et al.* Alkyl transfer from C-C cleavage. *Angew. Chemie Int. Ed.* **52**, 8432–8436 (2013).
82. Buzzetti, L., Prieto, A., Roy, S. R. & Melchiorre, P. Radical-Based C-C Bond-Forming Processes Enabled by the Photoexcitation of 4-Alkyl-1,4-dihydropyridines. *Angew. Chem. Int. Ed.* **56**, 15039–15043 (2017).
83. Foucaud, A. & Moison, H. Reaction de Knoevenagel et de Wittig-Horner En Presence D'oxydes Metalliques. Modification de la Selectivite Du Catalyseur Par Addition De Solvants Ou De Sels Metalliques. *Mol. Cryst. Liq. Cryst. Inc. Nonlinear Opt.* **161**, 517–520 (1988).
84. Khatun, N., Kim, M. J. & Woo, S. K. Visible-Light Photoredox-Catalyzed Hydroalkoxymethylation of Activated Alkenes Using α-Silyl Ethers as Alkoxymethyl Radical Equivalents. *Org. Lett.* **20**, 6239–6243 (2018).
85. Goti, G., Bieszczad, B., Vega-Peñaloza, A. & Melchiorre, P. Stereocontrolled Synthesis of 1,4-Dicarbonyl Compounds by Photochemical Organocatalytic AcylRadical AdditiontoEnals. *Angew. Chemie Int. Ed.* **58**, 1213–1217 (2019).
86. Yu, X.-X. *et al.* Iodine-Promoted Formal [3+2] Cycloaddition of Enaminone: Access to 2-Hydroxy-1,2-dihydro-pyrrol-3-ones with Quaternary Carbon Center. *J. Org. Chem.* **86**, 12141–12147 (2021).
87. Watanuki, S. *et al.* Acid-mediated Cyclization of 3-Benzoyl-2-cyanobutyronitrile to 2-Amino-4-methyl-5-phenylfuran-3-carbonitrile. *Heterocycles* **62**, 127–130 (2004).
88. Wan, Q., Li, S., Kang, Q., Yuan, Y. & Du, Y. Chiral-at-Metal Rh(III) Complex Catalyzed Cascade Reduction- Michael Addition Reaction. *J. Org. Chem.* **84**, 15201–15211 (2019).
89. de Abrantes, P. G., de Abrantes, P. G., Ferreira, J. M. G. de O. & Vale, J. A. NaCl as an eco-friendly and efficient promoter for Knoevenagel condensation at room temperature. *Synth. Commun.* **53**, 135–145 (2023).
90. Salaverri, N., Carli, B., Gratal, P. B., Marzo, L. & Alemán, J. Remote Giese Radical Addition by Photocatalytic Ring Opening of Activated Cycloalkanols. *Adv. Synth. Catal.* **364**, 1689–1694 (2022).
91. Shan, X. *et al.* Visible-Light-Promoted Trifluoromethylthiolation and Trifluoromethylselenolation of 1,4-Dihydropyridines. *J. Org. Chem.* **88**, 319–328 (2023).
92. Zhao, L. *et al.* Eosin Y-Containing Metal–Organic Framework as a Heterogeneous Catalyst for Direct Photoactivation of Inert C–H Bonds. *Inorg. Chem.* **61**, 7256–7265 (2022).
93. Wang, G. Z., Shang, R., Cheng, W. M. & Fu, Y. Decarboxylative 1,4-Addition of α-Oxocarboxylic Acids with Michael Acceptors Enabled by Photoredox Catalysis. *Org. Lett.* **17**, 4830–4833 (2015).
94. Vu, M. D., Das, M. & Liu, X. W. Direct Aldehyde Csp2-H Functionalization through Visible-Light-Mediated Photoredox Catalysis. *Chem. Eur. J.* **23**, 15899–15902 (2017).